Supporting Information

Mesolytic Cleavage of Homobenzylic Ethers for Programmable End-of-Life Function in Redoxmers

Hai Qian,[†,a,b,c] Michael J. Counihan,[†,a,c] Hieu A. Doan,[†,a,e] Nafisa Ibrahim,[a,c] Andrew S. Danis,[a,c] Worapol Setwipatanachai,[c] Nathan S. Purwanto,[d] Joaquín Rodríguez-López,*[,a,b,c] Rajeev S. Assary,*[,a,e] and Jeffrey S. Moore*[,a,b,c,d]

[a]Joint Center for Energy Storage Research, Argonne National Laboratory, 9700 South Cass Avenue, Lemont, Illinois 60439, United States; [b]The Beckman Institute for Advanced Science and Technology, [c]Department of Chemistry, [d]Department of Materials Science and Engineering, University of Illinois at Urb ana-Champaign, Urbana, Illinois 61801, United States; [e]Materials Science Division, Argonne National Laboratory, Lemont, IL, 60439, USA..

*Email: jsmoore@illinois.edu; joaquinr@illinois.edu; assary@anl.gov.

[†]H.Q., M.J.C, and H.A.D. contributed equally to this work

Table of Contents

1. General Methods **S2**

2. Synthesis and Characterizations **S3**

3. Fragmentation Studies **S27**

4. Electrochemistry Studies **S30**

5. Chemical Trapping Analysis **S50**

6. Computational Studies **S53**

7. NMR Spectra **S86**

8. Reference **S119**

1 General Methods

All reagents and starting materials were purchased from commercial vendors and were used as supplied unless otherwise indicated. All experiments were conducted in air unless otherwise noted. Column chromatography was performed on Biotage Isolera using Silicycle SiliaSep HP flash cartridges. Deuterated solvents were purchased from Cambridge Isotope Laboratories, Inc. and used as received. ^{1}H NMR, ^{13}C NMR and 2D NMR spectra were recorded on a Bruker 500 MHz NMR spectrometer, with working frequencies of 499.87 MHz for ^{1}H nuclei, and 125.7 MHz for ^{13}C nuclei. Chemical shifts are quoted in ppm relative to tetramethylsilane (TMS), using the residual solvent peak as the reference standard. Hi-Res mass spectra were obtained on a Waters Synapt G2-Si ESI mass spectrometer. Analytical gel permeation chromatography (GPC) experiments were performed on an Agilent 1260 Infinity system equipped with an isocratic pump (G1310B), a refractive index detector (G1362A), a thermostatted column compartment (G1316A), a standard auto-sampler (G1329B), a Wyatt Viscostar II viscometer detector, a Wyatt MiniDAWN Treos 3-angle light-scattering detector, and a series of 4 Waters HR Styragel columns (7.8 × 300 mm, HR1, HR3, HR4, and HR5) in THF at 30 °C and a flow rate of 1 mL/min. Molecular weights and molecular weight distributions were calculated based on the dn/dc value (0.1870 mL/g) of polystyrene, or calibration curves by linear polystyrene standards. Elemental analyses were performed on Exeter Analytical CE 440 and Perkin Elmer 2440, Series II. The theoretical polymer formula is calculated based on Mn value by GPC. Infrared spectra were recorded on a Perkin-Elmer UATR-2 FT-IR spectrophotometer.

2 Synthetic and Characterizations

General procedure for methylation of homobenzylic alcohol (S1)**:** To a stirred solution of a homobenzylic alcohol (1 equiv) in dry THF at 0 °C was slowly added NaH (2.0 equiv). The reaction mixture was further stirred at 0 °C for 1 h before slow addition of iodomethane (1.5 equiv). The mixture was then stirred at r.t. overnight. The mixture was quenched with the addition of saturated NH_4Cl and extracted with ethyl acetate (EtOAc) three times. The combined organic extracts were washed with brine and dried over $MgSO_4$. The crude product was collected by filtration and purified by silica gel column chromatography to afford homobenzylic ethers (HBEs).

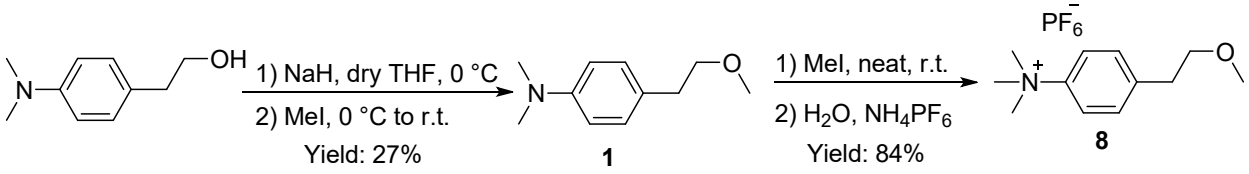

4-(2-Methoxyethyl)-N,N-dimethylaniline (1): This compound was synthesized following the general procedure for methylation of homobenzylic alcohol, while using 2-(4-(dimethylamino)phenyl)ethanol (1.49 g, 9.0 mmol, 1.0 equiv), NaH (0.43 g, 18.0 mmol, 2.0 equiv), and iodomethane (MeI, 0.84 mL, 13.5 mmol, 1.5 equiv) as the starting materials in dry THF (10 mL). The crude product was subjected to silica gel column chromatography using hexanes/EtOAc as eluent to give HBE **1** (0.440 g, 27%) as an orange oil. ^{1}H NMR (500 MHz, $CDCl_3$) δ 7.10 (dd, *J* = 23.2, 7.2 Hz, 1H), 6.73 (d, *J* = 7.5 Hz, 1H), 3.58 (t, *J* = 7.3 Hz, 1H), 3.38 (d, *J* = 0.9 Hz, 2H), 2.96 (d, *J* = 14.7 Hz, 3H), 2.82 (t, *J* = 7.2 Hz, 1H) ppm; ^{13}C NMR (126 MHz, $CDCl_3$) δ 129.46, 126.87, 112.98, 74.17, 58.64, 43.75, 40.87, 35.20 ppm; Hi-Res MS (ESI): *m/z* found [M–H$^+$] for $C_{11}H_{18}NO^+$ 180.1384 (calcd. 180.1388).

4-(2-Methoxyethyl)-N,N,N-trimethylbenzenaminium hexafluorophosphate salt (8): This compound was synthesized using a modified reported procedure (S2). To a vial with a magnetic stir bar was added **1** (0.144 g, 0.80 mmol, 1.0 equiv) and MeI (1.14 g, 8.0 mmol, 10.0 equiv). The neat reaction mixture was stirred at r.t. for 24 hrs. The MeI was removed in vacuum to

furnish the quaternary ammonium iodide. The iodide salt was dissolve in water, followed by the addition of saturated ammonium hexafluorophosphate solution. The off-white flake-shaped crystal crashed out and collected by filtration to give HBE **8** (0.23 g, 84%). ^{1}H NMR (500 MHz, CD_3CN) δ 8.51 (d, *J* = 8.9 Hz, 2H), 8.32 (d, *J* = 9.1 Hz, 2H), 4.46 (t, *J* = 6.4 Hz, 2H), 4.35 (s, 9H), 4.12 (s, 3H), 3.76 (t, *J* = 6.3 Hz, 2H) ppm; ^{13}C NMR (126 MHz, CD_3CN) δ 145.61, 143.62, 131.39, 120.42, 72.83, 58.41, 57.74, 35.47 ppm; Hi-Res MS (ESI): *m/z* found [M^+] for $C_{12}H_{20}NO^+$ 194.1540 (calcd. 194.1545).

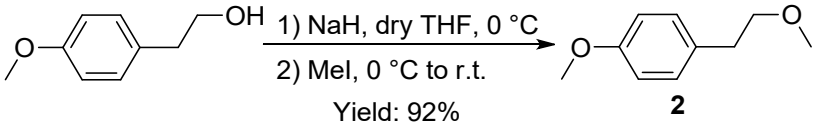

1-Methoxy-4-(2-methoxyethyl)benzene (2): This compound was synthesized following the general procedure for methylation of homobenzylic alcohol, while using 2-(4-methoxyphenyl)ethanol (1.52 g, 10.0 mmol, 1.0 equiv), NaH (0.48 g, 20.0 mmol, 2.0 equiv), and iodomethane (MeI, 0.93 mL, 15.0 mmol, 1.5 equiv) as the starting materials in dry THF (10 mL). The crude product was subjected to silica gel column chromatography using hexanes/EtOAc as eluent to give HBE **2** (1.55 g, 92%) as a pale yellow oil. The identity of **2** was confirmed by comparing the obtained ^{1}H NMR with the published one (S3). ^{1}H NMR (500 MHz, $CDCl_3$) δ 7.19 – 7.14 (m, 2H), 6.88 – 6.84 (m, 2H), 3.81 (s, 3H), 3.59 (t, *J* = 7.1 Hz, 2H), 3.38 (s, 3H), 2.85 (t, *J* = 7.1 Hz, 2H) ppm.

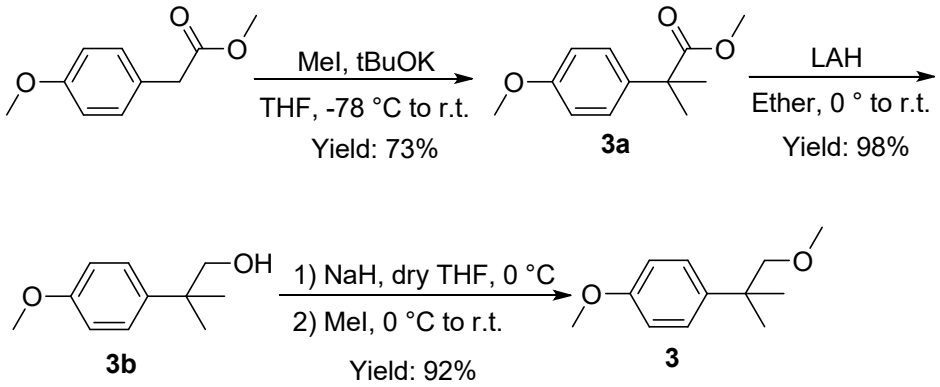

Methyl 2-(4-methoxyphenyl)-2-methylpropanoate (3a): To a solution of methyl 2-(4-methoxyphenyl)acetate (5.00 g, 27.7 mmol, 1.0 equiv) in THF (50.0 mL) at -78 °C was added MeI (11.82 g, 83.2 mmol, 3.0 equiv) very slowly. Potassium tert-butoxide (9.34 g, 83.2 mmol, 3 equiv) was then added portionwise over 10 min and the reaction mixture was stirred at -78 °C for 1.5 hrs, followed by stirring at r.t. overnight. The reaction was quenched by the addition of water and extracted with EtOAc three times. The combined organic extracts were washed with brine and dried over Na_2SO_4. The crude product was subjected to silica gel column chromatography using hexanes/EtOAc as eluent to give **3a** (4.24 g, 73%) as a colorless oil. The identity of **3a** was confirmed by comparing the obtained ^{1}H NMR with the published one (S4). ^{1}H NMR (400 MHz, $CDCl_3$) δ 7.30 – 7.24 (m, 2H), 6.89 – 6.84 (m, 2H), 3.80 (s, 3H), 3.65 (s, 3H), 1.56 (s, 6H) ppm.

1-Methoxy-4-(1-methoxy-2-methylpropan-2-yl)benzene (3): The **3b** alcohol was obtained from the reduction of **3a**. To an oven-dried flask was charged **3a** (2.08 g, 10.0 mmol, 1 equiv) and dry THF (80 mL). The solution was cooled in an ice bath. To this mixture, lithium aluminum hydride (LAH, 0.86 g, 22.5 mmol, 2.25 equiv) was added portionwise over 10 mins. The reaction was then left at r.t. overnight. The reaction mixture was cooled down in an ice bath and quenched with 1 M aqueous HCl (20 mL). The mixture was extracted with diethyl ether three times. The combined organic extracts were washed with brine and dried over anhydrous $MgSO_4$. After removing the organic solvent under vacuum, the primary alcohol product was obtained and immediately used for next step without further purification. HBE **3** was synthesized following the general procedure for methylation of homobenzylic alcohol, while using **3b** (1.00 g, 5.6 mmol, 1.0 equiv), NaH (0.27 g, 11.2 mmol, 2.0 equiv), and iodomethane (MeI, 0.52 mL, 8.4 mmol, 1.5 equiv) as the starting materials in dry THF (10 mL). The crude product was subjected to silica gel column chromatography using hexanes/EtOAc as eluent to give HBE **3** (2.00 g, 92%) as a colorless oil. ^{1}H NMR (500 MHz, $CDCl_3$) δ 7.35 – 7.31 (m, 2H), 6.93 – 6.84 (m, 2H), 3.82 (s, 3H), 3.39 (s, 2H), 3.34 (s, 3H), 1.33 (s, 6H) ppm; ^{13}C NMR (126 MHz, $CDCl_3$) δ 157.61, 139.73, 126.98, 113.44, 83.06, 59.40, 55.21, 38.44, 26.19 ppm; Hi-Res MS (ESI): *m/z* found [M–

Na^+] for $C_{12}H_{18}O_2Na^+$ 217.1208 (calcd. 217.1204).

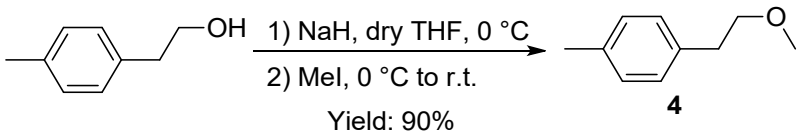

1-(2-Methoxyethyl)-4-methylbenzene (4): This compound was synthesized following the general procedure for methylation of homobenzylic alcohol, while using 2-(p-tolyl)ethanol (2.04 g, 15.0 mmol, 1.0 equiv), NaH (0.72 g, 30.0 mmol, 2.0 equiv), and MeI (1.40 mL, 22.5 mmol, 1.5 equiv) as the starting materials in dry THF (15 mL). The crude product was subjected to silica gel column chromatography using hexanes/EtOAc as eluent to give HBE **4** as a yellow oil (2.02 g, 90%) The identity of **4** was confirmed by comparing the obtained ^{1}H NMR with the published one (S3). ^{1}H NMR (500 MHz, $CDCl_3$) δ 7.20 – 7.08 (m, 4H), 3.62 (t, J = 7.2 Hz, 2H), 3.39 (s, 3H), 2.89 (t, J = 7.2 Hz, 2H), 2.36 (s, 3H) ppm.

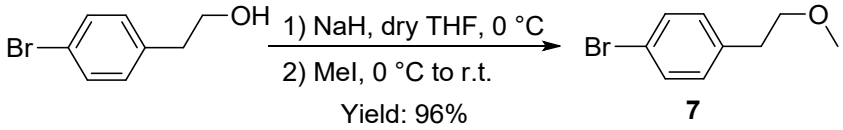

1-Bromo-4-(2-methoxyethyl)benzene (7): This compound was synthesized following the general procedure for methylation of homobenzylic alcohol, while using 2-(4-bromophenyl)ethanol (4.02 g, 20.0 mmol, 1.0 equiv), NaH (0.96 g, 40.0 mmol, 2.0 equiv), and MeI (1.87 mL, 30.0 mmol, 1.5 equiv) as the starting materials in dry THF (20 mL). The crude product was subjected to silica gel column chromatography using hexanes/EtOAc as eluent to give HBE **7** as a yellow oil (4.12 g, 96%). The identity of **7** was confirmed by comparing the obtained ^{1}H NMR with the published one (S3). ^{1}H NMR (500 MHz, $CDCl_3$) δ 7.47 – 7.38 (m, 2H), 7.13 (d, J = 8.2 Hz, 2H), 3.60 (t, J = 6.9 Hz, 2H), 3.37 (s, 3H), 2.86 (t, J = 6.8 Hz, 2H) ppm.

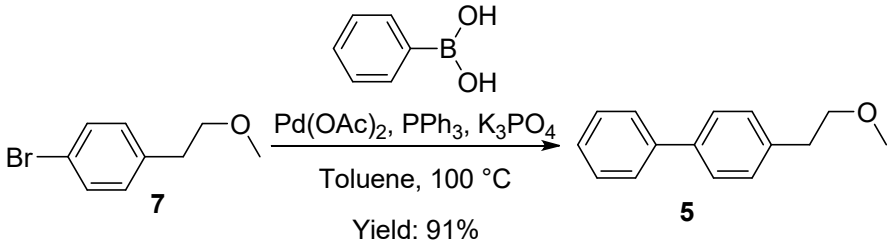

4-(2-Methoxyethyl)-1,1'-biphenyl (5): This compound was synthesized using a modified reported procedure (S5). To a solution of HBE **7** (1.07 g, 5.0 mmol, 1.0 equiv) and phenylboronic acid (0.68 g, 5.5 mmol, 1.1 equiv) in toluene (20 mL) was added triphenylphosphine (PPh_3, 24 mg, 0.09 mmol, 0.018 equiv), palladium acetate ($Pd(OAc)_2$, 6.7 mg, 0.03 mmol, 0.006 equiv), and K_3PO_4 (3.18 g, 15 mmol, 3 equiv). The solution was heated to 100 ^oC and stirred 22 hrs. After cooling to ambient temperature, the precipitate was removed by filtration and the solvent was concentrated under reduced pressure. The crude product was subjected to silica gel column chromatography using hexanes/EtOAc as eluent to give **5** (0.96 g, 91%) as a pale yellow oil. ^1H NMR (500 MHz, $CDCl_3$) δ 7.61 (d, J = 7.1 Hz, 2H), 7.56 (d, J = 8.2 Hz, 2H), 7.49 – 7.42 (m, 2H), 7.39 – 7.31 (m, 3H), 3.68 (t, J = 7.0 Hz, 2H), 3.41 (s, 3H), 2.96 (t, J = 7.0 Hz, 2H) ppm; ^{13}C NMR (126 MHz, $CDCl_3$) δ 141.07, 139.21, 138.11, 129.27, 128.73, 127.16, 127.08, 127.04, 73.57, 58.73, 35.85 ppm; Hi-Res MS (ESI): *m/z* found [M–Na^+] for $C_{15}H_{16}ONa^+$ 235.1110 (calcd. 235.1099).

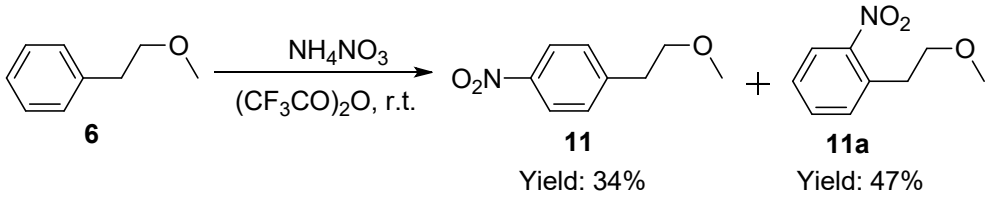

1-(2-Methoxyethyl)-4-nitrobenzene (11): This compound was synthesized using a modified reported procedure (S6). To a mixture of HBE **6** (2.72 g, 20.0 mmol, 1.0 equiv) and ammonium nitrate (NH_4NO_3, 1.6 g, 20.0 mmol, 1.0 equiv) was added trifluoroacetic anhydride ($(CF_3CO)_2O$, 14.7 g, 70 mmol, 10 mL, 3.5 equiv). The reaction mixture was stirred at r.t. for 2 hrs until all the inorganic salt was dissolved. The reaction mixture was then poured into ice water (50 mL) and

extracted three times with chloroform. The combined organic extracts were washed with brine and dried over Na_2SO_4. The crude product was subjected to silica gel column chromatography using hexanes/EtOAc as eluent to give **11** (1.23 g, 34%) as an off-white solid and **11a** (1.69 g, 47%) as a yellow oil. **11**: ^{1}H NMR (500 MHz, $CDCl_3$) δ 8.31 – 8.04 (m, 2H), 7.44 (t, J = 21.3 Hz, 2H), 3.67 (t, J = 6.5 Hz, 2H), 3.38 (d, J = 4.1 Hz, 3H), 3.01 (t, J = 6.5 Hz, 2H) ppm; ^{13}C NMR (126 MHz, $CDCl_3$) δ 147.18, 146.66, 129.70, 123.61, 72.47, 58.82, 36.10 ppm; Hi-Res MS (ESI): *m/z* found [M–Na$^+$] for $C_9H_{11}NO_3Na^+$ 204.0633 (calcd. 204.0637).

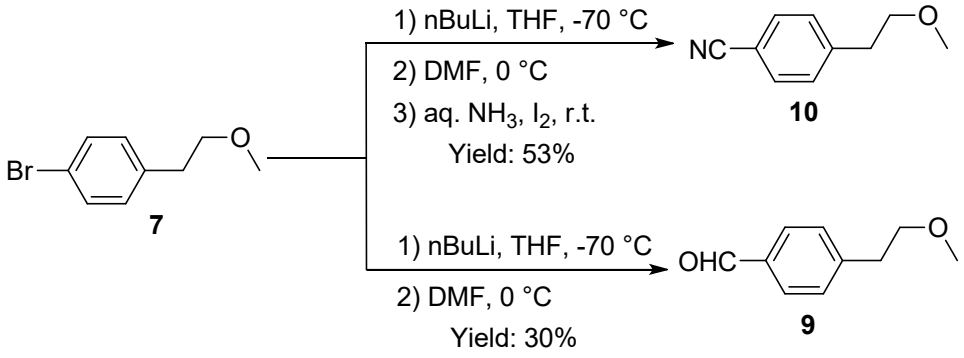

4-(2-Methoxyethyl)benzonitrile (10): This compound was synthesized using a modified reported procedure (S7). To a solution of HBE **7** (0.43 g, 2.0 mmol, 1.0 equiv) in dry THF (3 mL) was dropwise added 1.6 M n-butyllithium in hexane (1.5 mL, 2.4 mmol, 1.2 equiv) at -78 °C. After 30 min, the resulting mixture was warmed and stirred for 5 min at 0 °C. Then, dry DMF (0.185 mL, 2.4 mmol, 1.2 equiv) was added to the mixture, and the obtained mixture was stirred at 0 °C for 1 hr. The aq NH_3 (28-30%, 4 mL, 60 mmol, 30 equiv) and I_2 (0.56 g, 2.2 mmol, 1.1 equiv) were added, and the obtained mixture was stirred for 2 h at r.t. The reaction mixture was quenched with sat. aq Na_2SO_3 and then extracted with Et_2O three times. The combined organic extracts were washed with brine and dried over Na_2SO_4. The crude product was purified by silica gel column chromatography using hexanes/EtOAc as eluent to give **10** (0.17 g, 53%) as a colorless oil. ^{1}H NMR (500 MHz, $CDCl_3$) δ 7.70 – 7.53 (m, 2H), 7.36 (d, J = 8.0 Hz, 2H), 3.64 (t, J = 6.6 Hz, 2H), 3.37 (s, 3H), 2.96 (t, J = 6.6 Hz, 2H) ppm; ^{13}C NMR (126 MHz, $CDCl_3$) δ 144.96, 132.17, 129.67, 119.06, 110.16, 72.54, 58.79, 36.32 ppm; Hi-Res MS (ESI): *m/z* found

[M–H$^+$] for $C_{10}H_{12}NO^+$ 162.0912 (calcd. 162.0919).

4-(2-Methoxyethyl)benzaldehyde (9): This compound was synthesized following a modified procedure for HBE **10**. To a solution of HBE **7** (0.43 g, 2.0 mmol, 1.0 equiv) in dry THF (3 mL) was dropwise added 1.6 M n-butyllithium in hexane (1.5 mL, 2.4 mmol, 1.2 equiv) at -78 °C. After 30 min, the resulting mixture was warmed and stirred for 5 min at 0 °C. Then, dry DMF (0.185 mL, 2.4 mmol, 1.2 equiv) was added to the mixture, and the obtained mixture was stirred at 0 °C for 1 hr. The reaction mixture was then quenched up with water and then extracted with Et_2O three times. The combined organic extracts were washed with brine and dried over Na_2SO_4. The crude product was purified by silica gel column chromatography using hexanes/EtOAc as eluent to give **9** (0.096 g, 30%) as a white solid. ^{1}H NMR (500 MHz, $CDCl_3$) δ 10.00 (s, 1H), 7.84 (d, *J* = 8.2 Hz, 2H), 7.42 (d, *J* = 8.0 Hz, 2H), 3.67 (t, *J* = 6.7 Hz, 2H), 3.38 (s, 3H), 2.99 (t, *J* = 6.7 Hz, 2H) ppm; ^{13}C NMR (126 MHz, $CDCl_3$) δ 192.01, 146.62, 134.82, 129.92, 129.55, 72.78, 58.78, 36.42 ppm; Hi-Res MS (ESI): *m/z* found [M–Na$^+$] for $C_{10}H_{12}O_2Na^+$ 187.0733 (calcd. 187.0735).

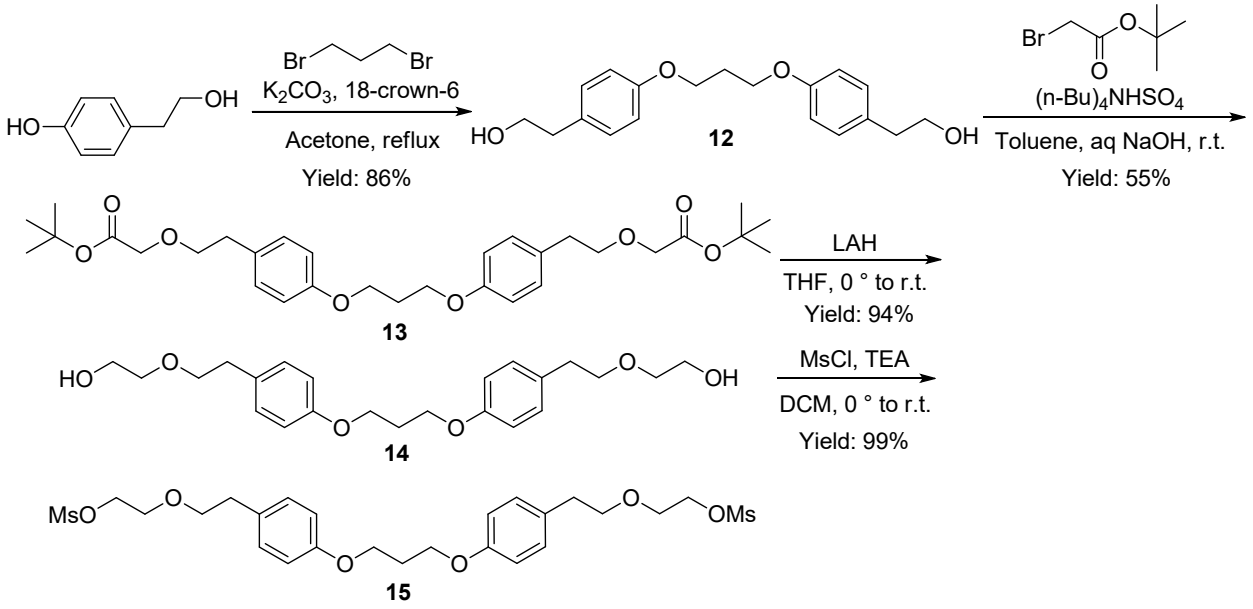

2,2'-((Propane-1,3-diylbis(oxy))bis(4,1-phenylene))diethanol (12): To a mixture of 4-(2-

hydroxyethyl)phenol (34.5g, 0.25 mol, 2.2 equiv), potassium carbonate (37.7 g, 0.273 mol, 2.4 equiv), 1,3-dibromopropane (22.93 g, 0.114 mol, 1 equiv), and 18-crown-6 (3.0 g, 11.36 mmol, 0.1 equiv) was added 625 mL acetone. The reaction mixture was refluxed and stirred for 42 hrs. The solution was then cooled in an ice bath. The precipitates were collected by filtration and washed with ice water three times to afford compound **12** (31.0 g, 86%) as a crystalline white power. ^{1}H NMR (500 MHz, CD_3CN) δ 7.20 – 7.08 (m, 4H), 6.92 – 6.85 (m, 4H), 4.15 (t, *J* = 6.2 Hz, 4H), 3.67 (tt, *J* = 7.7, 3.9 Hz, 4H), 2.73 (t, *J* = 6.9 Hz, 4H), 2.62 (t, *J* = 5.6 Hz, 2H), 2.23 – 2.17 (m, 2H) ppm; ^{13}C NMR (126 MHz, CD_3CN) δ 157.95, 132.22, 130.53, 114.89, 64.99, 63.56, 38.68, 38.64, 29.61 ppm; Hi-Res MS (ESI): *m/z* found [M–H$^+$] for $C_{19}H_{25}O_4^+$ 317.1765 (calcd. 317.1753).

Di-tert-butyl-2,2'-((((propane-1,3-diylbis(oxy))bis(4,1-phenylene))bis(ethane-2,1-diyl))bis(oxy))diacetate (13): This compound was synthesized using a modified reported procedure (S8). To a mixture of compound **12** (4.0 g, 12.64 mmol, 1.0 equiv), tert-butyl 2-bromoacetate (9.86 g, 101.2 mmol, 8.0 equiv) and tetrabutylammonium hydrogen sulfate (3.43 g, 10.11mmol, 0.8 equiv) in 120 mL toluene were added 300 mL 5 M aqueous sodium hydroxide over 10 mins. The reaction mixture was stirred at r.t for 7 hrs. The aqueous layer was then extracted with four portions of EtOAc and dried over Na_2SO_4. The crude product was subjected to silica gel column chromatography using hexanes/EtOAc as eluent to give **13** (4.0 g, 55%) as a yellow oil. ^{1}H NMR (500 MHz, CD_3CN) δ 7.26 – 7.09 (m, 4H), 6.92 – 6.82 (m, 4H), 4.14 (t, *J* = 6.3 Hz, 4H), 3.93 (s, 4H), 3.67 (t, *J* = 6.9 Hz, 4H), 2.81 (t, *J* = 6.9 Hz, 4H), 2.20 – 2.19 (m, 3H), 1.46 (s, 18H) ppm; ^{13}C NMR (126 MHz, CD_3CN) δ 170.19, 158.01, 131.75, 130.44, 114.91, 81.39, 72.54, 68.96, 65.00, 35.40, 29.60, 27.87 ppm; Hi-Res MS (ESI): *m/z* found [M–Na$^+$] for $C_{31}H_{44}O_8Na^+$ 567.2953 (calcd. 567.2934).

2,2'-((((Propane-1,3-diylbis(oxy))bis(4,1-phenylene))bis(ethane-2,1-diyl))bis(oxy))diethanol (14): To an oven-dried flask was charged **13** (4.0 g, 7.35 mmol, 1 equiv) and dry THF (150 mL).

The solution was cooled in an ice bath. To this mixture, LAH (1.26 g, 33.07 mmol, 4.5 equiv) was added portionwise over 10 mins. The reaction was then left at r.t. overnight. The reaction mixture was cooled down in an ice bath and quenched with 1 M aqueous HCl. The mixture was extracted with EtOAc three times. The combined organic extracts were washed with brine, dried over anhydrous $MgSO_4$, and removed under vacuum to afford **14** (2.80 g, 94%) as a white flaky solid. ^{1}H NMR (500 MHz, CD_3CN) δ 7.22 – 7.12 (m, 4H), 6.92 – 6.85 (m, 4H), 4.15 (t, *J* = 6.3 Hz, 4H), 3.63 (t, *J* = 7.0 Hz, 4H), 3.60 – 3.56 (m, 4H), 3.48 (dd, *J* = 6.2, 3.7 Hz, 4H), 2.80 (t, *J* = 7.0 Hz, 4H), 2.63 (t, *J* = 5.8 Hz, 2H), 2.23 – 2.17 (m, 2H) ppm; ^{13}C NMR (126 MHz, CD_3CN) δ 158.15, 132.26, 130.62, 115.07, 72.68, 72.53, 65.18, 61.70, 35.67, 29.78 ppm; Hi-Res MS (ESI): *m/z* found [M–H$^+$] for $C_{23}H_{33}O_6^+$ 405.2282 (calcd. 405.2277).

((((Propane-1,3-diylbis(oxy))bis(4,1-phenylene))bis(ethane-2,1-diyl))bis(oxy))bis(ethane-2,1-diyl) dimethanesulfonate (15): This compound was synthesized using a modified reported procedure (S9). Compound **14** (2.08 g, 5.15 mmol, 1 equiv) and triethylamine (1.72 mL, 12.36 mmol, 2.4 equiv) were dissolved in 50 mL dichloromethane. Methanesulfonyl chloride (2.12 g, 12.36 mmol, 3.6 equiv) was added dropwise to the mixture at 0 °C. The mixture was then stirred overnight and filtered. The filtrate was washed with saturated Na_2CO_3 solution and dried over anhydrous Na_2SO_4. The crude product was subjected to silica gel column chromatography using hexanes/EtOAc as eluent to give **15** (2.85 g, 99%) as a white solid. ^{1}H NMR (500 MHz, $CDCl_3$) δ 7.14 (d, *J* = 8.6 Hz, 4H), 6.90 – 6.81 (m, 4H), 4.38 – 4.30 (m, 4H), 4.14 (t, *J* = 6.1 Hz, 4H), 3.70 (dt, *J* = 10.5, 4.9 Hz, 8H), 2.94 (s, 6H), 2.84 (t, *J* = 6.9 Hz, 4H), 2.25 (p, *J* = 6.1 Hz, 2H) ppm; ^{13}C NMR (126 MHz, $CDCl_3$) δ 157.49, 130.76, 129.86, 114.49, 72.42, 69.42, 68.57, 64.47, 37.48, 35.24, 29.34 ppm; Hi-Res MS (ESI): *m/z* found [M–Na$^+$] for $C_{25}H_{36}O_{10}S_2Na^+$ 583.1647 (calcd. 583.1648).

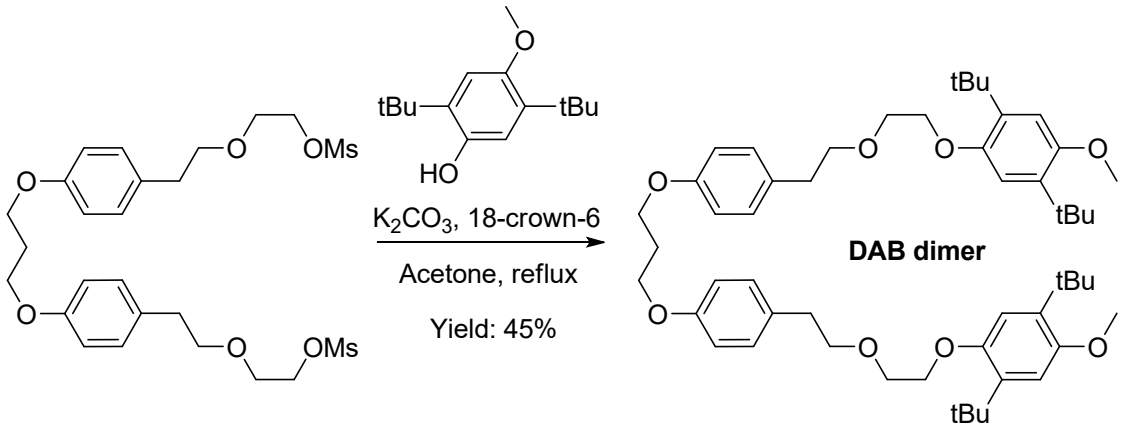

DAB dimer: This compound was synthesized using a modified reported procedure (S10). To a solution of compound **15** (111.0 mg, 0.198 mmol, 1 equiv) in acetone (16 mL) was added 18-crown-6 (5.3 mg, 0.020 mmol, 0.1 equiv), 2,5-di-*tert*-butyl-4-methoxyphenol (107.8 mg, 0.456 mmol, 2.3 equiv), and anhydrous pulverized K_2CO_3 (65.7 mg, 0.476 mmol, 2.4 equiv). The reaction mixture was reflux under N_2 for 44 hrs. After cooling the reaction to r.t., the mixture was filtered and the filtrate was concentrated under vacuum. The crude product was re-dissolved in methylene chloride, washed with saturated Na_2CO_3 and brine, dried over anhydrous Na_2SO_4, and finally subjected to silica gel column chromatography using hexanes/EtOAc as eluent to give **DAB dimer** (75 mg, 45%) as a colorless oil. ^{1}H NMR (500 MHz, $CDCl_3$) δ 7.17 (d, J = 8.6 Hz, 4H), 6.91 – 6.79 (m, 8H), 4.18 – 4.10 (m, 8H), 3.86 (dd, J = 9.1, 4.2 Hz, 4H), 3.84 (s, 6H), 3.75 (t, J = 7.2 Hz, 4H), 2.89 (t, J = 7.2 Hz, 4H), 2.26 (p, J = 6.1 Hz, 2H), 1.41 (s, 18H), 1.38 (s, 18H) ppm; ^{13}C NMR (126 MHz, $CDCl_3$) δ 157.38, 152.07, 151.09, 136.39, 136.31, 131.04, 129.86, 114.45, 112.36, 111.71, 72.64, 69.83, 68.03, 64.50, 55.92, 35.50, 34.68, 34.59, 29.92, 29.82, 29.39 ppm; Hi-Res MS (ESI): *m/z* found [M–Na$^+$] for $C_{53}H_{76}O_8Na^+$ 863.5413 (calcd. 863.5438).

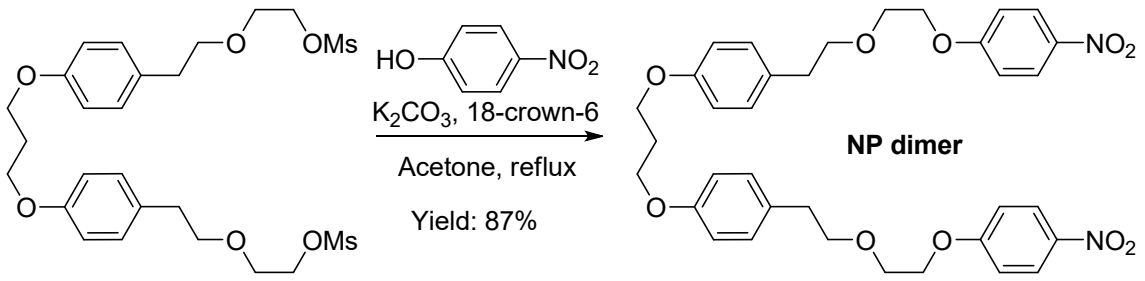

NP dimer: This compound was synthesized following the general procedure for **DAB dimer**, while using compound **15** (400.0 mg, 0.714 mmol, 1.0 equiv), 18-crown-6 (18.6 mg, 0.025 mmol, 0.1 equiv), *p*-nitrophenol (245.2 mg, 1.642 mmol, 2.3 equiv), and anhydrous pulverized K_2CO_3 (236.6 mg, 1.712 mmol, 2.4 equiv) as the starting materials in acetone (45 mL). The crude product was subjected to silica gel column chromatography using hexanes/EtOAc as eluent to give **NP dimer** (400 mg, 87%) as an off-white solid. ^{1}H NMR (500 MHz, $CDCl_3$) δ 8.26 – 8.15 (m, 4H), 7.19 – 7.10 (m, 4H), 7.02 – 6.93 (m, 4H), 6.88 – 6.79 (m, 4H), 4.26 – 4.18 (m, 4H), 4.15 (t, *J* = 6.1 Hz, 4H), 3.85 (dd, *J* = 5.3, 4.1 Hz, 4H), 3.74 (t, *J* = 7.1 Hz, 4H), 2.88 (t, *J* = 7.1 Hz, 4H), 2.26 (p, *J* = 6.1 Hz, 2H). ppm; ^{13}C NMR (126 MHz, $CDCl_3$) δ 163.90, 157.46, 141.62, 130.78, 129.84, 125.87, 114.63, 114.43, 72.80, 68.98, 68.22, 64.45, 35.33, 29.36 ppm; Hi-Res MS (ESI): *m/z* found [M–H$^+$] for $C_{35}H_{38}N_2O_{10}^+$ 647.2613 (calcd. 647.2605).

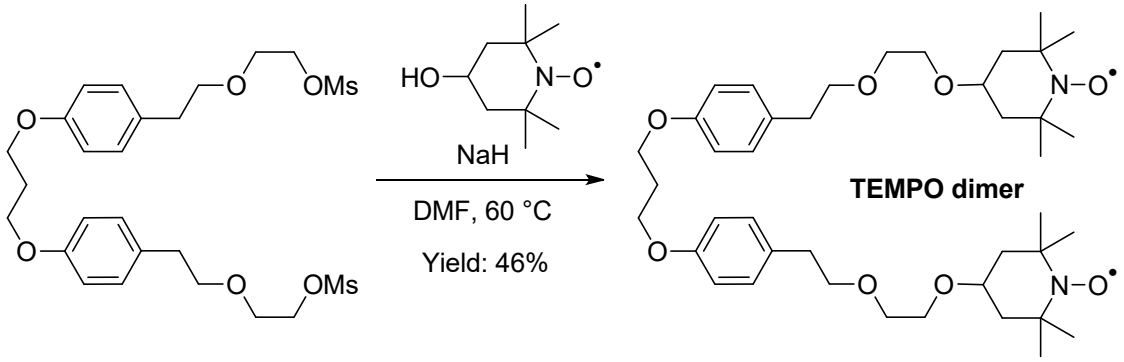

TEMPO dimer: 4-Hydroxyl-TEMPO (307.5 mg, 1.786 mmol, 4.0 equiv) was dissolved in dry DMF (5 mL). To the mixture was dropwise added NaH (43 mg, 1.786 mmol, 4.0 equiv) at 0 °C, and then the reaction mixture was brought to r.t. for 1 h. To the pale orange solution was added compound **15** (250 mg, 0.446 mmol, 1.0 equiv). The mixture was heated to 60 °C overnight. The reaction mixture was concentrated and re-dissolved in ethyl acetate. The organic phase was washed with water twice and brine, and dried over Na_2SO_4. The crude product was subjected to silica gel column chromatography using hexanes/EtOAc as eluent to give **TEMPO dimer** (146 mg, 46%) as a bright red viscous oil. The product was reduced with phenylhydrazine for NMR characterization. ^{1}H NMR (500 MHz, $CDCl_3$) δ 7.28 – 7.24 (m, 4H), 7.14 (dd, *J* = 12.9, 6.2 Hz,

4H), 4.19 – 4.11 (m, 4H), 3.75 – 3.62 (m, 6H), 3.62 – 3.55 (m, 8H), 2.90 – 2.79 (m, 4H), 2.26 (p, *J* = 6.1 Hz, 2H), 2.16 – 2.03 (m, 4H), 2.03 – 1.90 (m, 4H), 1.64 – 1.45 (m, 12H), 1.45 – 1.29 (m, 12H) ppm; ^{13}C NMR (126 MHz, $CDCl_3$) δ 157.33, 151.17, 129.83, 129.24, 128.35, 128.23, 119.53, 114.46, 114.42, 113.27, 112.20, 72.39, 70.50, 67.93, 64.55, 62.69, 60.63, 53.43, 45.47, 44.21, 35.34, 33.45, 29.38 ppm; Hi-Res MS (ESI): *m/z* found [M–H$^+$] for $C_{41}H_{65}N_2O_8^+$ 713.4741 (calcd. 713.4741).

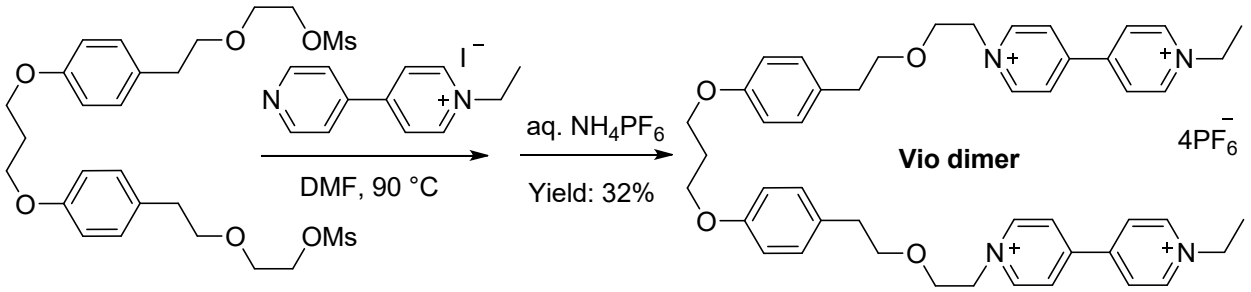

Vio dimer: To the solution of compound **15** (140 mg, 0.25 mmol, 1 equiv) in DMF (5 mL) was added ethyl viologen (172 mg, 0.55 mmol, 2.2 equiv). The mixture was stirred at 90 °C under N_2 atmosphere overnight. After cooling, the solvent was removed under vacuum, and the residue was subjected to silica gel column chromatography using MeOH / aq. NH_4Cl (2M) / $MeNO_2$ (7:2:1) as eluent, followed by counterion exchange (NH_4PF_6/H_2O) to give **Vio dimer** (106 mg, 32%) as an off-white solid. ^{1}H NMR (500 MHz, CD_3CN) δ 8.95 (d, *J* = 6.8 Hz, 4H), 8.82 (d, *J* = 7.0 Hz, 4H), 8.41 (d, *J* = 6.3 Hz, 4H), 8.32 (d, *J* = 6.8 Hz, 4H), 7.10 (d, *J* = 8.6 Hz, 4H), 6.83 (d, *J* = 8.6 Hz, 4H), 4.78 – 4.73 (m, 4H), 4.70 (q, *J* = 7.4 Hz, 4H), 4.09 (t, *J* = 6.3 Hz, 4H), 3.96 – 3.90 (m, 4H), 3.66 (t, *J* = 6.8 Hz, 4H), 2.76 (t, *J* = 6.7 Hz, 4H), 2.15 – 2.12 (m, 2H), 1.68 (t, *J* = 7.3 Hz, 6H) ppm; ^{13}C NMR (126 MHz, CD_3CN) δ 157.94, 150.58, 150.38, 146.62, 145.94, 131.67, 130.48, 127.77, 127.18, 115.00, 72.31, 68.56, 65.10, 62.27, 58.31, 35.03, 29.58, 16.20 ppm; Hi-Res MS (ESI): *m/z* found [M-4PF_6]$^{2+}$ for $C_{47}H_{56}N_4O_4^{2+}$ 370.2132 (calcd. 370.2151).

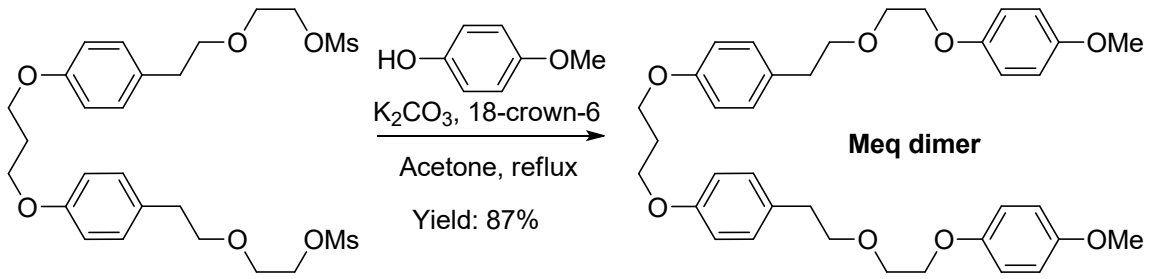

Meq dimer: This compound was synthesized following the general procedure for **DAB dimer**, while using compound **15** (112.0 mg, 0.2 mmol, 1.0 equiv), 18-crown-6 (5.3 mg, 0.02 mmol, 0.1 equiv), mequinol (57.1 mg, 0.46 mmol, 2.3 equiv), and anhydrous pulverized K_2CO_3 (66.3 mg, 0.48 mmol, 2.4 equiv) as the starting materials in acetone (10 mL). The crude product was subjected to silica gel column chromatography using hexanes/EtOAc as eluent to give **Meq dimer** (106 mg, 87%) as a white solid. ^{1}H NMR (500 MHz, $CDCl_3$) δ 7.16 (d, J = 8.5 Hz, 4H), 6.92 – 6.78 (m, 12H), 4.15 (t, J = 6.1 Hz, 4H), 4.11 – 4.05 (m, 4H), 3.83 – 3.77 (m, 10H), 3.73 (t, J = 7.3 Hz, 4H), 2.89 (t, J = 7.3 Hz, 4H), 2.26 (p, J = 6.1 Hz, 2H) ppm; ^{13}C NMR (126 MHz, $CDCl_3$) δ 157.39, 153.95, 153.00, 130.96, 129.87, 115.72, 114.59, 114.44, 72.74, 69.48, 68.16, 64.49, 55.73, 35.38, 29.39 ppm; Hi-Res MS (ESI): *m/z* found [M–H$^+$] for $C_{37}H_{45}O_8^+$ 617.3119 (calcd. 617.3114).

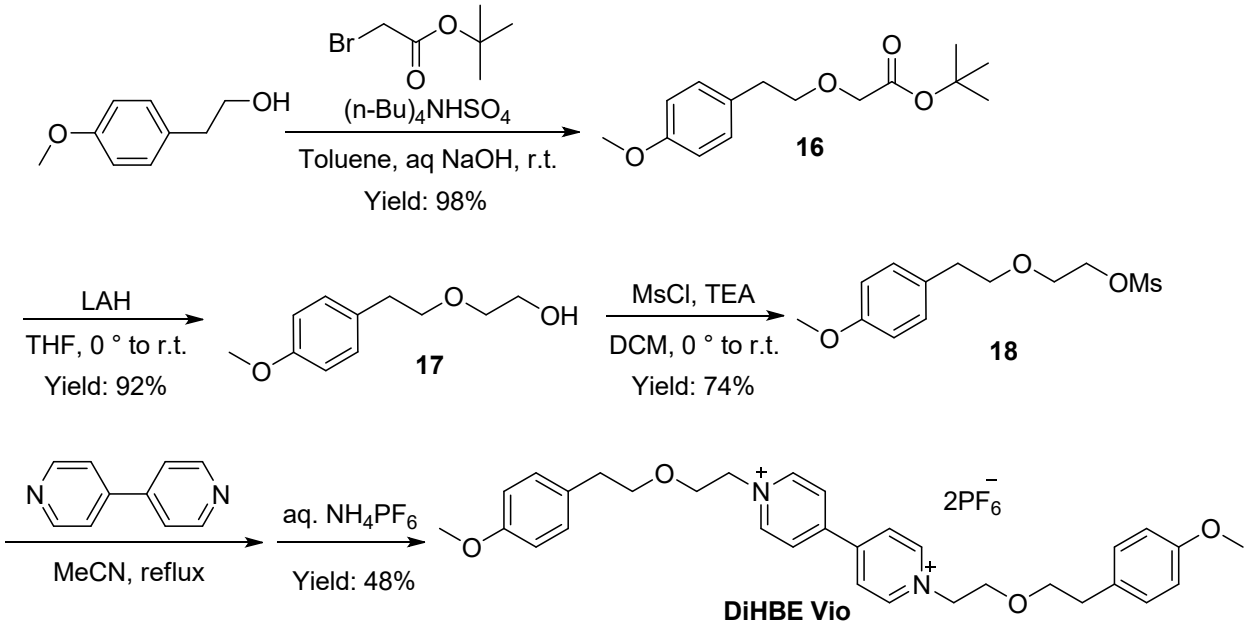

***tert*-Butyl 2-(4-methoxyphenethoxy)acetate (16)**: This compound was synthesized following

the general procedure for compound **13**, while using 2-(4-methoxyphenyl)ethanol (3.00 g, 19.71 mmol, 1.0 equiv), tert-butyl 2-bromoacetate (30.75 g, 157.68 mmol, 8.0 equiv) and tetrabutylammonium hydrogen sulfate (5.35 g, 15.77 mmol, 0.8 equiv) as the starting materials in toluene (200 mL) and 5 M aq. NaOH (150 mL). The crude product was subjected to silica gel column chromatography using hexanes/EtOAc as eluent to give **16** (4.5 g, 98 %) as a colorless oil. ^{1}H NMR (500 MHz, $CDCl_3$) δ 7.22 – 7.13 (m, 2H), 6.90 – 6.81 (m, 2H), 3.98 (s, 2H), 3.81 (s, 3H), 3.72 (t, *J* = 7.3 Hz, 2H), 2.91 (t, *J* = 7.3 Hz, 2H), 1.50 (s, 9H) ppm; ^{13}C NMR (126 MHz, $CDCl_3$) δ 169.71, 169.05, 158.13, 130.59, 129.87, 113.84, 81.86, 81.55, 72.75, 68.93, 68.51, 55.26, 35.34, 28.12 ppm; Hi-Res MS (ESI): *m/z* found [M–Na^+] for $C_{15}H_{22}O_4Na^+$ 289.1434 (calcd. 289.1420).

2-(4-Methoxyphenethoxy)ethanol (17): This compound was synthesized following the general procedure for compound **14**, while using compound **16** (2.1 g, 8.33 mmol, 1.0 equiv) and LAH (0.71 g, 18.74 mmol, 2.25 equiv) as the starting materials in dry THF (80 mL). The organic extracts were removed under vacuum to afford **17** (1.5 g, 92%) as a yellow oil. ^{1}H NMR (500 MHz, $CDCl_3$) δ 7.18 – 7.15 (m, 2H), 6.88 – 6.85 (m, 2H), 3.81 (s, 3H), 3.73 (dd, *J* = 5.7, 3.5 Hz, 2H), 3.69 (t, *J* = 7.1 Hz, 2H), 3.60 – 3.56 (m, 2H), 2.87 (t, *J* = 7.1 Hz, 2H) ppm; ^{13}C NMR (126 MHz, $CDCl_3$) δ 158.14, 130.84, 129.79, 113.86, 72.30, 71.80, 61.80, 55.27, 35.36 ppm; Hi-Res MS (ESI): *m/z* found [M–Na^+] for $C_{11}H_{16}O_3Na^+$ 219.1001 (calcd. 219.0997).

2-(4-Methoxyphenethoxy)ethyl methanesulfonate (18): This compound was synthesized following the general procedure for compound **15**, while using compound **17** (0.784 g, 4.0 mmol, 1.0 equiv), triethylamine (0.67 mL, 4.8 mmol, 1.2 equiv), and methanesulfonyl chloride (0.825 g, 7.2 mmol, 1.8 equiv) as the starting materials in dry dichloromethane (20 mL). The crude product was subjected to silica gel column chromatography using hexanes/EtOAc as eluent to give **18** (0.81 g, 74%) as a colorless oil. ^{1}H NMR (500 MHz, $CDCl_3$) δ 7.19 – 7.09 (m, 2H), 6.91 – 6.81 (m, 2H), 4.42 – 4.31 (m, 2H), 3.81 (s, 3H), 3.74 – 3.67 (m, 4H), 2.96 (s, 3H), 2.88 – 2.82

(m, 2H) ppm; ^{13}C NMR (126 MHz, $CDCl_3$) δ 158.20, 130.59, 129.81, 113.86, 72.49, 69.25, 68.61, 55.28, 37.55, 35.25 ppm; Hi-Res MS (ESI): *m/z* found [M–Na^+] for $C_{13}H_{14}N_4ONaS^+$ 297.0785 (calcd. 297.0786).

DiHBE Vio: To the solution of compound **18** (109.6 mg, 0.40 mmol, 3.0 equiv) in CH_3CN (5 mL) was added 4,4'-bipyridine (20.3 mg, 0.13 mmol, 1.0 equiv). The mixture was stirred at reflux under N_2 atmosphere for 2 days. After cooling, the solvent was removed under vacuum, and the residue was subjected to silica gel column chromatography using MeOH / aq. NH_4Cl (1.4 M) / $MeNO_2$ (210:50:5) as eluent, followed by counterion exchange (NH_4PF_6/H_2O) to give **DiHBE Vio** (50 mg, 48%) as an off-white solid. ^{1}H NMR (500 MHz, CD_3CN) δ 8.79 (d, *J* = 6.9 Hz, 4H), 8.24 (d, *J* = 6.7 Hz, 4H), 7.08 (d, *J* = 8.6 Hz, 4H), 6.81 – 6.74 (m, 4H), 4.76 (t, 4H), 3.93 (t, 4H), 3.73 – 3.65 (m, 10H), 2.77 (t, *J* = 6.4 Hz, 4H) ppm; ^{13}C NMR (126 MHz, CD_3CN) δ 158.74, 150.39, 146.73, 131.82, 130.52, 127.18, 114.40, 72.23, 68.62, 62.44, 55.55, 35.12 ppm; Hi-Res MS (ESI): *m/z* found [M-2PF_6]$^+$ for $C_{32}H_{38}N_2O_4^+$ 514.2844 (calcd. 514.2832).

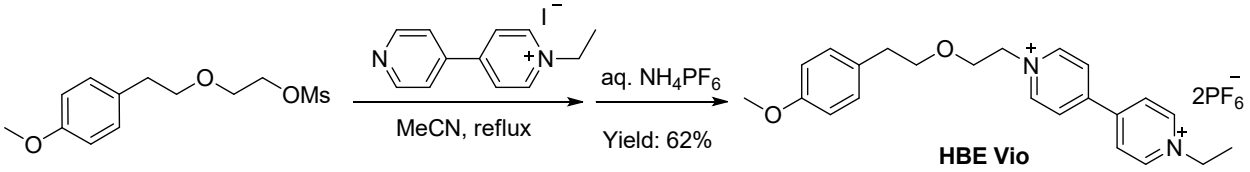

HBE Vio: To the solution of compound **18** (275 mg, 1.0 mmol, 2 equiv) in MeCN (15 mL) was added ethyl viologen (156 mg, 0.5 mmol, 1 equiv). The mixture was reflux under N_2 atmosphere for 3 days. After cooling, the solvent was removed under vacuum. The residue was re-dissolved in water, followed by counterion exchange (NH_4PF_6/H_2O). The precipitates were collected by filtration to afford **HBE Vio** (203 mg, 62%) as an off-white solid. ^{1}H NMR (500 MHz, CD_3CN) δ 8.97 (d, *J* = 6.7 Hz, 2H), 8.76 (d, *J* = 6.9 Hz, 2H), 8.39 (d, *J* = 6.3 Hz, 2H), 8.25 (d, *J* = 6.7 Hz, 2H), 7.11 – 7.01 (m, 2H), 6.81 – 6.75 (m, 2H), 4.79 – 4.68 (m, 4H), 3.97 – 3.85 (m, 2H), 3.72 – 3.66 (m, 5H), 2.76 (t, *J* = 6.4 Hz, 2H), 1.70 (t, *J* = 7.3 Hz, 3H) ppm; ^{13}C NMR (126 MHz, CD_3CN) δ 158.40, 150.24, 146.38, 145.80, 131.51, 130.18, 127.57, 126.86, 114.07, 71.85, 68.26,

62.07, 58.17, 55.25, 34.78, 16.06 ppm; Hi-Res MS (ESI): *m/z* found $[M\text{-}2PF_6]^+$ for $C_{23}H_{28}N_2O_2^+$ 364.2113 (calcd. 364.2132).

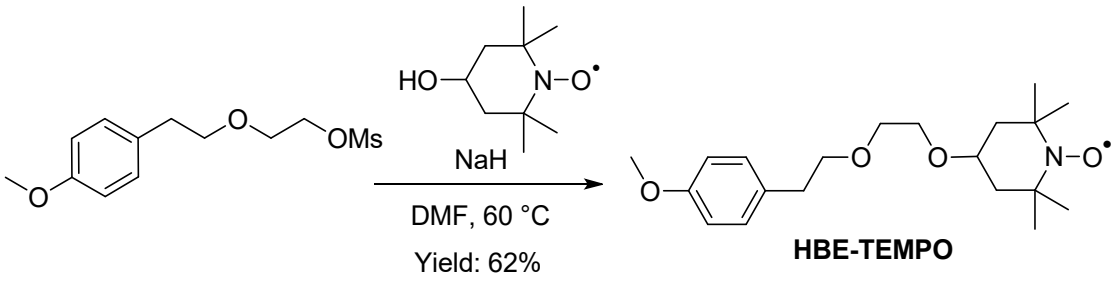

HBE-TEMPO: This compound was synthesized following the general procedure for **TEMPO dimer**, while using compound **18** (274 mg, 1.0 mmol, 1.0 equiv), TEMPO (206 mg, 1.2 mmol, 1.2 equiv), and NaH (36 mg, 1.5 mmol, 1.5 equiv) as the starting materials in dry DMF (5 mL). The crude product was subjected to silica gel column chromatography using hexanes/EtOAc as eluent to give **HEB-TEMPO** (217 mg, 62%) as a bright reddish oil. The product was reduced with phenylhydrazine for NMR characterization. ^{1}H NMR (499 MHz, $CDCl_3$) δ 7.29 – 7.24 (m, 2H), 7.19 – 7.12 (m, 2H), 3.85 – 3.80 (m, 3H), 3.79 – 3.72 (m, 1H), 3.67 (ddd, *J* = 11.5, 7.6, 3.0 Hz, 2H), 3.64 – 3.55 (m, 4H), 2.90 – 2.81 (m, 2H), 2.17 (d, *J* = 37.6 Hz, 2H), 1.98 (s, 2H), 1.54 (s, 6H), 1.40 (s, 6H) ppm; ^{13}C NMR (126 MHz, $CDCl_3$) δ 130.84, 129.80, 129.76, 129.64, 129.38, 128.69, 128.35, 128.24, 120.98, 115.62, 115.34, 113.82, 113.79, 113.29, 72.62, 72.53, 71.76, 70.56, 70.28, 68.65, 68.57, 68.04, 67.76, 67.43, 60.68, 55.27, 44.20, 42.02, 38.97, 35.40, 35.32, 31.97, 28.80, 28.52, 26.91, 21.80, 21.72, 21.21 ppm; Hi-Res MS (ESI): *m/z* found $[M^+]$ for $C_{20}H_{32}NO_4^+$ 350.2338 (calcd. 350.2331).

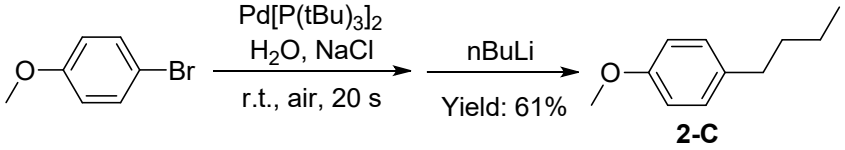

1-Butyl-4-methoxybenzene (2-C): This compound was synthesized using a modified reported procedure (S11). In a 20 mL test tube, NaCl (11.0 mg, 0.2 mmol, 1.0 equiv), 1-bromo-4-methoxybenzene (37.4 mg, 0.2 mmol, 1.0 equiv), and $Pd[P(tBu)_3]_2$ (2.5 mg, 0.005 mmol, 0.025

equiv) were sequentially added to 1.0 mL of deionized water at r.t. and under air. The mixture was vigorously stirred for 10 min. During this time, the color of the mixture changed from slightly yellow to dark orange. 1.6 M n-butyllithium (0.138 mL, 0.22 mmol, 1.1 equiv) was rapidly spread over the mixture under air and with vigorous stirring at room temperature to generate an emulsion. After 20 s, the reaction mixture was directly extracted with Et_2O. The organic layer was filtered through a Celite pad and the solvent was removed under reduced pressure. The crude was purified by silica gel column chromatography using hexanes/EtOAc as eluent to afford **2-C** (20 mg, 61%) as a colorless oil. The identity of **2-C** was by comparing the obtained ^{1}H NMR with the published one (S11). ^{1}H NMR (500 MHz, $CDCl_3$) δ 7.17 – 7.07 (m, 2H), 6.88 – 6.80 (m, 2H), 3.81 (s, 3H), 2.61 – 2.52 (m, 2H), 1.59 (ddd, *J* = 9.3, 8.0, 4.6 Hz, 2H), 1.41 – 1.32 (m, 2H), 0.94 (t, *J* = 7.4 Hz, 3H) ppm.

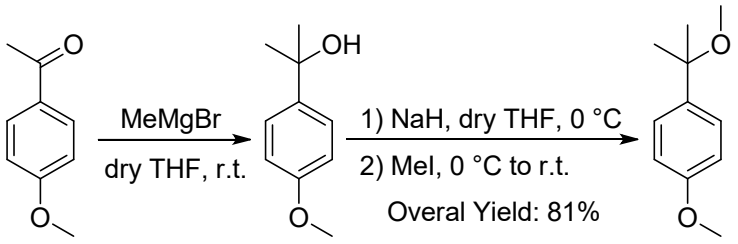

19

1-Methoxy-4-(2-methoxypropan-2-yl)benzene (19): To a stirred solution of a 1-(4-methoxyphenyl)ethanone (1.00 g, 6.66 mmol, 1.0 equiv) in dry THF (12 mL) at 0 °C was dropwise added MeMgBr (2.38 g, 19.98 mmol, 3.0 equiv). The mixture was stirred at r.t. for 12 hrs. The reaction mixture was quenched with the addition of saturated NH_4Cl and extracted with ethyl acetate (EtOAc) three times. The combined organic extracts were washed with brine and dried over Na_2SO_4. The crude product was immediately used for methylation without further purification. To a stirred solution of the above alcohol (0.33 g, 2.0 mmol, 1.0 equiv) in dry THF (2 mL) at 0 °C was slowly added NaH (0.096 g, 4.0 mmol, 2.0 equiv). The reaction mixture was further stirred at 0 °C for 1 h before slow addition of iodomethane (0.43 g, 3.0 mmol, 1.5 equiv). The mixture was then stirred at r.t. overnight. The mixture was quenched with the addition of saturated NH_4Cl and extracted with ethyl acetate (EtOAc) three times. The combined organic

extracts were washed with brine and dried over $MgSO_4$. The crude was purified by silica gel column chromatography using hexanes/EtOAc as eluent to afford **19** (0.29 g, 81%) as a colorless oil. ^{1}H NMR (500 MHz, CD_3CN) δ 7.40 – 7.30 (m, 2H), 6.97 – 6.86 (m, 2H), 3.80 (s, 3H), 3.00 (s, 3H), 1.48 (s, 6H) ppm; ^{13}C NMR (126 MHz, CD_3CN) δ 159.25, 138.92, 127.77, 114.05, 76.70, 55.57, 50.28, 28.01 ppm; Hi-Res MS (ESI): *m/z* found [M^+] for $C_{11}H_{16}O_2Na^+$ 203.1008 (calcd. 203.1004).

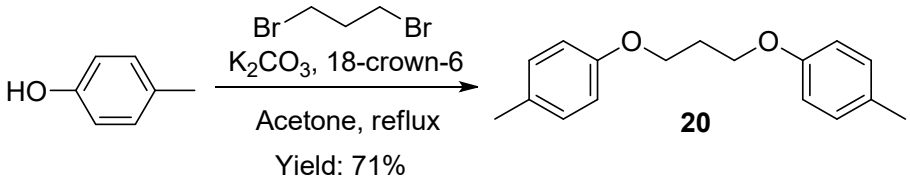

1,3-Bis(p-tolyloxy)propane (20): This compound was synthesized following a modified procedure for compound **12**, while using 1,3-dibromopropane (1.01 g, 5.0 mmol, 1 equiv), 18-crown-6 (35.0 mg, 0.13 mmol, 0.027 equiv), *p*-cresol (1.44g, 13.3 mmol, 2.7 equiv), and anhydrous pulverized K_2CO_3 (1.84 g, 13.0 mmol, 2.6 equiv) as the starting materials in acetone (30 mL). After cooling the reaction to r.t., the mixture was concentrated under vacuum. The crude product was re-dissolved in methylene chloride, washed with saturated Na_2CO_3 and brine, dried over anhydrous Na_2SO_4, and finally subjected to silica gel column chromatography using hexanes/EtOAc as eluent to afford **20** (0.912 g, 71%) as an off-white solid. ^{1}H NMR (500 MHz, $CDCl_3$) δ 7.09 (t, *J* = 7.5 Hz, 4H), 6.88 – 6.78 (m, 4H), 4.15 (t, *J* = 6.2 Hz, 4H), 2.31 (s, 6H), 2.26 (p, *J* = 6.2 Hz, 2H) ppm; ^{13}C NMR (126 MHz, $CDCl_3$) δ 156.77, 129.92, 129.89, 114.39, 64.60, 29.43, 20.47 ppm; Hi-Res MS (ESI): *m/z* found [M–Na^+] for $C_{17}H_{20}O_2Na^+$ 279.1359 (calcd. 279.1361).

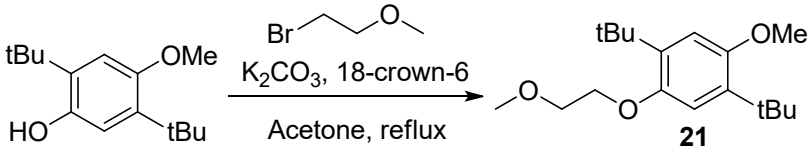

1,4-Di-tert-butyl-2-methoxy-5-(2-methoxyethoxy)benzene (21): This compound was

synthesized using a reported procedure (S12). The crude product was subjected to silica gel column chromatography using hexanes/EtOAc as eluent to give **21** as a white crystalline solid. The identity of **21** was confirmed by comparing the obtained ^{1}H NMR with the published one (S12). ^{1}H NMR (500 MHz, $CDCl_3$) δ 6.86 (d, *J* = 6.8 Hz, 2H), 4.18 – 4.09 (m, 2H), 3.83 (s, 3H), 3.82 – 3.79 (m, 2H), 3.48 (s, 3H), 1.41 (s, 9H), 1.37 (s, 9H) ppm.

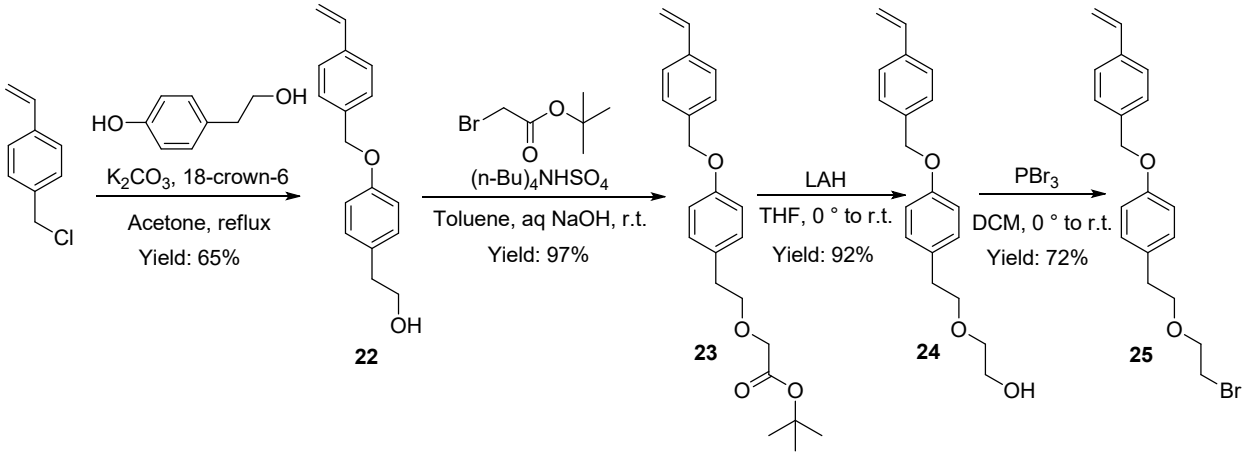

2-(4-((4-Vinylbenzyl)oxy)phenyl)ethanol (22): This compound was synthesized following a modified procedure for compound **12**, while using 4-vinylbenzyl chloride (15.2 g, 100 mmol, 1.00 equiv), 18-crown-6 (264 mg, 1 mmol, 0.01 equiv), 4-(2-hydroxyethyl)phenol (15.2 g, 110 mmol, 1.10 equiv), and anhydrous pulverized K_2CO_3 (25.0 g, 181 mmol, 1.81 equiv)) as the starting materials in acetone (150 mL). After refluxing for 17hrs, the reaction was cooled to r.t. The mixture was filtered and the filtrate was concentrated under vacuum. The crude product was recrystallized in acetone/water. The precipitates were collected by filtration and subsequently washed with ice water and cold ether to afford compound **22** (16.5 g, 65%) as a crystalline white power. ^{1}H NMR (500 MHz, $CDCl_3$) δ 7.47 – 7.43 (m, 2H), 7.41 (d, *J* = 8.2 Hz, 2H), 7.19 – 7.14 (m, 2H), 6.97 – 6.93 (m, 2H), 6.75 (dd, *J* = 17.6, 10.9 Hz, 1H), 5.78 (d, *J* = 17.6 Hz, 1H), 5.31 – 5.26 (m, 1H), 5.06 (s, 2H), 3.85 (q, *J* = 6.4 Hz, 2H), 2.84 (t, *J* = 6.5 Hz, 2H), 1.43 (t, *J* = 6.0 Hz, 1H) ppm; ^{13}C NMR (126 MHz, $CDCl_3$) δ 157.48, 137.32, 136.64, 136.45, 130.73, 130.02, 127.66, 126.43, 115.04, 114.09, 69.82, 63.82, 38.29, 30.95 ppm; Hi-Res MS (ESI): *m/z* found [M–Na^+] for $C_{17}H_{18}O_2Na^+$ 277.1204 (calcd. 277.1204).

tert-Butyl 2-(4-((4-vinylbenzyl)oxy)phenethoxy)acetate (23): This compound was synthesized following the general procedure for compound **13**, while using compound **22** (5.08 g, 20.0 mmol, 1.0 equiv), *tert*-butyl 2-bromoacetate (16.5 g, 80.0 mmol, 4.0 equiv) and tetrabutylammonium hydrogen sulfate (4.5 g, 14.0 mmol, 0.7 equiv) as the starting materials in toluene (150 mL) and 5 M aq. NaOH (100 mL). The crude product was subjected to silica gel column chromatography using hexanes/EtOAc as eluent to give **23** (7.27 g, 97 %) as a colorless oil. ^{1}H NMR (500 MHz, $CDCl_3$) δ 7.47 – 7.43 (m, 2H), 7.40 (d, *J* = 8.2 Hz, 2H), 7.20 – 7.15 (m, 2H), 6.94 – 6.90 (m, 2H), 6.74 (dd, *J* = 17.6, 10.9 Hz, 1H), 5.78 (d, *J* = 17.6 Hz, 1H), 5.28 (d, *J* = 10.9 Hz, 1H), 5.05 (s, 2H), 3.98 (s, 2H), 3.72 (t, *J* = 7.3 Hz, 2H), 2.91 (t, *J* = 7.3 Hz, 2H), 1.50 (s, 9H) ppm; ^{13}C NMR (126 MHz, $CDCl_3$) δ 169.71, 169.05, 157.32, 137.28, 136.72, 136.47, 130.92, 129.90, 127.66, 126.41, 114.83, 114.05, 81.85, 81.55, 72.71, 69.79, 68.93, 68.51, 35.36, 28.13 ppm; Hi-Res MS (ESI): *m/z* found [M–Na^+] for $C_{23}H_{28}O_4Na^+$ 391.1895 (calcd. 391.1885).

2-(4-((4-Vinylbenzyl)oxy)phenethoxy)ethanol (24): This compound was synthesized following the general procedure for compound **14**, while using compound **23** (5.0 g, 13.58 mmol, 1.0 equiv) and LAH (1.16 g, 30.6 mmol, 2.25 equiv) as the starting materials in dry THF (150 mL). The organic extracts were removed under vacuum to afford **24** (3.74 g, 92%) as a white solid. ^{1}H NMR (500 MHz, $CDCl_3$) δ 7.47 – 7.43 (m, 2H), 7.41 (d, *J* = 8.2 Hz, 2H), 7.19 – 7.13 (m, 2H), 6.96 – 6.90 (m, 2H), 6.75 (dd, *J* = 17.6, 10.8 Hz, 1H), 5.78 (d, *J* = 17.6 Hz, 1H), 5.28 (d, *J* = 10.9 Hz, 1H), 5.06 (s, 2H), 3.76 – 3.71 (m, 2H), 3.71 – 3.66 (m, 2H), 3.60 – 3.56 (m, 2H), 2.86 (q, *J* = 6.9 Hz, 2H), 1.93 (t, *J* = 6.1 Hz, 1H) ppm; ^{13}C NMR (126 MHz, CDCl3) δ 157.33, 137.30, 136.69, 136.46, 131.17, 129.82, 127.68, 126.42, 114.85, 114.07, 72.27, 71.80, 69.81, 61.81, 35.38 ppm; Hi-Res MS (ESI): *m/z* found [M–Na^+] for $C_{19}H_{22}O_3Na^+$ 321.1461 (calcd. 321.1467).

1-(2-(2-Bromoethoxy)ethyl)-4-((4-vinylbenzyl)oxy)benzene (25): This compound was synthesized using a modified reported procedure (S13). A solution of tetrabromomethane (1.82 g,

5.55 mmol, 1.1 equiv) in dichloromethane (4.5 mL) was added dropwise to a solution of compound **24** (1.5 g, 5.03 mmol, 1.0 equiv) and PPh_3 (1.45 g, 5.53 mmol, 1.1 equiv) in dichloromethane (10 mL) at 0 °C. The reaction mixture was stirred at r.t. for 24 hrs and the solvent was removed under vacuum. The crude product was purified by flash silica gel column chromatography using hexanes/EtOAc as eluent to afford **25** (1.3 g, 72%) as a white solid. ^{1}H NMR (500 MHz, $CDCl_3$) δ 7.44 (dd, *J* = 9.8, 5.7 Hz, 2H), 7.40 (d, *J* = 8.2 Hz, 2H), 7.19 – 7.13 (m, 2H), 6.95 – 6.90 (m, 2H), 6.75 (dd, *J* = 17.6, 10.9 Hz, 1H), 5.78 (d, *J* = 17.6 Hz, 1H), 5.28 (d, *J* = 10.9 Hz, 1H), 5.06 (s, 2H), 3.78 (t, *J* = 6.3 Hz, 2H), 3.70 (t, *J* = 7.2 Hz, 2H), 3.47 (t, *J* = 6.3 Hz, 2H), 2.87 (t, *J* = 7.1 Hz, 2H) ppm; ^{13}C NMR (126 MHz, $CDCl_3$) δ 157.33, 137.29, 136.70, 136.46, 131.01, 129.89, 127.66, 126.41, 114.82, 114.06, 72.36, 70.79, 69.80, 35.36, 30.37 ppm; Hi-Res MS (ESI): *m/z* found [M–Na$^+$] for $C_{19}H_{21}O_2BrNa^+$ 383.0617 (calcd. 383.0623).

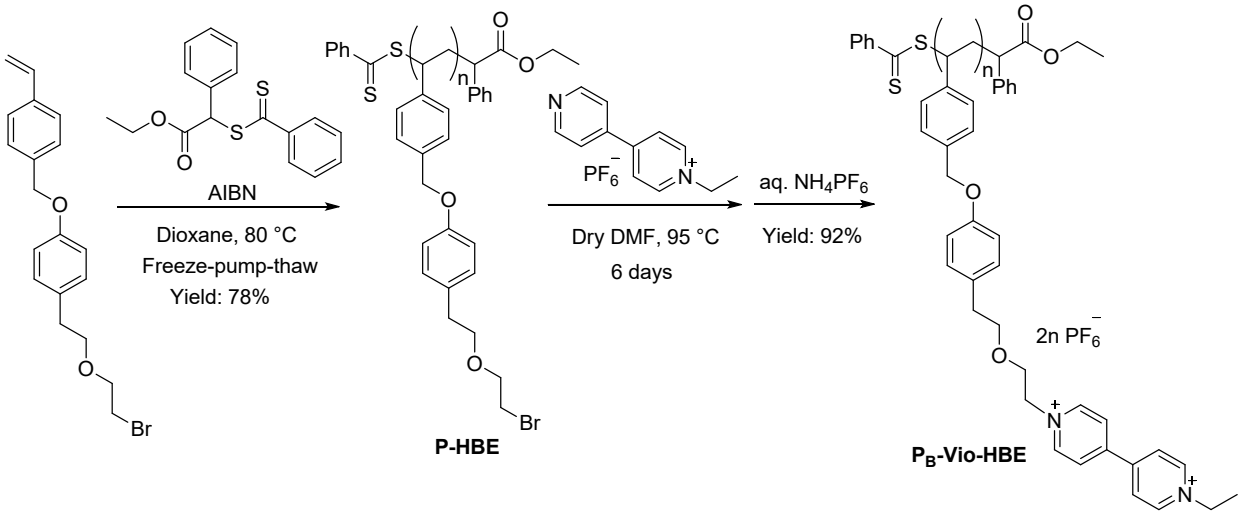

P-HBE: In a 10 mL Schlenk tube, **25** (360 mg, 1.0 mmol, 50 equiv), AIBN (0.328 mg, 0.002 mmol, 0.2 equiv), ethyl 2-(phenylcarbonothioylthio)-2-phenylacetate (6.32 mg, 0.02 mmol, 1 equiv) were dissolved in dioxane (0.5 mL). The mixture was degassed by freeze-pump-thaw (× 4) and stirred at 80 °C for 42 hrs. The reaction mixture was cooled to r.t. and transferred to Et_2O. The precipitate was collected by centrifuge to afford a slightly pink solid **P-HBE** (285 mg, 78%). ^{1}H NMR (500 MHz, $CDCl_3$) δ 7.22–6.95 (4H), 6.94–6.75 (2H), 6.76–6.21 (2H), 5.05–4.72 (2H), 3.84–3.57 (4H), 3.48–3.39 (2H), 2.92–2.74 (s, 2H), 2.08–1.66 (1H), 1.56–1.14 (2H) ppm. The

repeating unit was estimated to be n ≈ 31 using Mn from GPC results.

P_B-Vio-HBE: This polymer was synthesized using a modified reported procedure (S14). Dry DMF (2 mL) was added to a vial containing **P-HBE** (150 mg, 0.42 mmol repeating units) and ethyl viologen (693 mg, 2.1 mmol, 5.0 equiv) under nitrogen. Reaction mixture was stirred at 95 °C for 6 days. Concentrated aqueous solution of NH_4PF_6 (5 g) was added to the above reaction mixture. The brownish solid crashed out and was collected by filtration. The crude solid was redissolved in minimal MeCN and precipitated in NH_4PF_6 aqueous solution to afford a brownish solid **P_B-Vio-HBE** (293 mg, 92%). ^{1}H NMR (500 MHz, CD_3CN) δ 9.10–8.52 (4H), 8.53–8.03 (4H), 7.32–6.90 (4H), 6.89–6.30 (4H), 5.10–4.41 (6H), 4.00–3.73 (2H), 3.71–3.48 (2H), 2.81–2.55 (2H), 1.88–1.22 (5H) ppm.

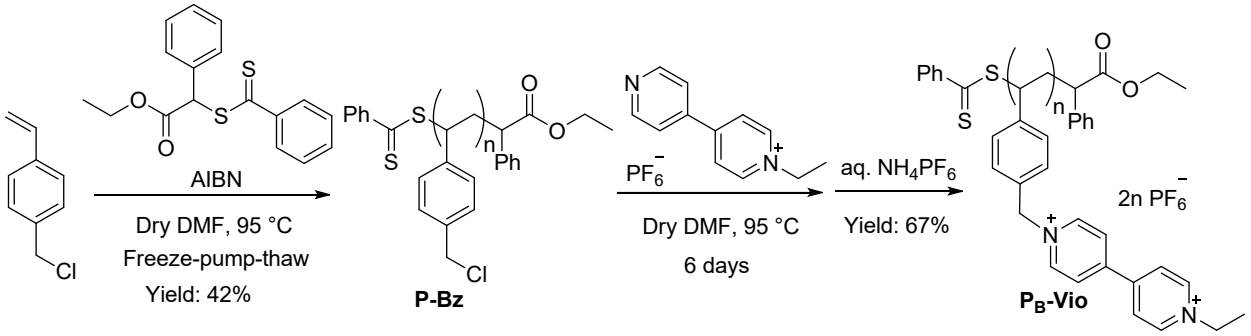

P-Bz: In a 10 mL Schlenk tube, 4-vinylbenzyl chloride (3.82 g, 25 mmol, 50 equiv), AIBN (8.21 mg, 0.05 mmol, 0.1 equiv), and ethyl 2-(phenylcarbonothioylthio)-2-phenylacetate (158 mg, 0.5 mmol, 1.0 equiv) were dissolved in dry DMF (2.5 mL). The mixture was degassed by freeze-pump-thaw (× 4) and stirred at 95 °C for 23 hrs. The reaction mixture was cooled to r.t. and then transferred to MeOH. The precipitate was collected by filtration. The crude solid was redissolved in minimal DCM and precipitated in MeOH to afford a slightly pink solid **P-Bz** (1.62 g, 42%). ^{1}H NMR (500 MHz, $CDCl_3$) δ 7.27–6.87 (2H), 6.85–6.18 (2H), 4.76–4.34 (2H), 2.60–1.59 (2H), 1.52–1.22 (1H) ppm. The repeating unit was estimated to be n ≈ 27 using Mn from GPC results.

P_B-Vio: This polymer was synthesized following the general procedure for **P_B-Vio-HBE**, while using **P-Bz** (150 mg, 0.99 mmol repeating units) and ethyl viologen (1.63 g, 4.95 mmol, 5.0 equiv) as the starting materials in dry DMF (4.5 mL). Reaction mixture was stirred at 95 °C for 6 days. Concentrated aqueous solution of NH_4PF_6 (5 g) was added to the above reaction mixture. The brownish solid crashed out and was collected by filtration. The crude solid was redissolved in minimal MeCN and precipitated in NH_4PF_6 aqueous solution to afford a brownish solid **P_B-Vio** (392 mg, 67%). ^{1}H NMR (500 MHz, Acetone) δ 9.52–9.06 (4H), 8.90–8.55 (4H), 7.12–6.44 (4H), 6.18–5.77 (2H), 5.10–4.87 (s, 2H), 1.95–1.51 (6H) ppm.

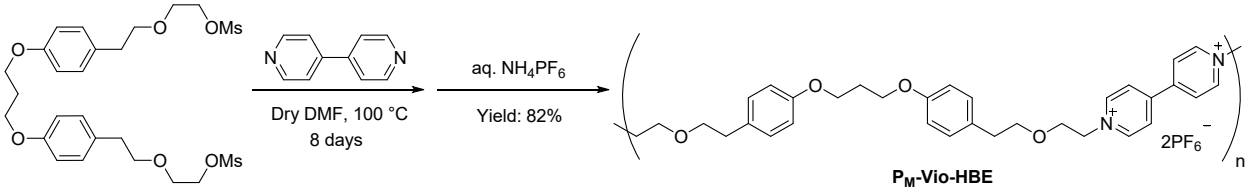

P_M-Vio-HBE: This polymer was synthesized using a modified reported procedure.[S15] Dry DMF (1.4 mL) was added to a vial containing compound **15** (560 mg, 1.0 mmol) and 4,4'-bipyridine (159 mg, 1.02 mmol, 1.02 equiv) under nitrogen. Reaction mixture was stirred at 100 °C for 8 days. The reaction mixture was cooled to r.t. and then transferred to a concentrated aqueous solution of NH_4PF_6. The brownish solid crashed out and was collected by filtration. The crude solid was redissolved in minimal MeCN and precipitated in NH_4PF_6 aqueous solution to afford a brownish solid **P_M-Vio-HBE** (670 mg, 82%). ^{1}H NMR (500 MHz, CD_3CN) δ 8.84 (d, J = 6.2 Hz, 4H), 8.38 – 8.28 (m, 4H), 7.11 (d, J = 7.6 Hz, 4H), 6.84 (d, J = 7.7 Hz, 4H), 4.76 (s, 4H), 4.09 (s, 4H), 3.93 (s, 4H), 3.66 (t, J = 6.6 Hz, 4H), 2.77 (t, J = 6.4 Hz, 4H), 2.19 – 2.03 (m, 2H) ppm. The repeating unit was estimated to be n ≈ 8 using the average integration of viologen end-groups.

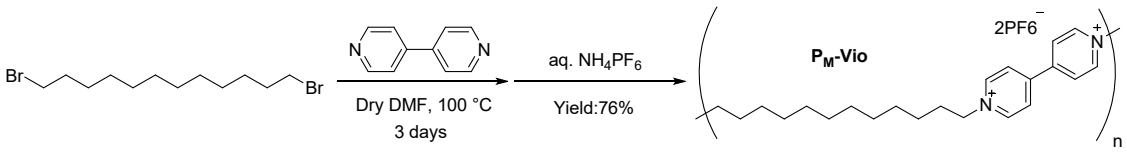

P_M-Vio: This polymer was synthesized following the general procedure for **P_M-Vio-HBE**, while using 1,12-dibromododecane (328 mg, 1.0 mmol, 1.0 equiv) and 4,4'-bipyridine (159 mg, 1.02 mmol, 1.02 equiv) as the starting materials in dry DMF (1.4 mL) under nitrogen. Reaction mixture was stirred at 100 °C for 3 days. The reaction mixture was cooled to r.t. and then transferred to a concentrated aqueous solution of NH_4PF_6. The off-white solid crashed out and was collected by filtration. The crude solid was redissolved in minimal MeCN and precipitated in NH_4PF_6 aqueous solution to afford an off-white solid **P_M-Vio** (470 mg, 76%). ^{1}H NMR (500 MHz, CD_3CN) δ 8.81 (d, *J* = 6.3 Hz, 4H), 8.28 (t, *J* = 10.6 Hz, 4H), 4.51 (dd, *J* = 16.2, 8.6 Hz, 4H), 1.93 (d, *J* = 6.7 Hz, 4H), 1.30 (s, 8H), 1.23 (s, 8H) ppm. The repeating unit was estimated to be n ≈ 12 using the average integration of viologen end-groups.

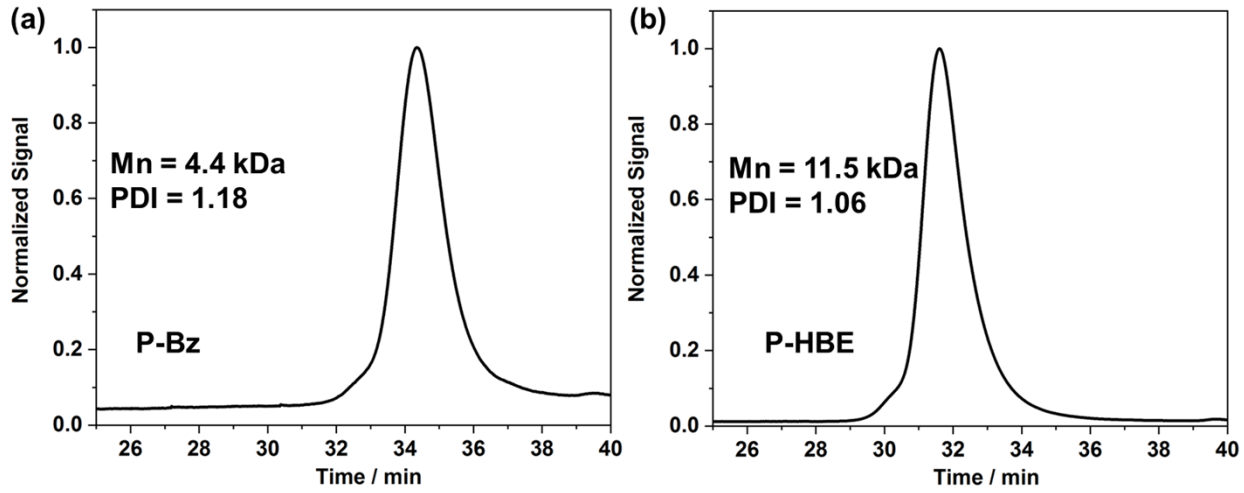

Figure S1. GPC chromatograms of polymers (a) **P-Bz** and (b) **P-HBE**

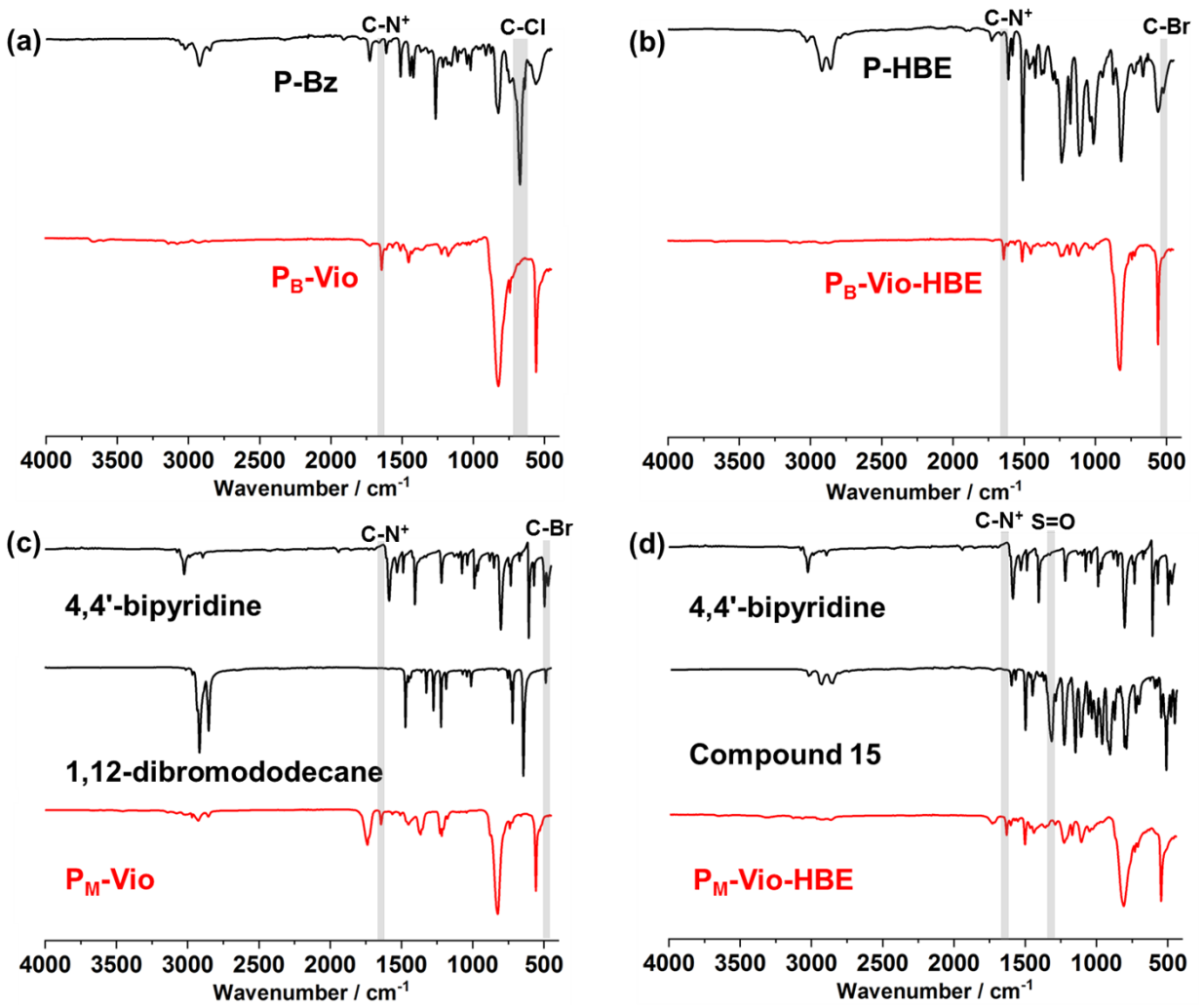

Figure S2. FT-IR spectra of (a) **P-Bz** and (b) **P-HBE** before (black lines) and after (red lines) the attachment of viologen redox moieties, and (c) **P_M-Vio** and (d) **P_M-Vio-HBE** before (black lines) and after (red lines) the condensation reaction between 4,4'-bipyridine and corresponding ditopic linkers.

Table S1. Elemental Analysis (C, H, N) of polymers.

Polymers	Elements	C	H	N
P-HBE[b]	Theoretical (%)[a]	63.2	5.84	-
	Experimental (%)	62.91	5.69	-
	Difference (%)	-0.29	-0.15	-
P_B-Vio-HBE	Theoretical (%)[a]	49.42	4.54	3.65
	Experimental (%)	48.04	4.36	3.69
	Difference (%)	-1.38	-0.18	0.04
P-Bz[b]	Theoretical (%)[a]	70.38	5.88	-
	Experimental (%)	70.72	5.88	-
	Difference (%)	0.34	0.00	-
P_B-Vio	Theoretical (%)[a]	43.01	3.77	4.64
	Experimental (%)	45.02	4.10	4.56
	Difference (%)	2.01	0.33	-0.08
P_M-Vio-HBE	Theoretical (%)[c]	47.80	4.49	3.93
	Experimental (%)	45.37	4.46	4.00
	Difference (%)	-2.43	-0.03	0.07
P_M-Vio	Theoretical (%)[c]	42.76	5.02	4.92
	Experimental (%)	41.26	4.92	4.77
	Difference (%)	-1.50	-0.10	-0.15

[a] Theoretical values are calculated based on Mn value from GPC; [b] Polymers do not contain element N; [c] Theoretical values are calculated based on the repeating unit determined by the integration of NMR signals.

3 Fragmentation Studies

Chromatograms of fragmentation were acquired using a GC-MS system (Agilent Inc, CA, USA) consisting of an Agilent 6890 gas chromatograph, an Agilent 5973 MSD and a HP 7683B autosampler. Gas chromatography was performed on a ZB-5MS (60m×0.32mm I.D. and 0.25μm film thickness) capillary column (Phenomenex, CA, USA). The inlet and MS interface temperatures were set at 250 ^{o}C, and the ion source temperature was adjusted to 230 ^{o}C. An aliquot of 5 μL was injected in split mode (10:1). The helium carrier gas was kept at a constant flow rate of 2 mL/min. The temperature program was: 1 min at 50 ^{o}C, followed by temperature ramp of 40 ^{o}C min^{-1} to 300 ^{o}C for 6 min. The mass spectrometer was operated in positive electron impact mode (EI) at 69.9 or 50 eV ionization energy at m/z 25–500 scan range. The threshold was 100. The instrument variability was within the standard acceptance limit (5%). The spectra of target peaks were evaluated using the MSD Chemstaion E.02.01.1177 software (Agilent Inc, CA, USA). All results were reproduced on a Shimadzu Gas Chromatograph/Mass Spectrometer (GCMS-QP2010Plus) equipped with an auto injector (AOC-20i) to confirm the accuracy of fragmentation pattern. The mass spectrometer was operated in positive electron impact mode (EI) at 70 eV ionization energy.

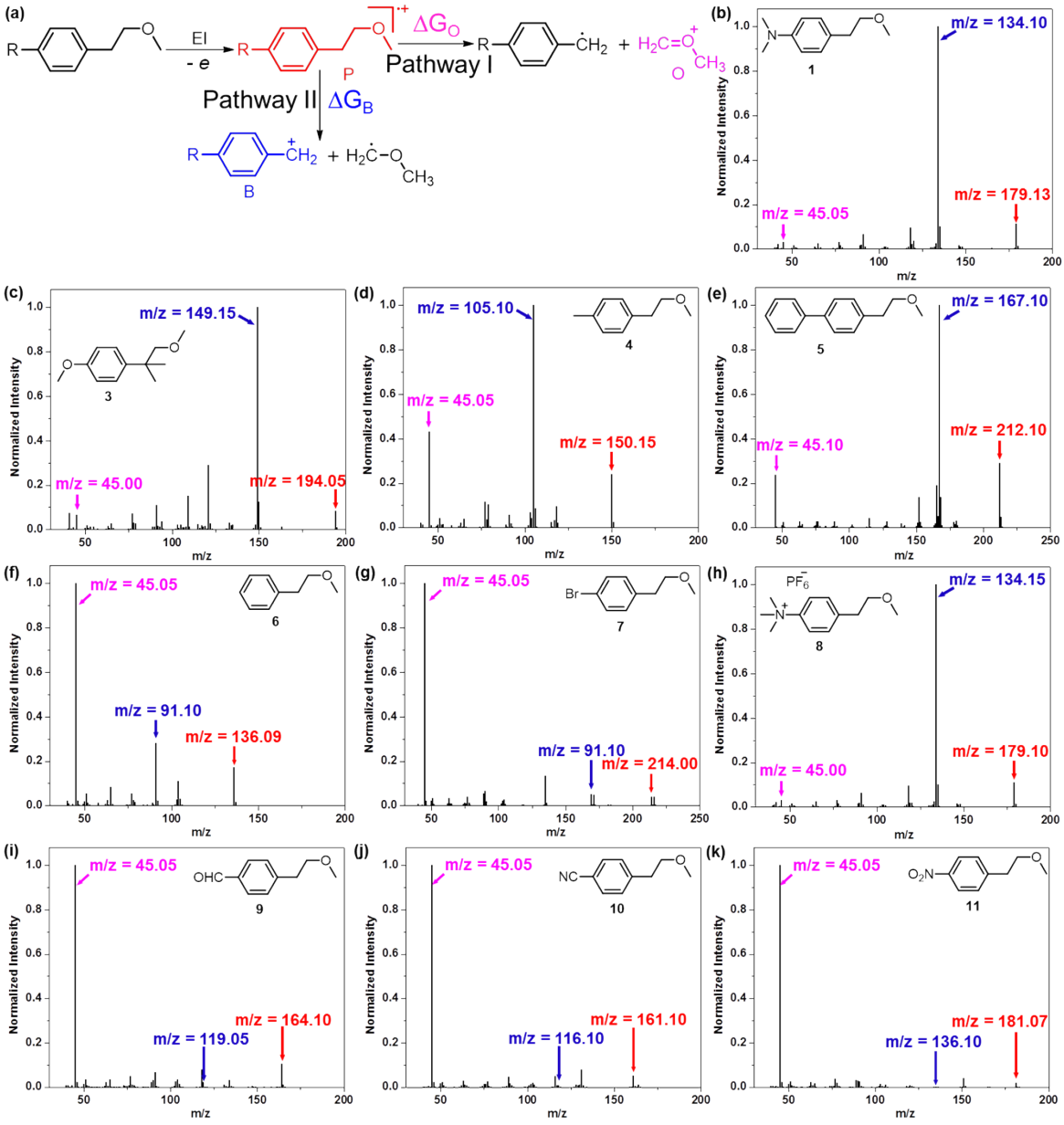

Figure S3. Proposed mesolytic cleavage pathways (a) and GC-MS results of HBEs (b) **1**, (c) **3**, (d) **4**, (e) **5**, (f) **6**, (g) **7**, (h) **8**, (i) **9**, (j) **10**, and (k) **11**, labeled with corresponding radical cation (red), benzylic cation (blue), and oxocarbenium cation (pink).

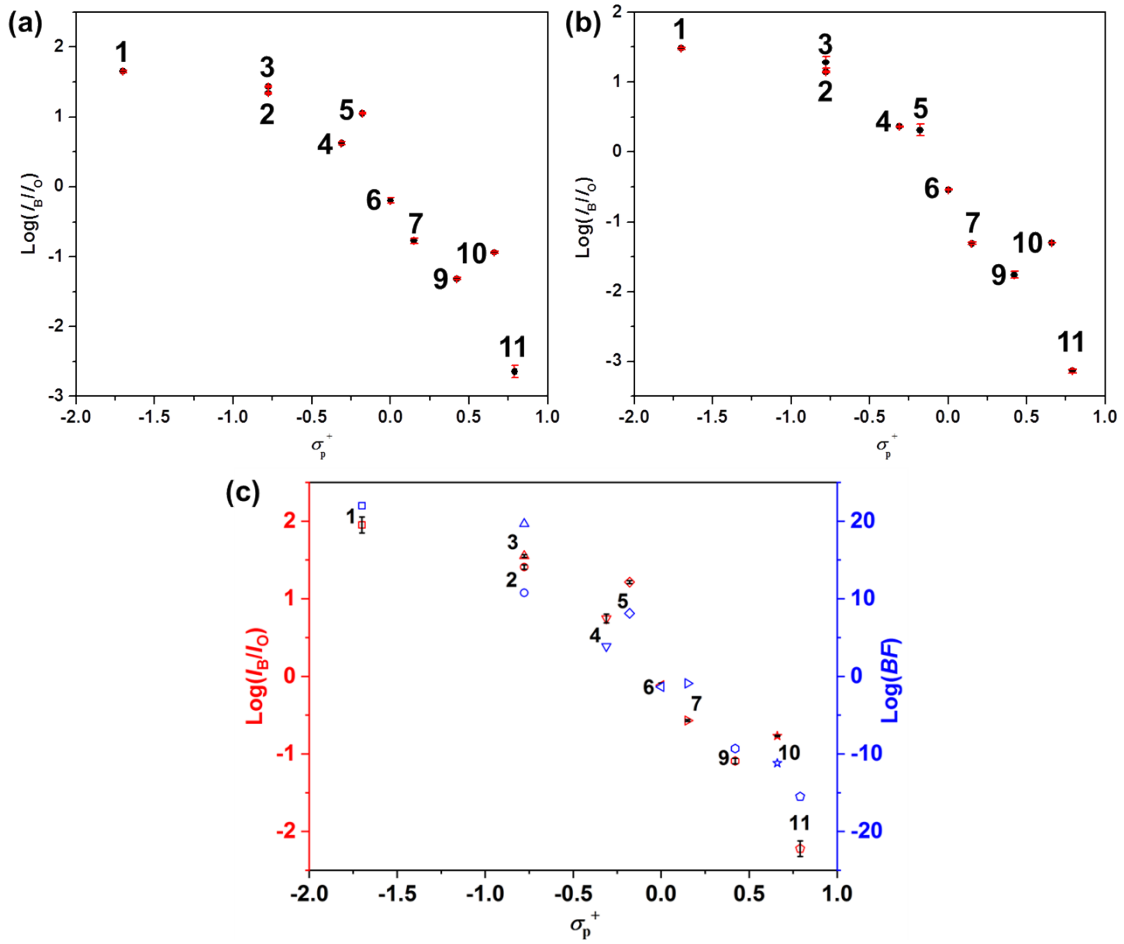

Figure S4. The plot of the logarithmic m/z intensity ratio between benzylic and oxocarbenium cations (Log(I_B/I_O)) as a function of the Hammett constant (σ_p^+) under (a) 50 and (b) 70 eV ionization energy on Agilent and Shimadzu instruments, respectively. (c) The combined plot of Log(I_B/I_O) *vs*. σ_p^+ (70 eV, Agilent) and Log(*BF*) *vs*. σ_p^+ clearly shows that the empirical σ_p^+ parameter is able to bridge experimental and computational results of the distribution ratio of two major mesolytic cleavage pathways for various HBEs. The error bar was estimated from standard deviation of the average of three measurements. All plots show similar decreasing trend and shape as the σ_p^+ increases. Fragmentation ratio of HBE **8** is not included in all plots because the ammonium-based compound is known to undergo demethylation, first under the high injection temperature of 250 ˚C (S16), followed by a similar fragmentation pattern as found for HBE **1**.

4 Electrochemistry Studies

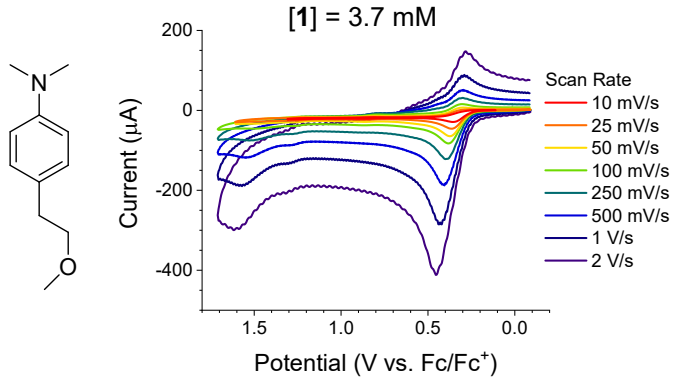

Figure S5. Cyclic voltammograms of HBEs **1**–**11**. Molecular structure and concentration used in experiments are given. A 3 mm diameter glassy carbon electrode was used for all CVs.

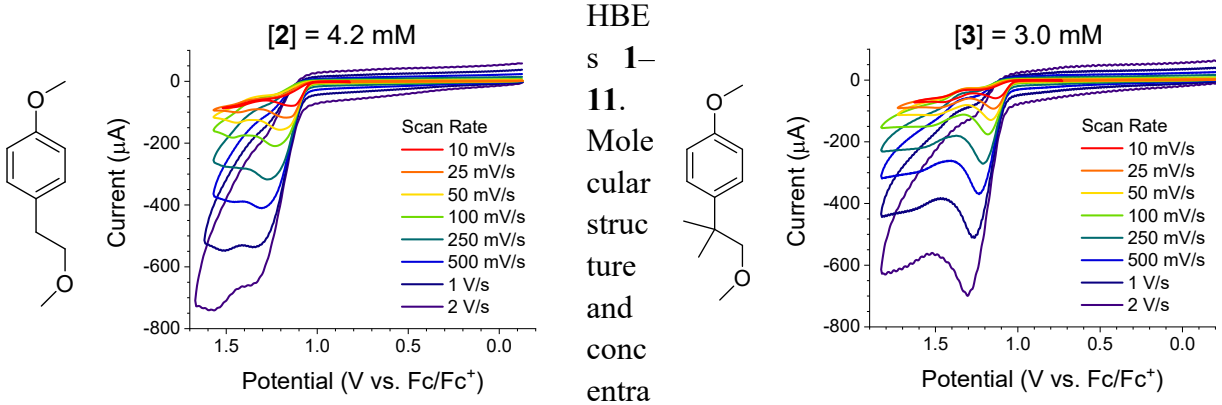

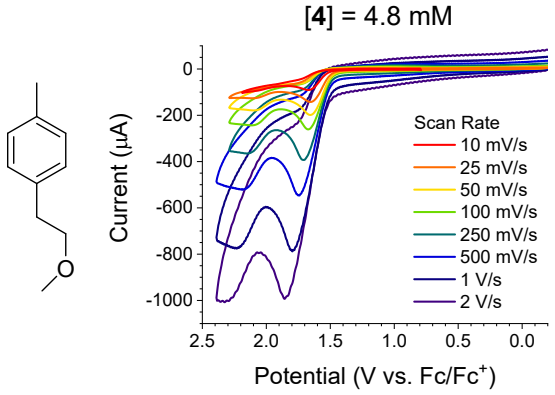

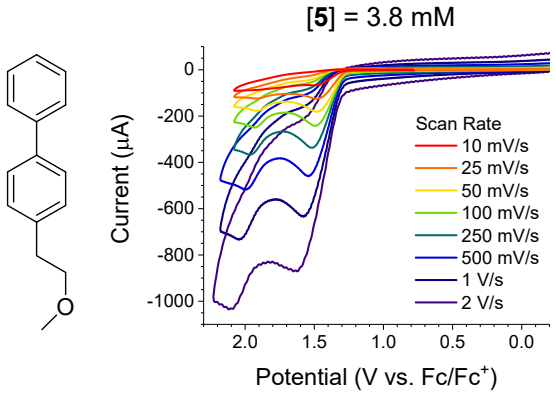

Figure S5 (continued).

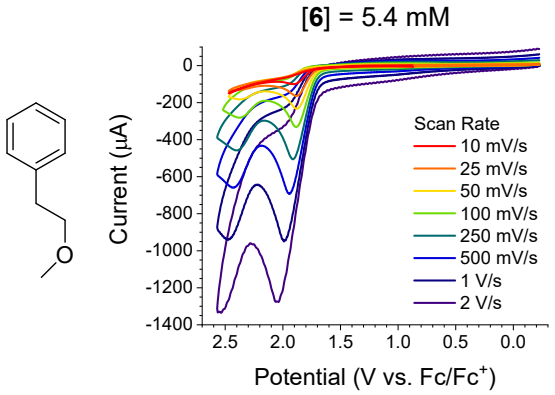

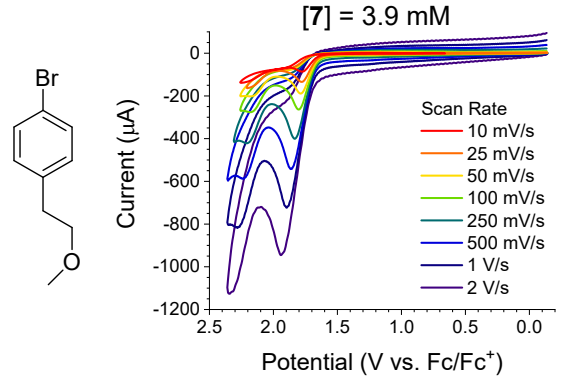

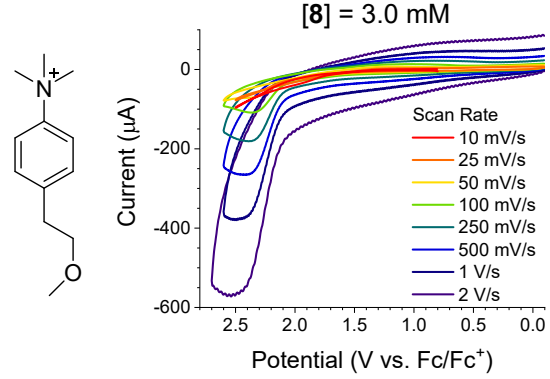

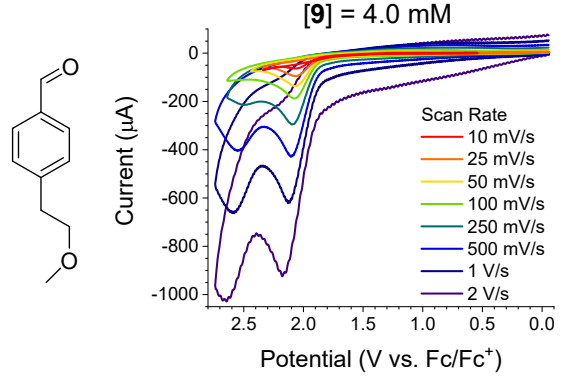

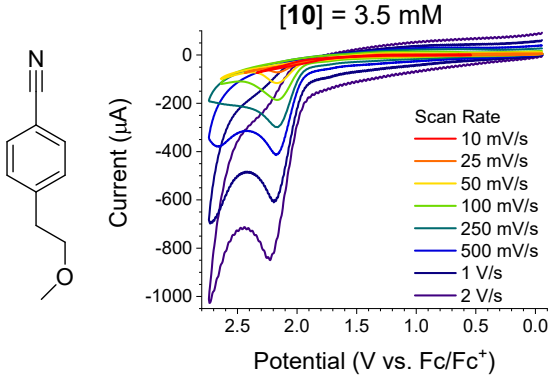
[10] = 3.5 mM
N
O
Current (μA)
0
-200
-400
-600
-800
-1000
2.5
2.0
1.5
1.0
0.5
0.0
Potential (V vs. Fc/Fc+)
Scan Rate
10 mV/s
25 mV/s
50 mV/s
100 mV/s
250 mV/s
500 mV/s
1 V/s
2 V/s

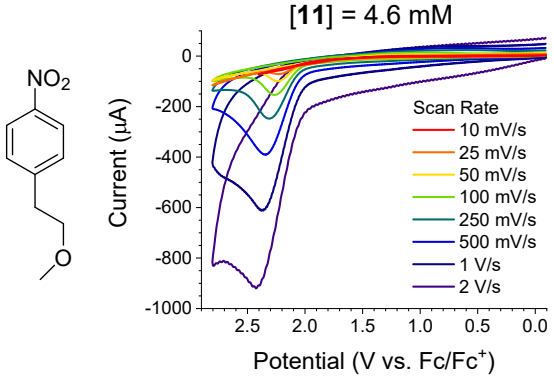
[11] = 4.6 mM
NO2
O
Current (μA)
0
-200
-400
-600
-800
-1000
2.5
2.0
1.5
1.0
0.5
0.0
Potential (V vs. Fc/Fc+)
Scan Rate
10 mV/s
25 mV/s
50 mV/s
100 mV/s
250 mV/s
500 mV/s
1 V/s
2 V/s

Figure S6. Theta-UME. (A) Micrograph of the theta-UME used for high-throughput generation-collection experiments. (B) Depiction of how generation-collection experiments are carried out with the theta-UME.

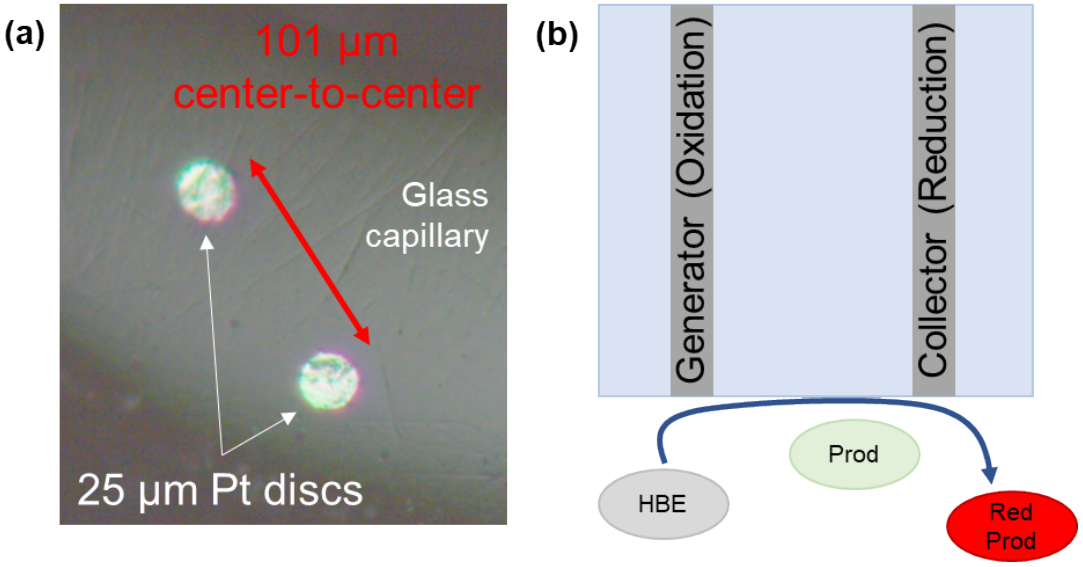

Figure S7. Generation-collection experiments of HBEs **1**–**11**. CVs taken in the same solutions as in **Figure S3** with 25 µm Pt working electrodes. Potential scales refer to $E_{collector}$. OCP denotes Open Circuit Potential.

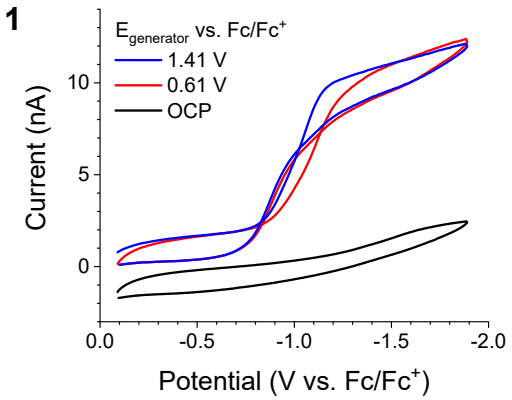

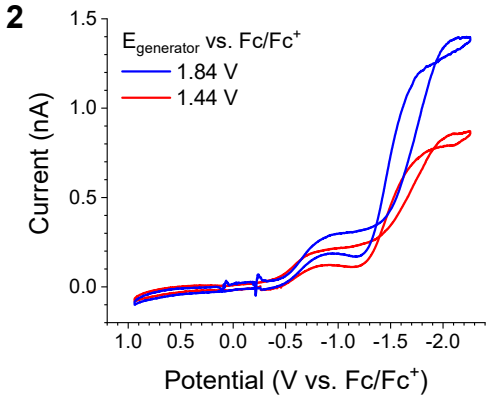

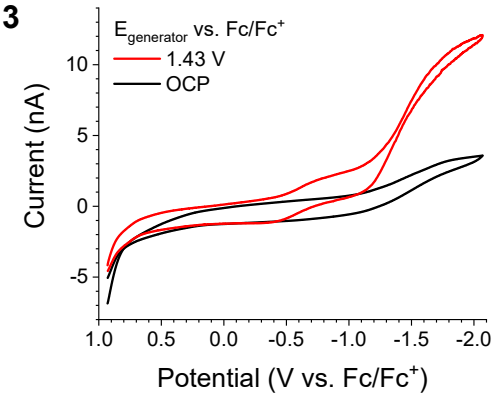

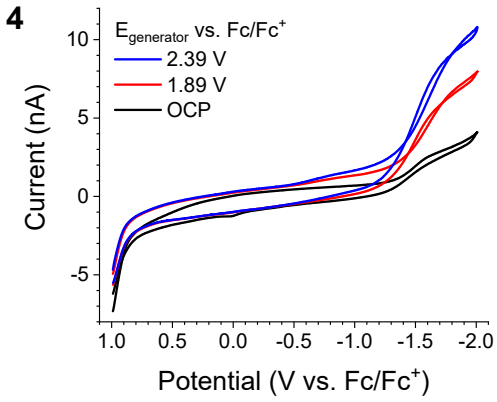

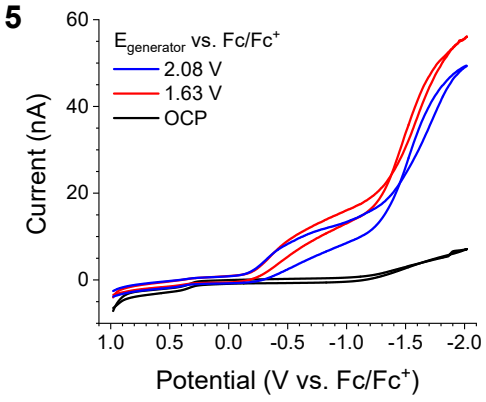

Figure S7 (continued).

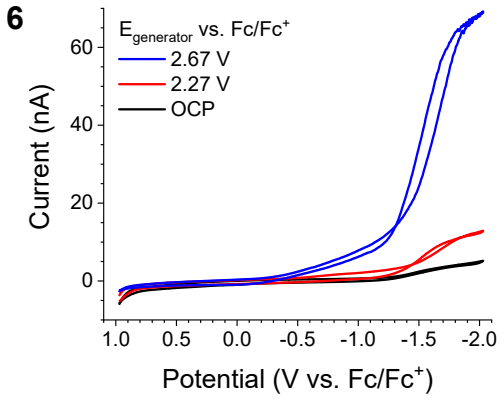

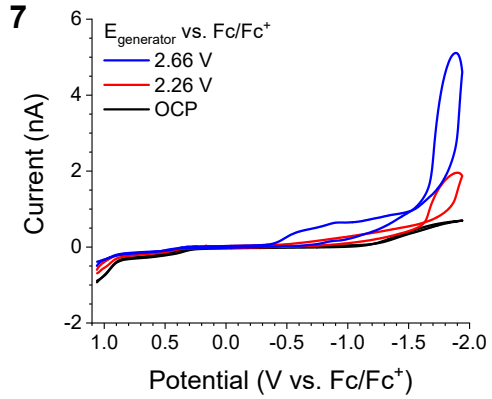

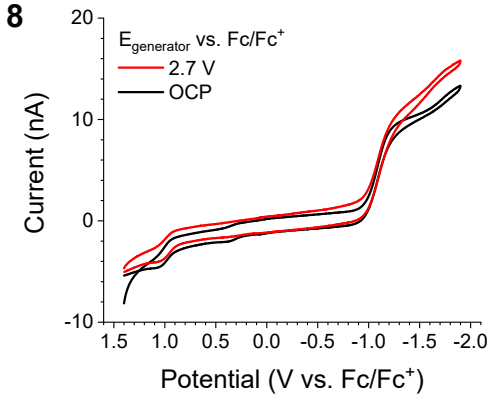

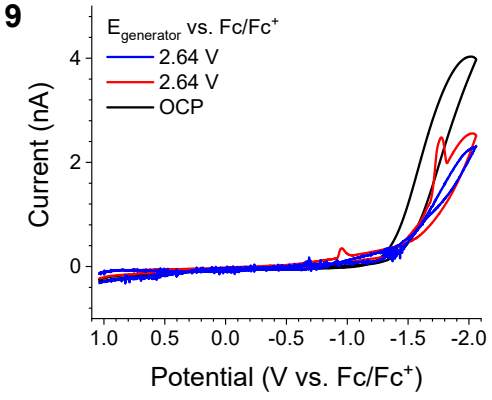

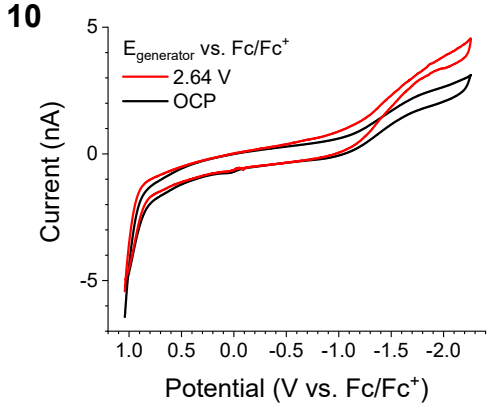

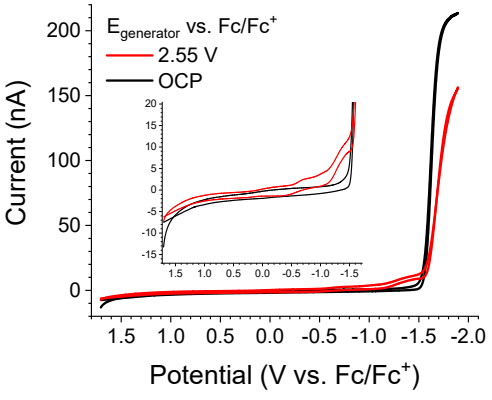

Figure S8. CVs of **2-C** (alkyl analogue of HBE **2**). (A) CVs with a glassy carbon macrodisk. (B) Collection results from generation-collection experiments with a theta-UME.

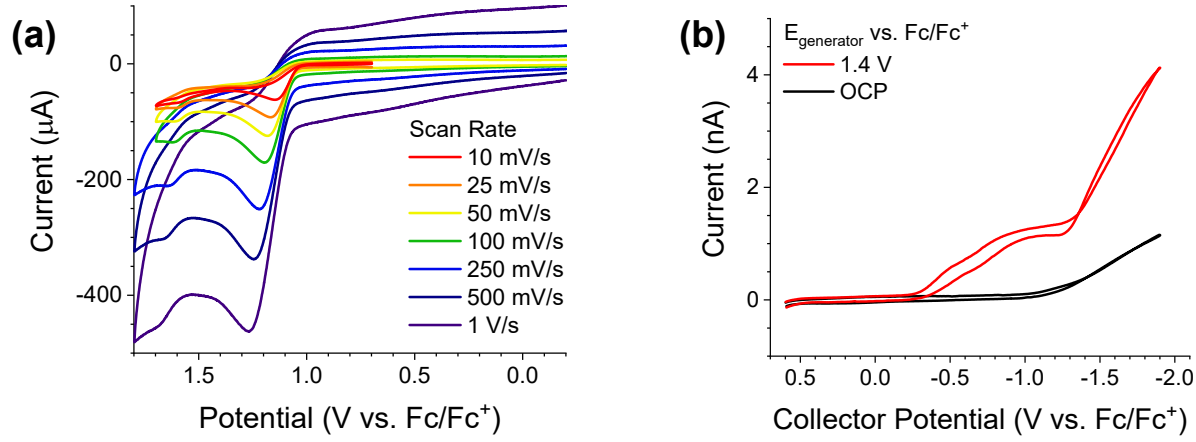

Figure S9. Reduction of HBE **11**. CVs of HBE **11** before (A) and after (B) stepping to oxidative potentials to cleave the HBE. Conditions are the same as in **Figure S3**. The nitrobenzene clearly loses electrochemical reversibility, which may be due to film formation on the electrode.

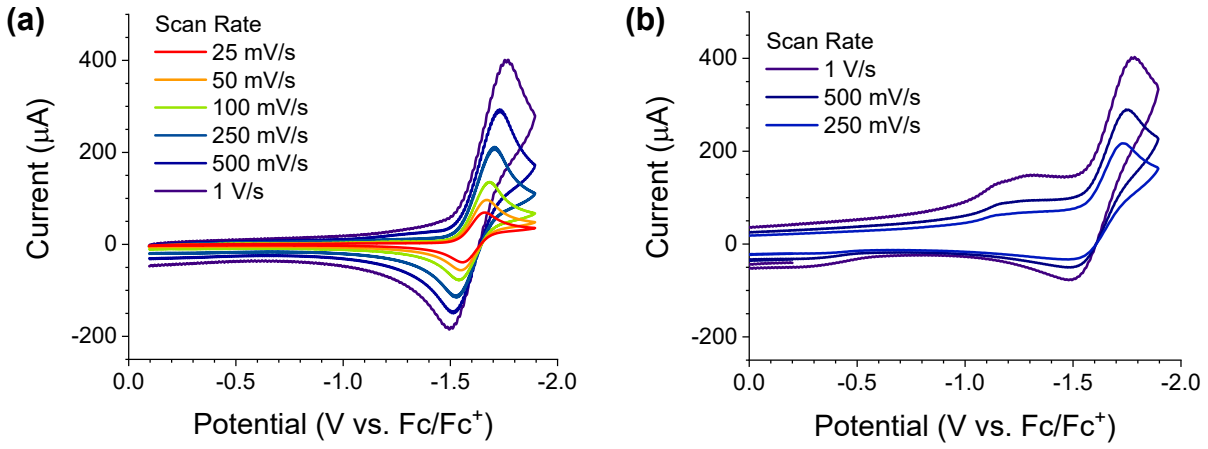

Figure S10. Randles-Sevcik calculations for HBE oxidation CVs. The peak currents obtained from our CVs depends on multiple factors, two of which are unknown, n and D. Using the Randles-Sevcik equation for a reversible electron transfer process (shown top left), the slopes of i_p vs. $v^{1/2}$ can be used to find n_{HBE} for HBE **11** since it undergoes reversible reduction and the HBE oxidation (i.e., D is cancelled out when comparing RS slopes). (a) Comparison of RS slopes for HBE **11** show a multi-electron process for HBE oxidation, since peak currents are higher than expected compared to the reduction peaks. (b) Calculation of n from RS slopes of all HBEs, assuming D = 1 × 10^{-5} cm^2/s (typical for small molecules in acetonitrile) and α = 0.5. n was estimated using RS equations for both reversible and irreversible electron transfer processes. Since most HBEs give values with n significantly higher than 1, it is likely that a two-electron ECE mechanism occurs when oxidizing these HBEs.

$$i_p = 0.4463nFAC\left(\frac{n_{rev}FvD}{RT}\right)^{1/2}$$

$$i_p = 0.4961nFAC\left(\frac{\alpha n_{irr}FvD}{RT}\right)^{1/2}$$

i_p = peak current, in A
n = number of electrons transferred
n_{rev} = for reversible reaction
n_{irr} = for irreversible reaction
A = electrode area, in cm^2
D = diffusion coefficient, in cm^2/s
C = concentration, in mol/cm^3
v = scan rate, in V/s
R = gas constant, in J/(K•mol)
T = temperature, in K
α = transfer coefficient

(a)

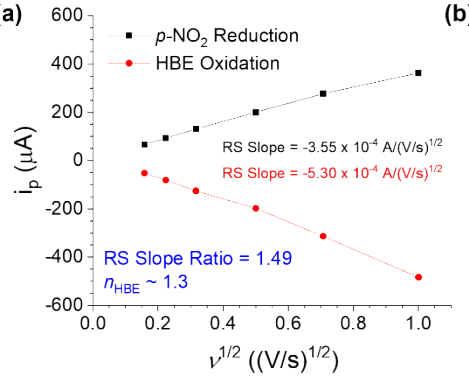

(b)

HBE	n_{rev}	n_{irr}
1	1.11	1.30
2	1.47	1.72
3	1.80	2.11
4	1.5	1.76
5	2.05	2.40
6	1.87	2.19
7	1.92	2.25
8	1.38	1.61
9	1.62	1.90
10	1.80	2.11
11	1.50	1.76

Figure S11. Bulk electrolysis and product detection. (a) Black: Bulk electrolysis of HBE **2** (5.9 mM, equal to 2.8 C for a one-electron oxidation) with a graphite rod at 1.54 V vs. Fc/Fc^+. Red: Bulk electrolysis of the same solution after oxidizing 2.8 C. (b) CVs with a 25 µm Pt UME of the solution after the oxidations in (a).

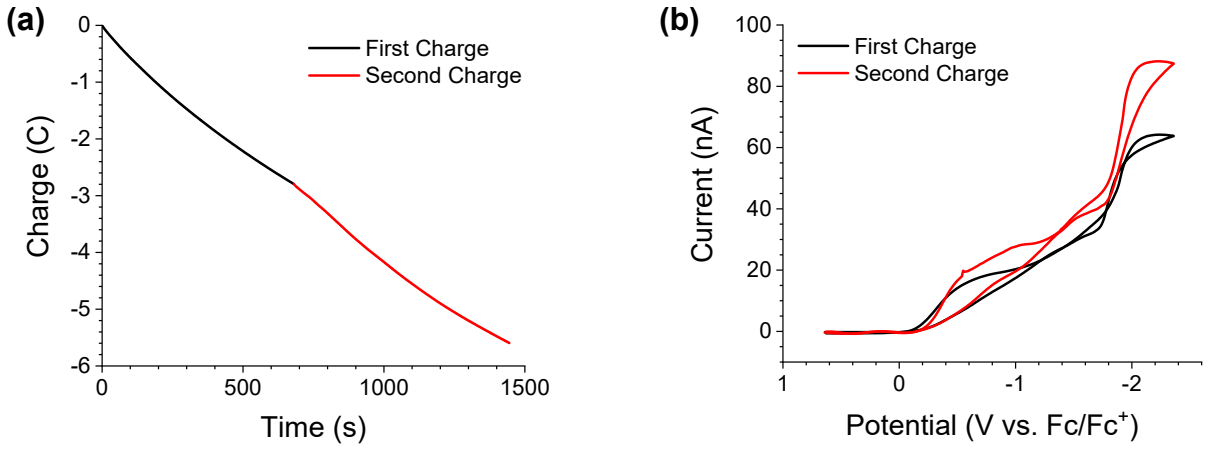

Figure S12. CVs of HBE-based redoxmers. Top: CVs of redox active centers; Bottom: CVs of HBE and redox centers in the same window. (a) 1 mM **DAB dimer**, (b) 0.57 mM **TEMPO dimer**, (c) 1 mM **DiHBE Vio**, (d) 1 mM **NP dimer**; 3 mm glassy carbon electrode was used.

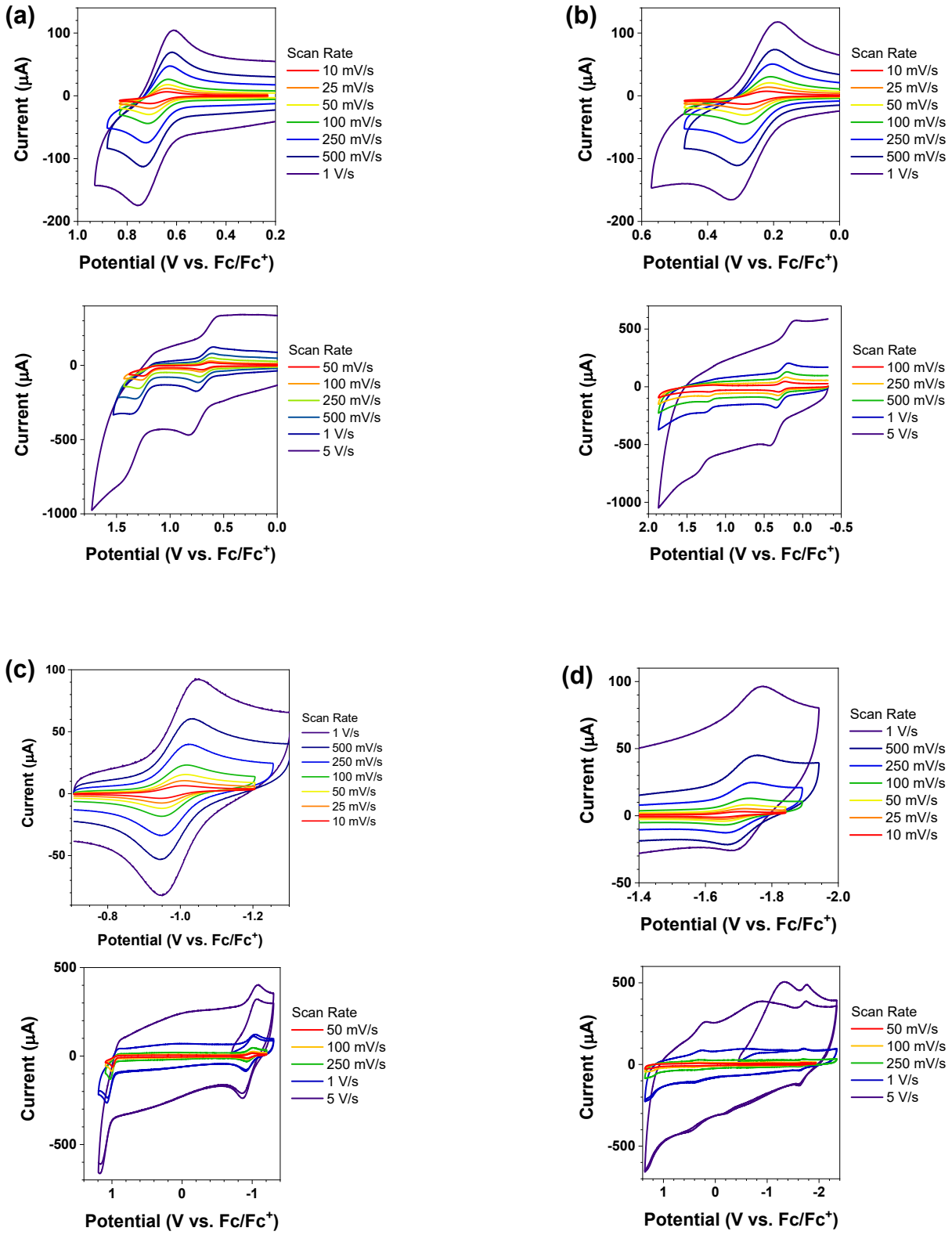

Figure S13. CVs of **TEMPO-HBE**. CVs of 2.0 mM **TEMPO-HBE** at a glassy carbon electrode (a) cycling only in the TEMPO oxidation range and (b) in the HBE oxidation and TEMPO oxidation regions. (c) Generation-collection results while oxidizing just TEMPO (0.46 V) and TEMPO and HBE (1.56 V).

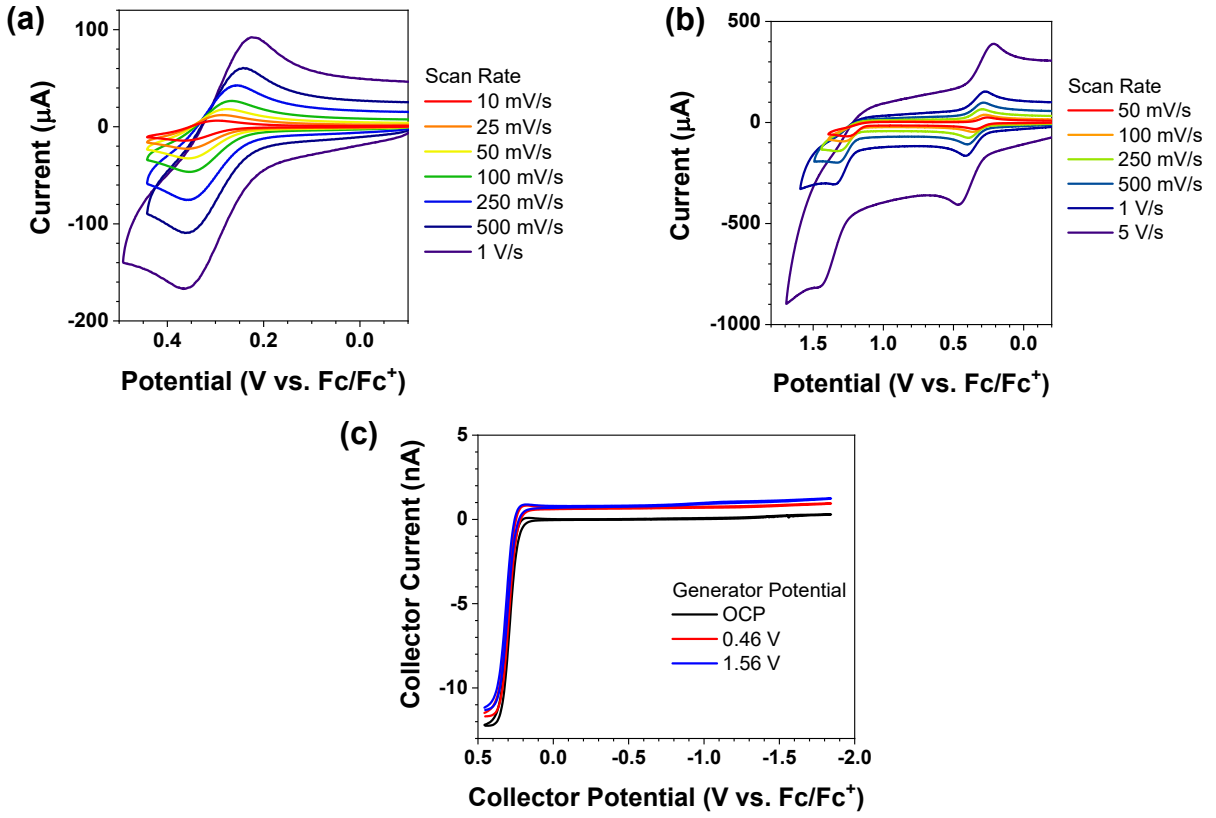

Figure S14. CVs of bulk electrolysis products of **TEMPO-HBE** after cleavage, charge, and discharge (resulting solution from main text Figure 4). (a) CVs (100 mV/s) before and after excursions to high oxidizing potentials show emergence of a $TEMPO^+$ reduction not present before oxidation. (b) CVs (50 mV/s) in the TEMPO redox window showing emergence of the redox wave after oxidizing solution near the electrode for 10 s followed immediately by CV. (c) Generation-collection experiment showing small but significant TEMPO wave upon oxidizing solution species. Blue arrows indicate TEMPO waves. The Ag^0 quasi-reference here is ca. +0.2 V vs. Fc/Fc^+.

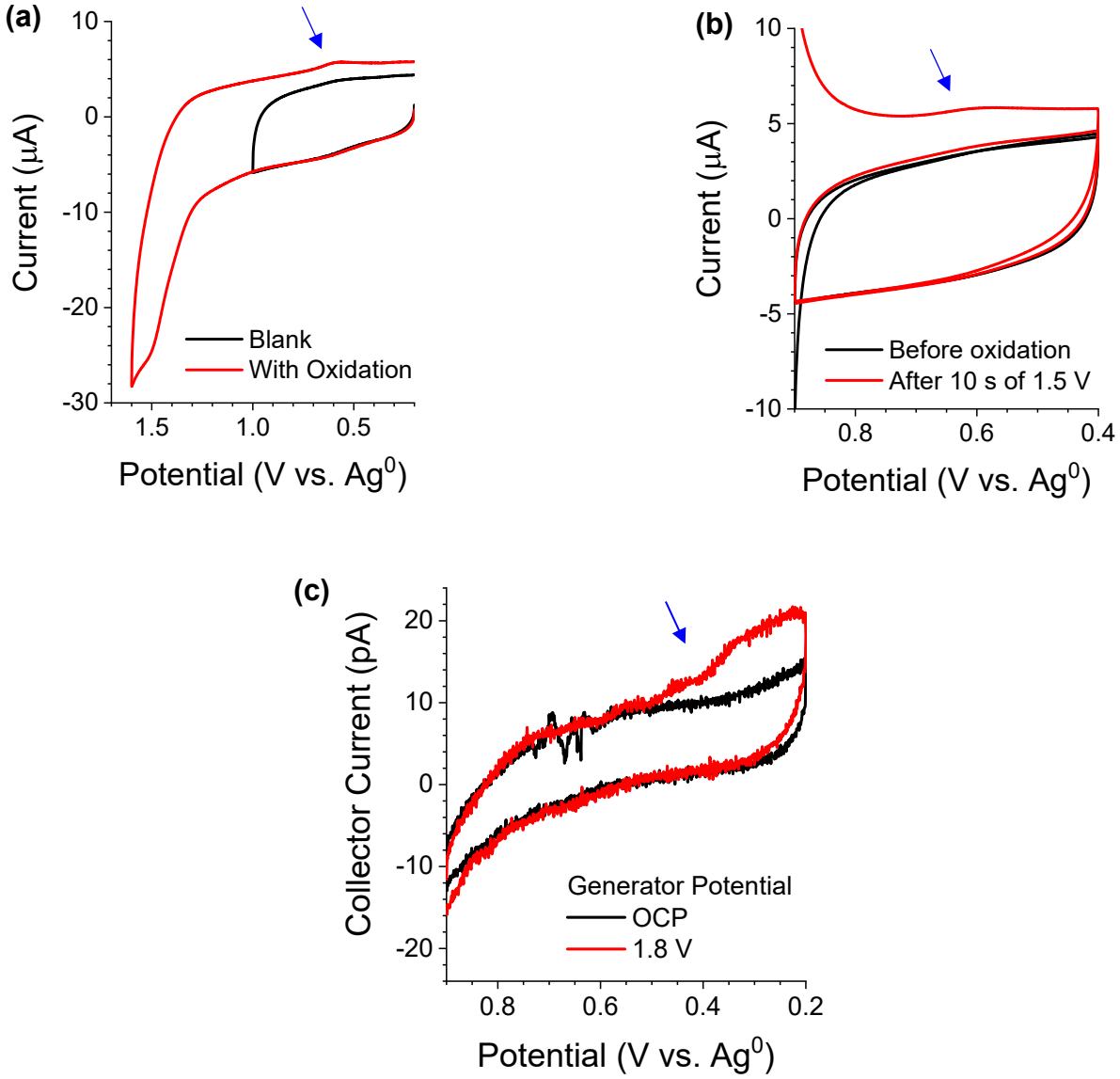

Figure S15. Bulk electrolysis results of **DiHBE-Vio**. (a) Pictures and CV results following bulk electrolysis (as shown in the scheme above the figures) of **DiHBE-Vio**. This system is initially electrochemically reversible, but the reduction of viologen mediates the reduction of cleavage products and seems to kill viologen reversibility when the bulk solution is charged. (b) Overlaid charge-discharge curves of the BE. (c) Overlaid UME CVs after the BE cycle noted.

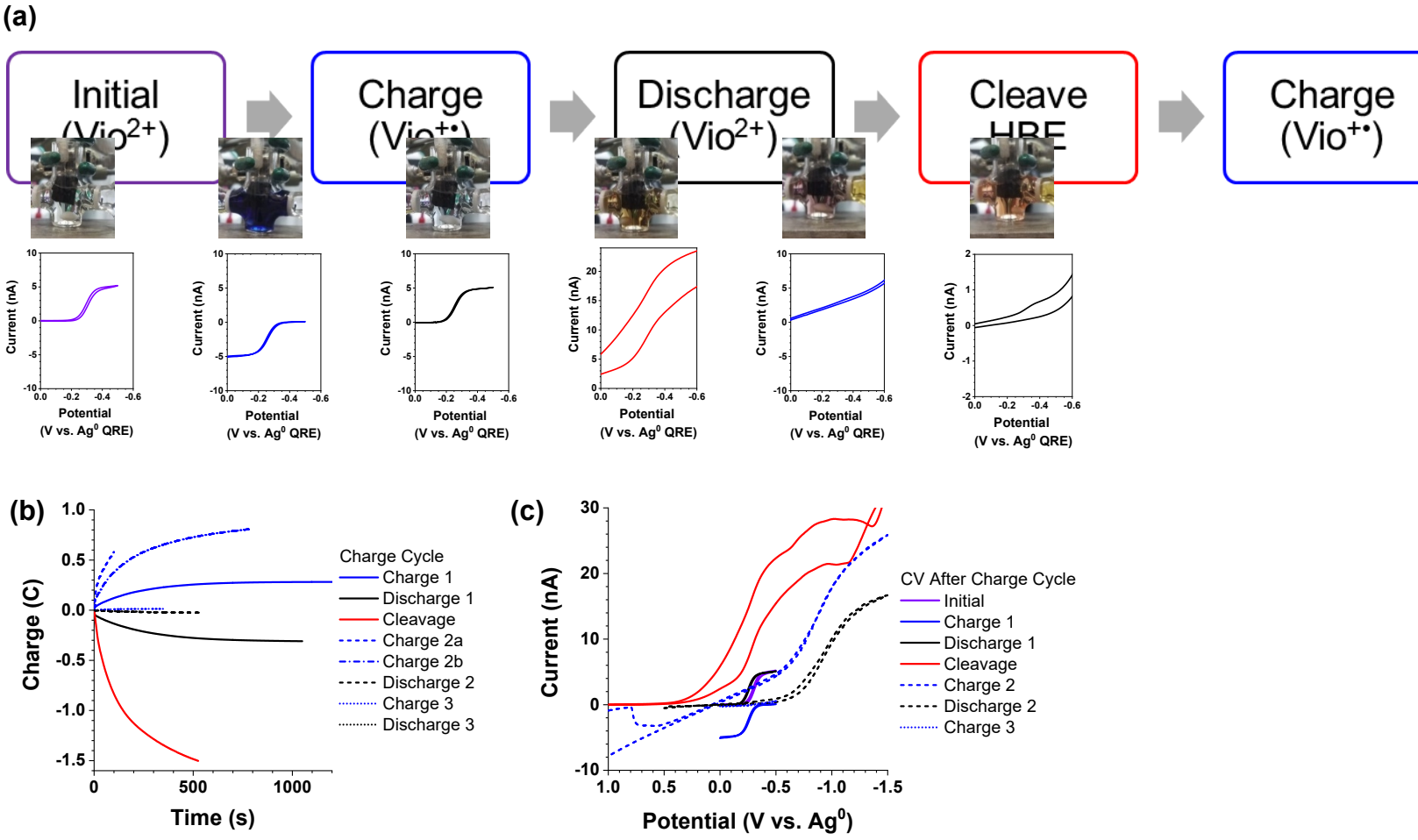

Figure S16. Membrane permeability studies. (a) Schematic of setup for testing membrane crossover rates of polymer solutions. Microelectrode CVs of neat (b) and cleaved (c) **P_B-Vio-HBE** solutions measured in the origin cell and in the blank cell at various time points throughout the experiments. Normalized [Vio] (C/C_0) as detected by UME CVs and corrected for constant evaporation of solution over time for neat (d) and cleaved (e) **P_B-Vio-HBE** in the blank cell. Evaporation rate was determined by the combined current of the origin and blank cells after 24 hrs, then the current of the blank cell was adjusted for each time point based on conservation of mass of the Vio species. For example, if the total current after 24 hrs was 3 nA, and the origin cell current was 2 nA at 0 hrs, then an increase of 0.042 nA/hr was determined and adjusted for each time point. Dashed line represents the theoretical maximum value for complete crossover.

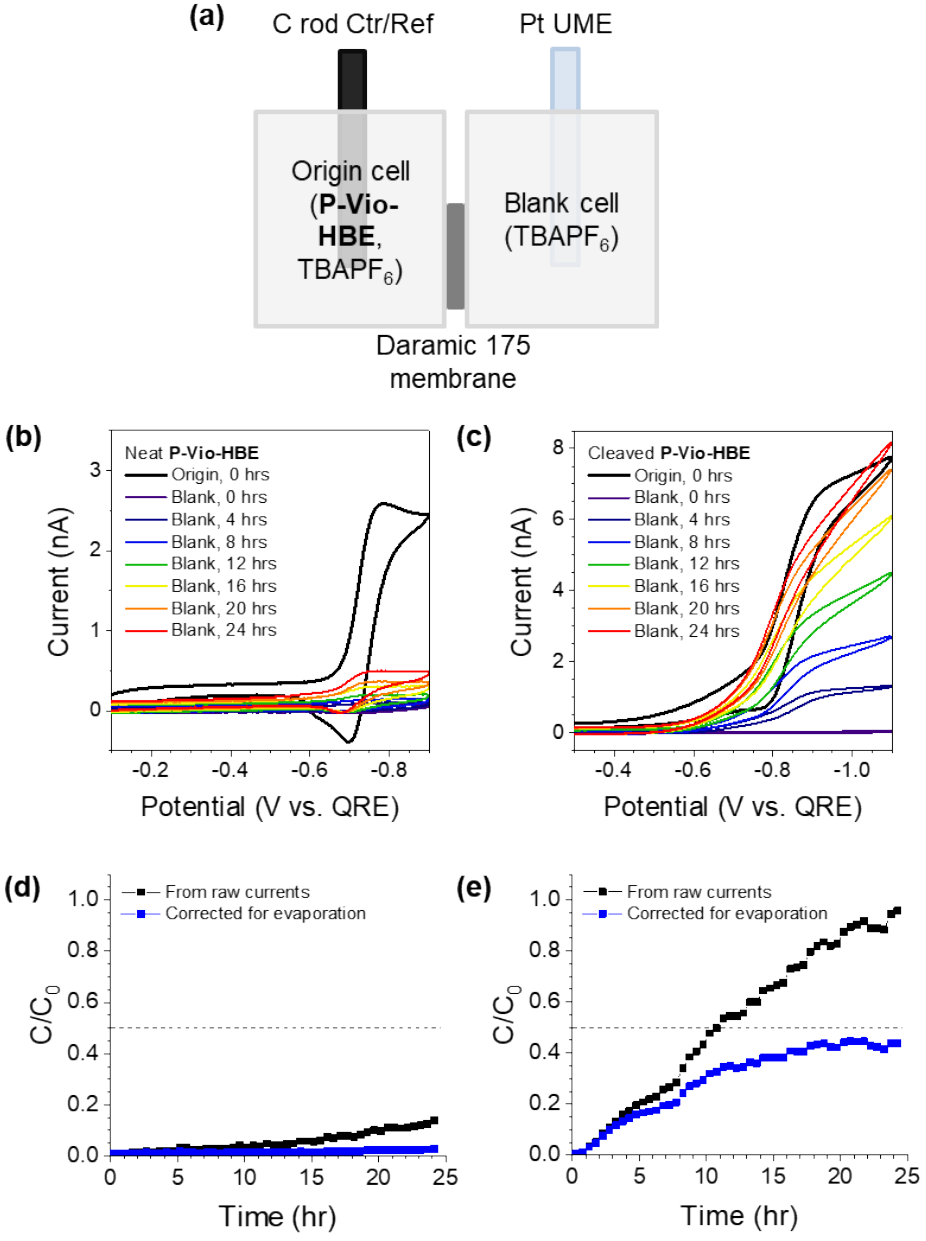

Calculation of Membrane Permeability. Permeability was calculated using the following equation:

$$P = \frac{V_{cell} \times T_{mem}}{A_{mem} \times (C_0 - C_t)} \times \frac{dC_t}{dt}$$

The parameters are defined as:

P is permeability in cm^2/min,
V_{cell} is the volume of the cells' solutions (3.6 mL each),
T_{mem} is the membrane thickness (175 μm),
A_{mem} is the cross-sectional area of the membrane between cells (2.85 cm^2),
C_0 is the concentration of Vio in the origin cell at time t = 0 (2 mM),
C_t is the concentration of Vio in the blank cell at time t (determined by CV), and
the derivative dC_t/dt is the slope of the concentration vs. time plot at time t.

P for both neat and cleaved **P_B-Vio-HBE** was evaluated at t = 10 hrs (here the C vs. t plot is linear, so the derivative equals the slope), and the concentrations and slopes used were adjusted for evaporation as reported above (so that V_{cell} is treated as a constant over time).

$P_{neat} = 1.2 \times 10^{-5}$ cm^2/min
$P_{cleaved} = 1.0 \times 10^{-3}$ cm^2/min

Figure S17. P_B-Vio-HBE voltammograms. (a) Macrodisk CVs at various scan rates of 1 mM (repeat unit) **P_B-Vio-HBE**, 100 mM $TBAPF_6$, MeCN; a 3 mm glassy carbon electrode was used. (b) Macrodisk CVs (50 mV/s) accessing the second reduction of viologen, show film accumulation with cycling over time (10 cycles shown); same parameters as (a). (c) CV of the redox active Vio film deposited in (b), tested in blank TBAPF6 solution (100 mV/s). (d) CVs of the Vio film before (blue line) and after (orange line) oxidation at E_{ox} (red line) and stirring, tested in blank $TBAPF_6$ solution (100 mV/s).

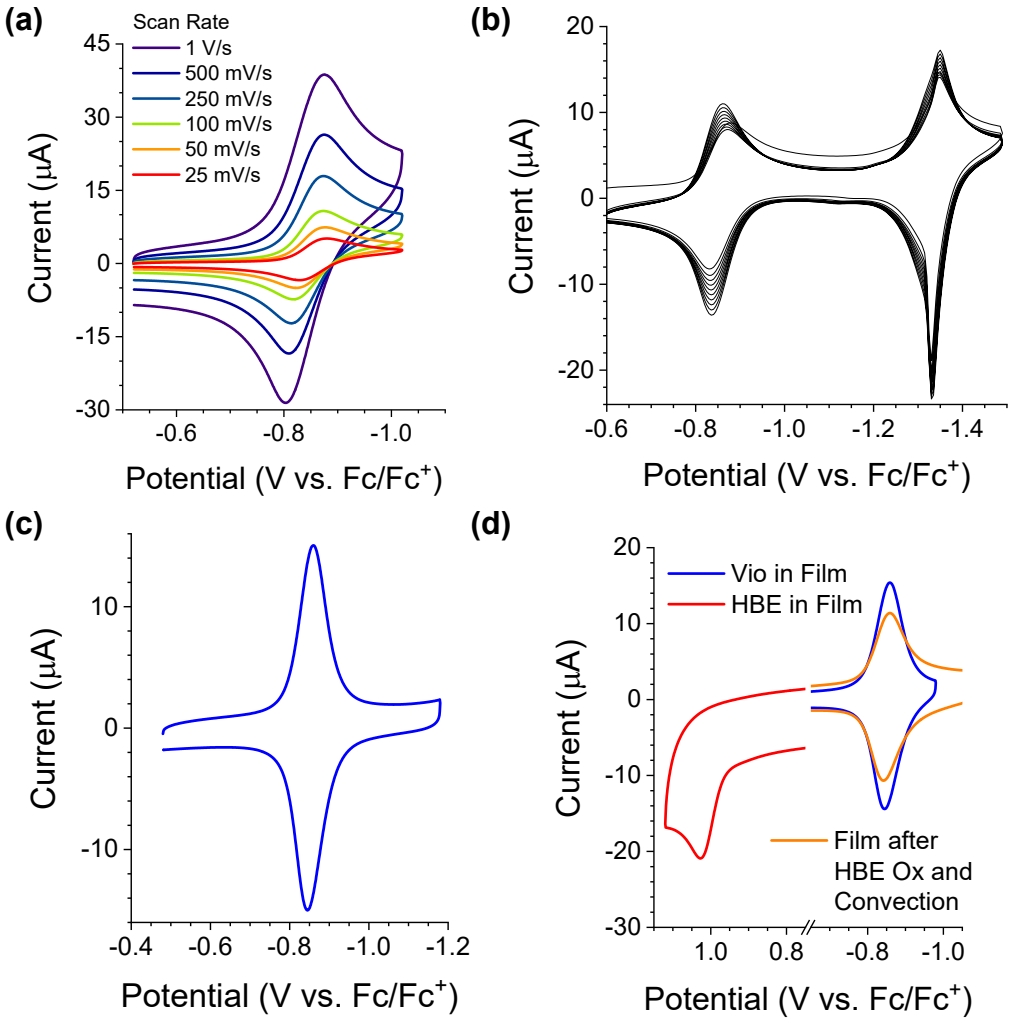

Figure S18. Film voltammograms. (a) Quantified parameters from CVs of Vio films: peak currents (i_p) and integrated charges (Q) from cathodic ($_{red}$) and anodic ($_{ox}$) sweeps. Film CVs from trials with (b) **P_B-Vio-HBE** and (c) **P_B-Vio** after oxidation then convection, and (d) **P_B-Vio-HBE** after convection then oxidation and convection.

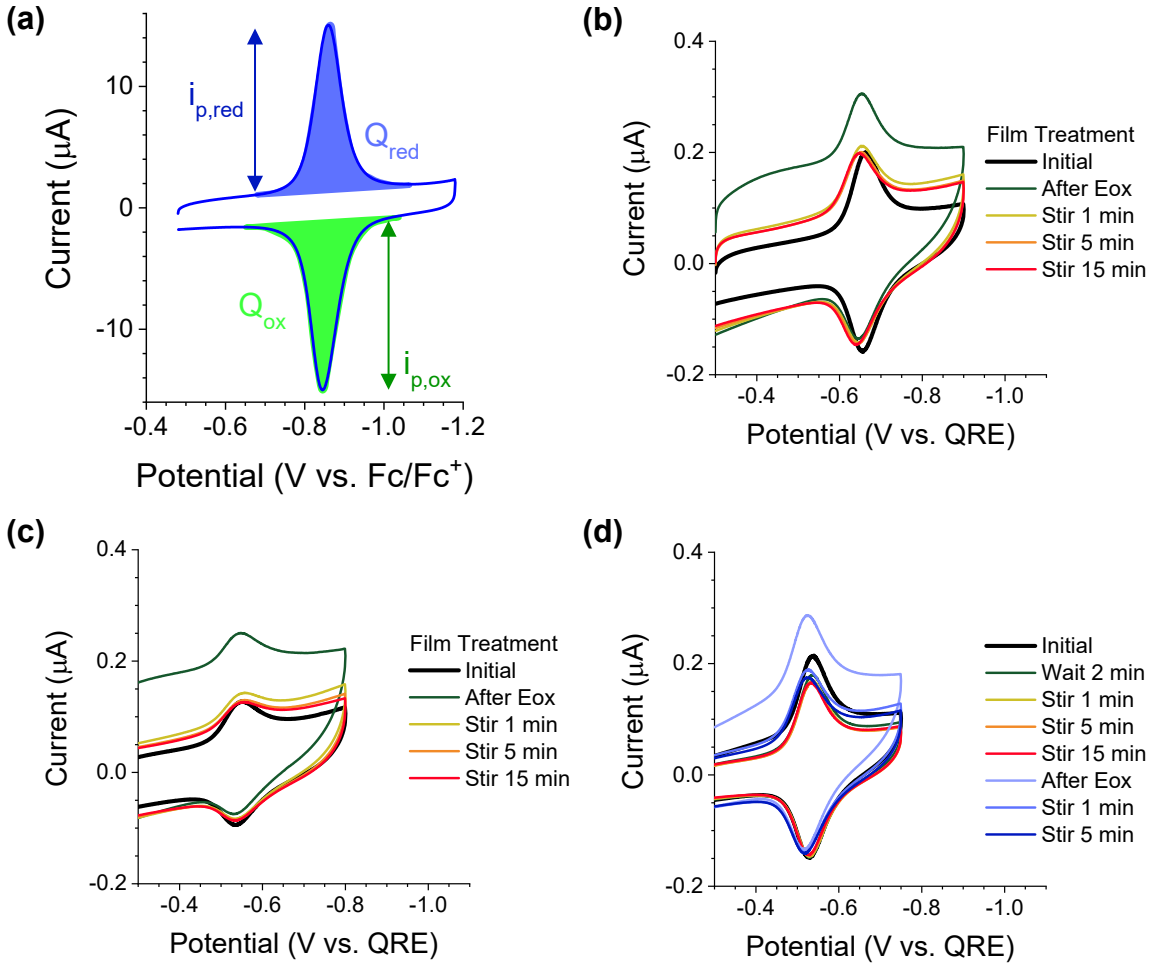

Figure S19. Deposition and oxidation of RAP films. Single electrodeposition cycles for (a) branched and (b) main-chain viologen RAPs. Application of E_{ox} for ~3 seconds via CV for (c) branched and (d) main-chain RAPs.

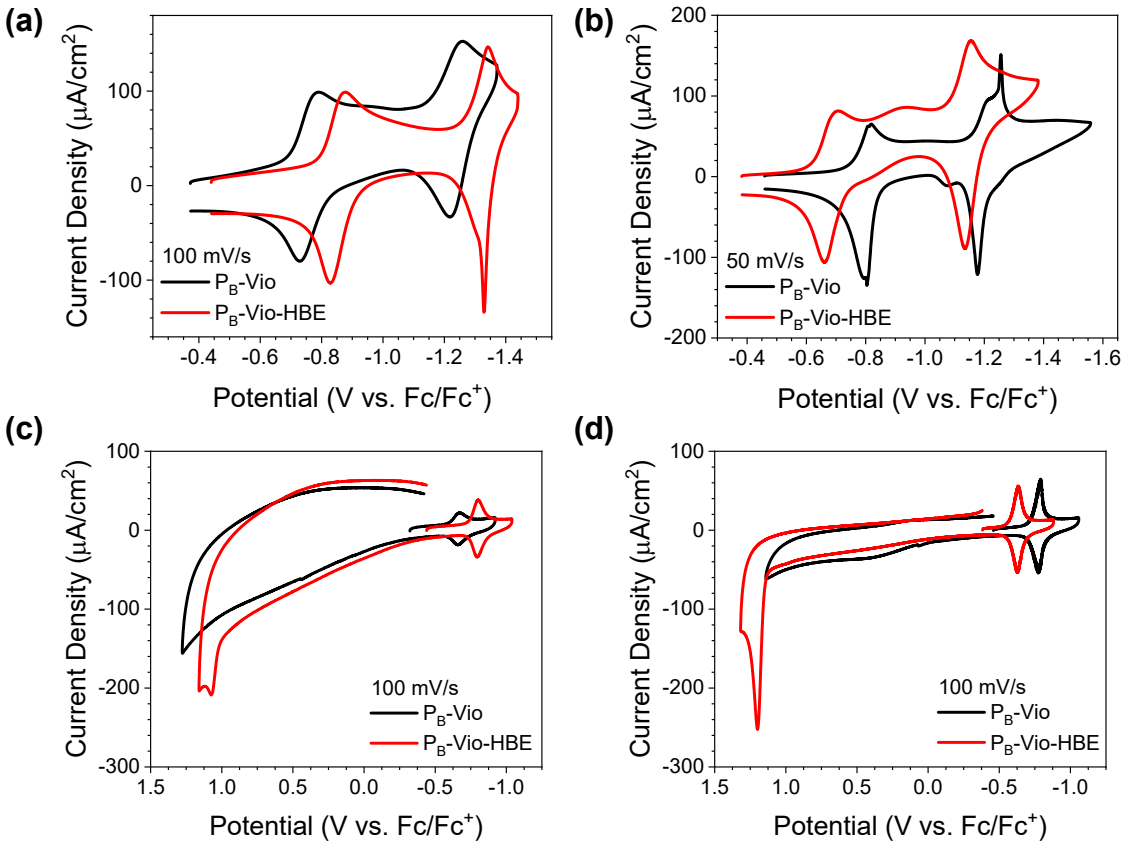

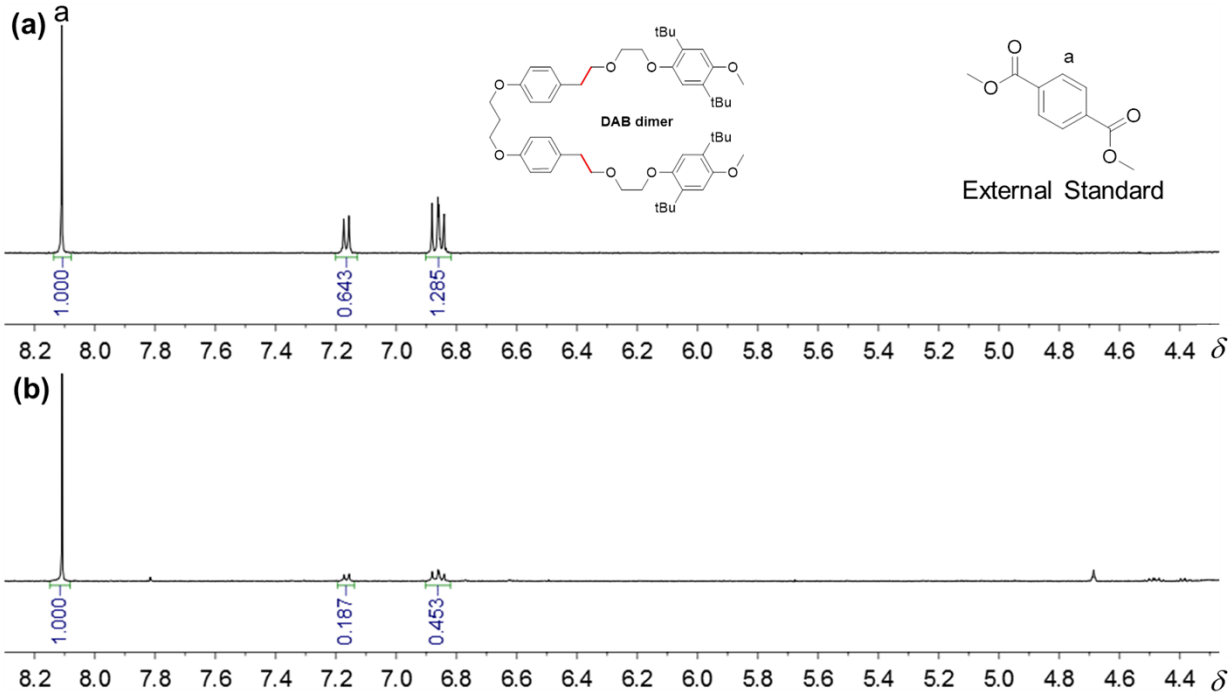

Figure S20. ^{1}H NMR spectra of **DAB dimer** (2 mM) in the MeCN solution containing 100 mM $TBAPF_6$ (a) before and (b) after bulk electrolysis. 20% v/v of MeCN-d_3 was added for locking and shimming during NMR collection. The dimethyl terephthalate was used as an external standard. The cleavage percentage of HBE linkers (red bonds) was calculated to be 68 % based on the remaining aromatic signals.

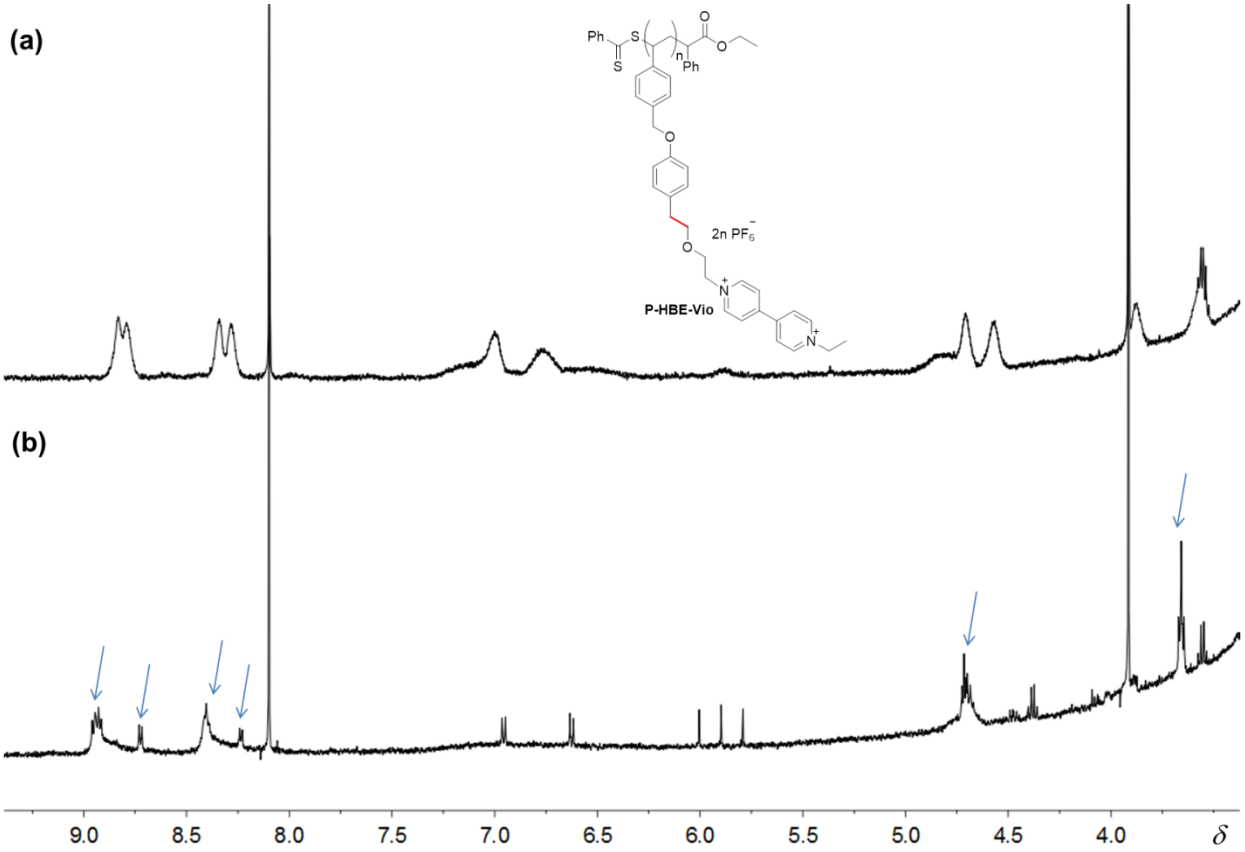

Figure S21. ^{1}H NMR spectra of **P_B-Vio-HBE** (2 mM) in the MeCN solution containing 100 mM $TBAPF_6$ (a) before and (b) after bulk electrolysis. 20% v/v of MeCN-d_3 was added for locking and shimming during NMR collection. The cleavage percentage of HBE linkers (red bonds) cannot be accurately calculated because of either the signal overlapping between remaining polymers and cleaved viologen redox moieties or baseline drift caused by giant signals of electrolytes. After cleavage, originally broad polymer signals disappear, accompanied with the emergence of sharp signals representing the cleaved viologen redox moieties (blue arrows) and other side products from the decomposition of electrolytes.

5 Chemical Trapping Analysis

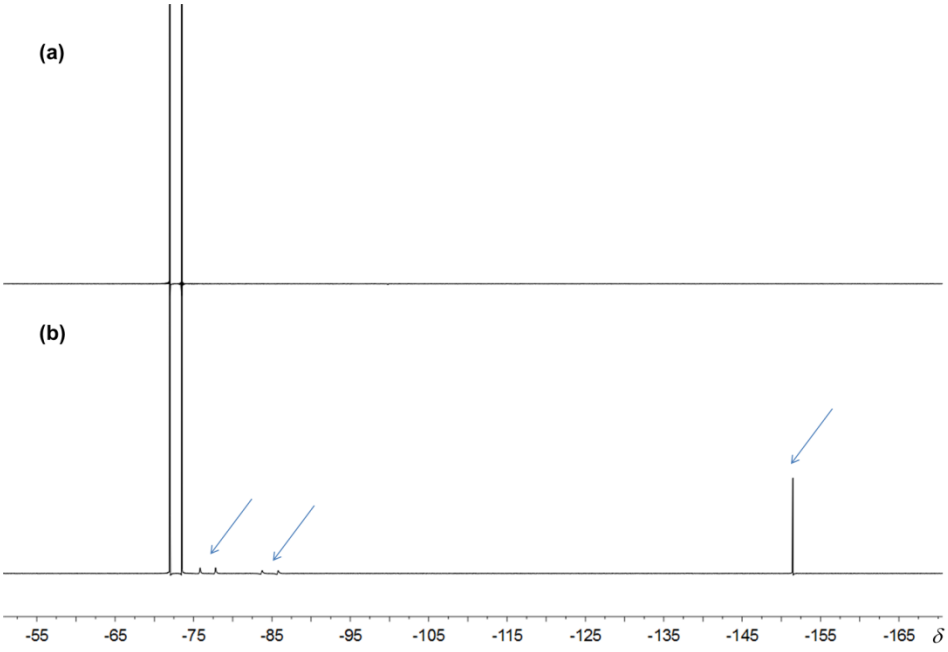

Figure S22. ^{19}F NMR spectra of HBE **2** in the MeCN solution containing 100 mM $TBAPF_6$ (a) before and (b) after bulk electrolysis. 20% v/v of MeCN-d_3 was added for locking and shimming during NMR collection. The arrows in (b) indicate the emergence of new fluorine adducts.

We also examined the mesolytic cleavage of HBEs initiated by a chemical oxidant, ceric ammonium nitrate (CAN), followed by a chemical trapping using a 13C-labled nucleophile. The oxidative capability of CAN is strong enough to oxidize HBEs **2** and **3** into the corresponding radical cations, which further undergo mesolytic cleavage. The generated cations were quenched up by the addition of the 13C-labeled methanol. The trapped dimethoxymethane was observed after comparing the quenched mixtures with the expected trapped products in (b) and (c) (Figures S23 and 24). ^1H NMR spectra comparison confirmed the formation of benzylic ether under the chemical oxidation condition (Figure S26). It might be the benzylic ethers were further oxidized by excess CAN to other species (Figure S17) (S17).

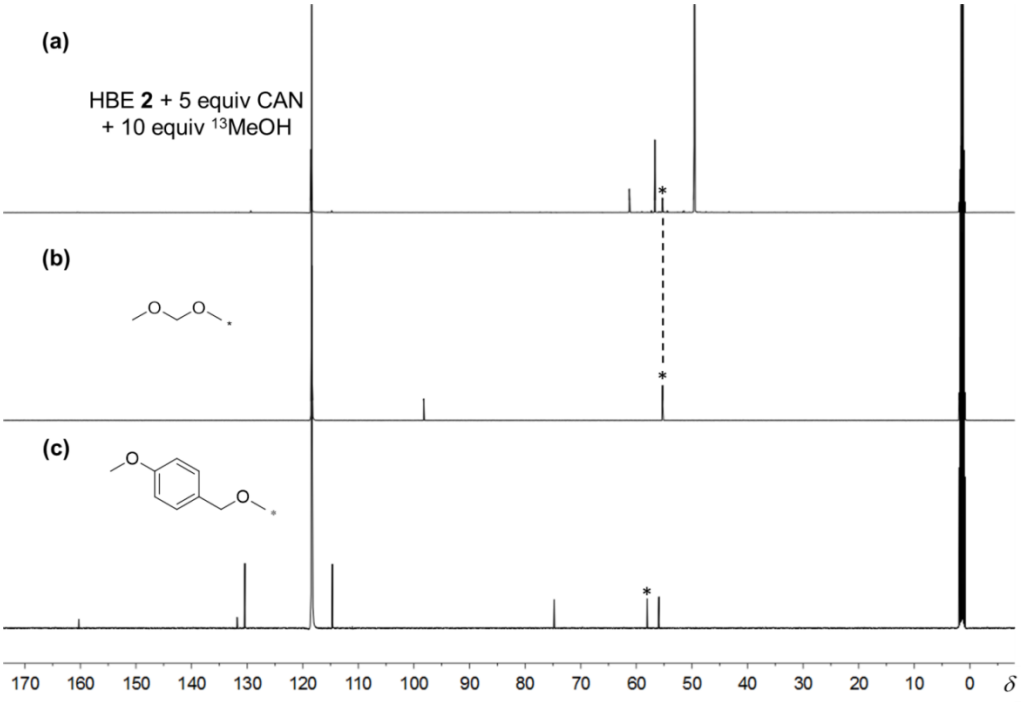

Figure S23. ^{13}C NMR spectra of (a) HBE **2** in the presence of CAN (5 equiv) oxidants and ^{13}MeOH (10 equiv) trapping reagents, and the expected trapped products (b) dimethoxymethane and (c) benzylic ether.

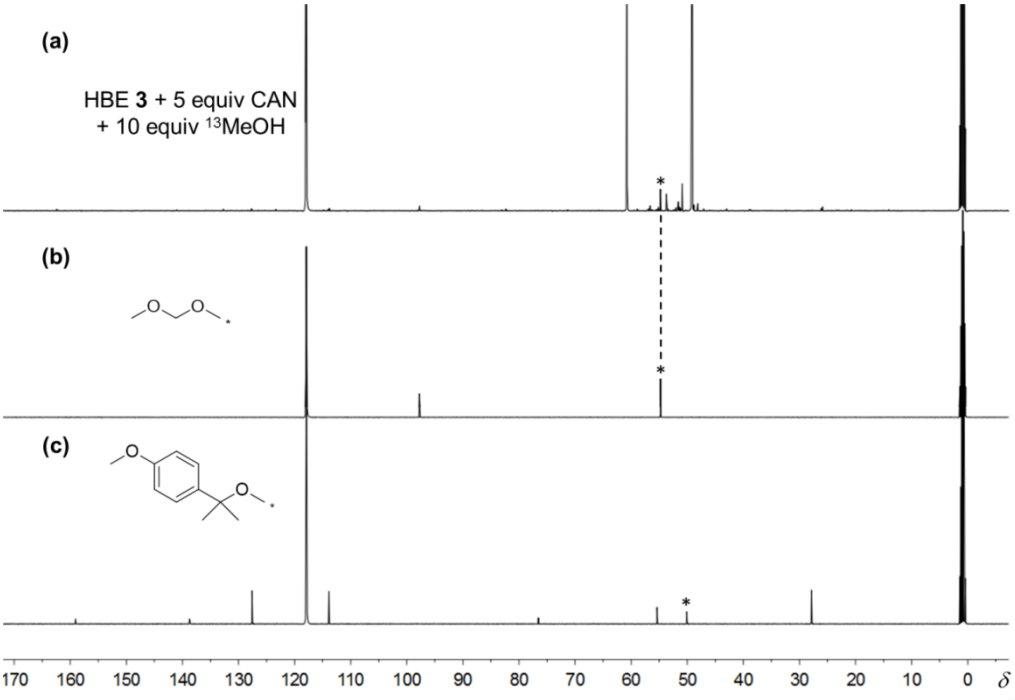

Figure S24. ^{13}C NMR spectra of (a) HBE **3** in the presence of CAN (5 equiv) oxidants and ^{13}MeOH (10 equiv) trapping reagents, and the expected trapped products (b) dimethoxymethane and (c) benzylic ether.

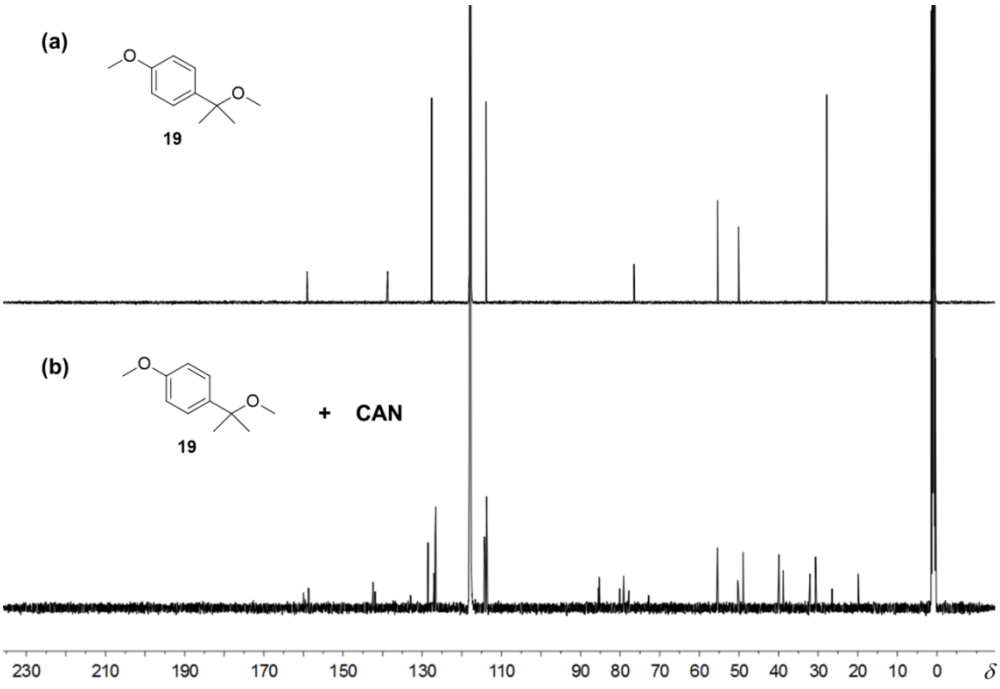

Figure S25. ^{13}C NMR spectra of the compound **19** (126 MHz, MeCN-d_3) in the (a) absence and (b) presence of excess CAN.

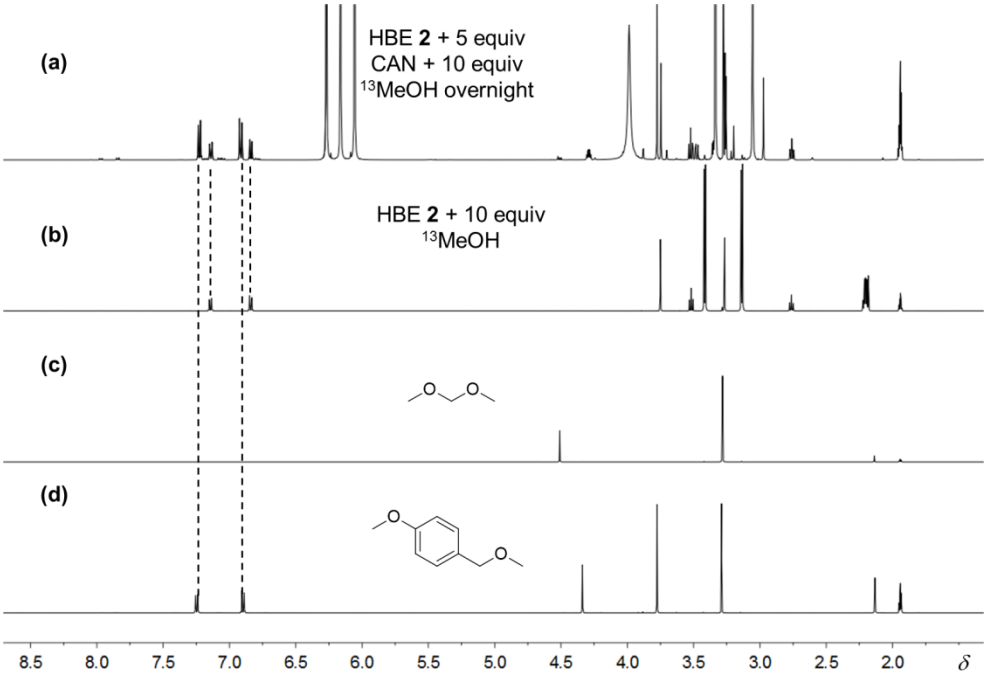

Figure S26. ^{1}H NMR spectra of the mixtures of HBE **2** and $^{13}MeOH$ (10 equiv) trapping reagents in the (a) presence and (b) absence of CAN (5 equiv) oxidants, and the expected trapped products (c) dimethoxymethane and (d) benzylic ether. Small NMR signals in (a) next to the

major aromatic peaks may indicate the formation of trace amounts of dimerized products.

6 Computational Studies

The oxidation potentials, E_{ox}, are computed from the Gibbs free energy change at 298K (ΔG_{ox}) for the elimination of an electron from the species of interest, using the equation (S18):

$$E_{ox}(V\ vs.\ NHE) = \frac{\Delta G_{ox}}{nF} - NHE \quad \text{Eq. S1}$$

where *n* is the number of electrons, *F* is the Faraday constant, and *NHE* is the absolute potential of the normal hydrogen electrode, 4.28 V (S19). To convert E_{ox}(V vs. NHE) to E_{ox}(V vs. Fc/Fc+), we used a constant conversion value of -0.40 V (S20–21).

The bond dissociation Gibbs free energy change of a radical cationic HBE (ΔG) was computed as follows:

$$\Delta G = G_{RC} - (G_R + G_C) \quad \text{Eq. S2}$$

where G_{RC} is the Gibbs free energy of the radical cationic parent molecule, G_R and G_C are the Gibbs free energies of the radical and cationic fragment, respectively.

Similarly, the bond dissociation free energy of a neutral HBE ($BDFE_{Sub}$) were calculated using the following equation:

$$BDFE_{Sub} = G_N - (G_{R1} + G_{R2}) \quad \text{Eq. S3}$$

where G_N is the Gibbs free energy of the neutral parent molecule, G_{R1} and G_{R2} are the Gibbs free energies of the first and second radical fragment, respectively.

In order to keep simulations consistent with CV and GC-MS experiments, all oxidation potentials were computed with implicit MeCN solvent whereas bond dissociation free energies were evaluated in gas phase.

Example Gaussian input:

```
%mem=16GB
%chk=HBE-2.chk
#p b3lyp/6-31+G(d,p) opt(MaxCycles=200) scf(xqc,MaxConventional=200) freq scrf(cpcm,solvent=acetonitrile)
```

O(C)C1=CC=C(C([H])([H])C([H])OC)C=C1 0 1

0 1

O	3.5428	0.5986	1.1043
C	4.6989	0.245	0.3564
C	2.3329	0.4208	0.4917
C	2.1292	-0.0604	-0.8011
C	0.8305	-0.1935	-1.3076
C	-0.2816	0.153	-0.5293
C	-1.6823	0.0125	-1.0814
C	-2.4735	-1.1342	-0.4405
O	-2.9453	-0.8195	0.8726
C	-4.1398	-0.0499	0.8719
C	-0.0695	0.6349	0.7669
C	1.227	0.7662	1.2701
H	4.6972	-0.8212	0.1065
H	4.7914	0.8625	-0.5431
H	5.5746	0.4379	0.9835
H	2.9567	-0.3416	-1.4432
H	0.698	-0.5715	-2.3189
H	-2.1969	0.972	-0.9609
H	-1.62	-0.1725	-2.161
H	-1.8417	-2.0254	-0.3527
H	-3.3248	-1.4065	-1.076
H	-4.4352	0.1223	1.9105
H	-3.9843	0.9205	0.3938
H	-4.9457	-0.5931	0.3691
H	-0.9132	0.9046	1.3986
H	1.3746	1.1385	2.2808

Table S2. Computed oxidation and reduction potentials (w.r.t. Fc/Fc+ reference electrode) of HBEs **1**–**11** and their corresponding mesolytic fragments.

HBE#	SMILES	2D Structure	E_{ox} (V)	E_{red} (V)
1	COCCc1ccc(N(C)C)cc1	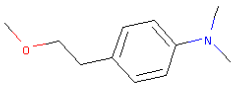	0.37	-3.71
1	[CH3]		2.18	-1.8
1	[N](C)c1ccc(CCOC)cc1	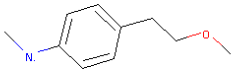	0.82	-1.25
1	[N](C)C		1.85	-1.78

1	[c]1ccc(CCOC)cc1	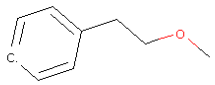	1.35	-1.26
1	[CH2]COC	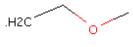	-0.94	-0.51
1	[c]1ccc(N(C)C)cc1	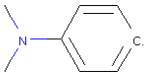	1.1	-1.3
1	[CH2]OC		-0.04	-2.2
1	[CH2]c1ccc(N(C)C)cc1	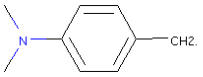	-0.52	-2.01

1	[CH2]Cc1ccc(N(C)C)cc1	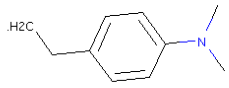	-0.76	-2.21
1	[O]C		-	-0.34
1	[O]CCc1ccc(N(C)C)cc1	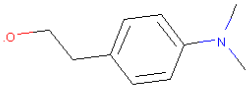	-0.93	-0.39
2	COCCc1ccc(OC)cc1	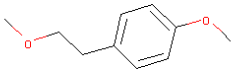	1.14	-3.49
2	[CH3]		2.18	-1.8

2	[O]c1ccc(CCOC)cc1	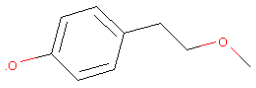	1.45	-0.42
2	[O]C		-	-0.34
2	[c]1ccc(CCOC)cc1	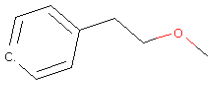	1.35	-1.26
2	[CH2]COC	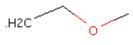	-0.94	-0.51
2	[c]1ccc(OC)cc1	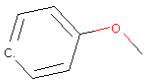	1.43	-1.2

2	[CH2]OC	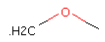	-0.04	-2.2
2	[CH2]c1ccc(OC)cc1	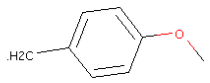	0.01	-1.93
2	[CH2]Cc1ccc(OC)cc1	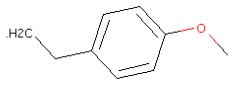	-0.26	-2.19
2	[O]CCc1ccc(OC)cc1	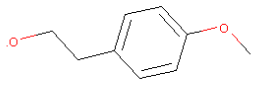	-0.46	-0.32
3	COCC(C)(C)c1ccc(OC)cc1	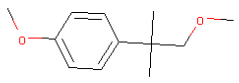	1.19	-3.66

3	[CH3]		2.18	-1.8
3	[O]c1ccc(C(C)(C)COC)cc1	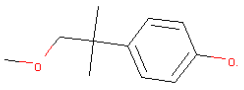	1.46	-0.38
3	[O]C		-	-0.34
3	[c]1ccc(C(C)(C)COC)cc1	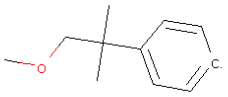	1.34	-1.21
3	[C](C)(C)COC	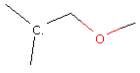	-0.11	-2.42

3	[c]1ccc(OC)cc1	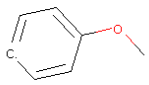	1.43	-1.2
3	[C](C)(COC)c1ccc(OC)cc1	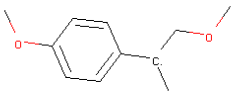	-0.25	-2.04
3	[C](C)(C)c1ccc(OC)cc1	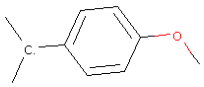	-0.4	-2.32
3	[CH2]OC	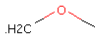	-0.04	-2.2
3	[CH2]C(C)(C)c1ccc(OC)cc1	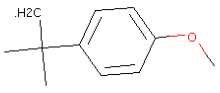	-0.62	-2.16

3	[O]CC(C)(C)c1ccc(OC)cc1	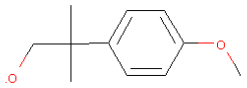	-1.15	-0.4
4	COCCc1ccc(C)cc1	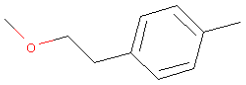	1.6	-3.69
4	[CH3]		2.18	-1.8
4	[c]1ccc(CCOC)cc1	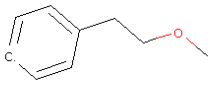	1.35	-1.26
4	[CH2]COC	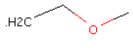	-0.94	-0.51

4	[c]1ccc(C)cc1	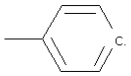	1.37	-1.24
4	[CH2]OC	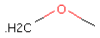	-0.04	-2.2
4	[CH2]c1ccc(C)cc1	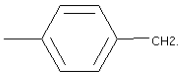	0.24	-1.83
4	[CH2]Cc1ccc(C)cc1	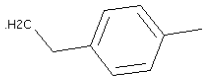	-0.63	-2.24
4	[O]C		-	-0.34

4	[O]CCc1ccc(C)cc1	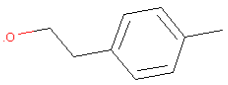	0.05	-0.27
5	COCCc1ccc(-c2ccccc2)cc1	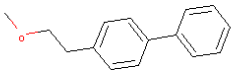	1.32	-2.87
5	[CH2]COC	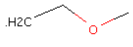	-0.94	-0.51
5	[c]1ccc(-c2ccccc2)cc1	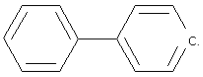	1.44	-1.16
5	[CH2]OC	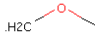	-0.04	-2.2

5	[CH2]c1ccc(-c2ccccc2)cc1	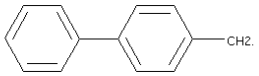	0.29	-1.59
5	[CH2]Cc1ccc(-c2ccccc2)cc1	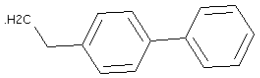	-0.0	-2.16
5	[O]C		-	-0.34
5	[CH3]		2.18	-1.8
5	[O]CCc1ccc(-c2ccccc2)cc1	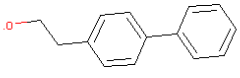	-0.18	-0.35

6	COCCc1ccccc1	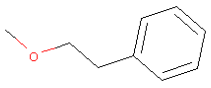	1.83	-3.6
6	[CH2]COC	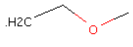	-0.94	-0.51
6	[c]1ccccc1		1.42	-1.22
6	[CH2]OC	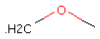	-0.04	-2.2
6	[CH2]c1ccccc1	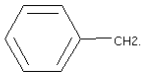	0.48	-1.72

6	[CH2]Cc1ccccc1	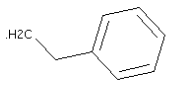	0.1	-2.09
6	[O]C		-	-0.34
6	[CH3]		2.18	-1.8
6	[O]CCc1ccccc1	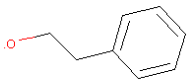	0.13	-0.32
7	COCCc1ccc(Br)cc1	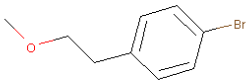	1.76	-2.11

7	[Br]		6.05	1.56
7	[c]1ccc(CCOC)cc1	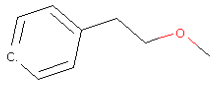	1.35	-1.26
7	[CH2]COC	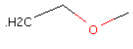	-0.94	-0.51
7	[c]1ccc(Br)cc1	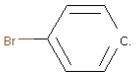	1.67	-1.02
7	[CH2]OC		-0.04	-2.2

7	[CH2]c1ccc(Br)cc1	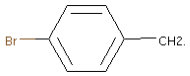	0.52	-1.6
7	[CH2]Cc1ccc(Br)cc1	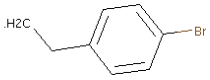	-0.42	-2.07
7	[O]C		-	-0.34
7	[CH3]		2.18	-1.8
7	[O]CCc1ccc(Br)cc1	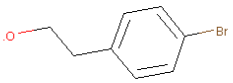	0.19	-0.23

8	COCCc1ccc([N+](C)(C)C)cc1	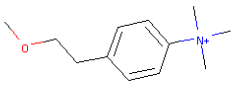	2.27	-2.85
8	[N+](C)(C)c1ccc(CCOC)cc1	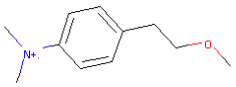	2.07	-
8	[N+](C)(C)C		-	-
8	[c]1ccc(CCOC)cc1	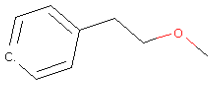	-	1.35
8	[c]1ccc(CCOC)cc1	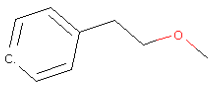	1.35	-1.26

8	[CH2]COC	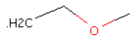	-0.94	-0.51
8	[CH2]COC	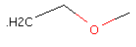	-	-0.94
8	[c]1ccc([N+](C)(C)C)cc1	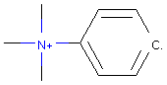	2.05	-
8	[CH2]c1ccc([N+](C)(C)C)cc1	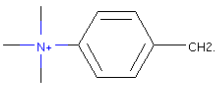	1.02	-
8	[CH2]Cc1ccc([N+](C)(C)C)cc1	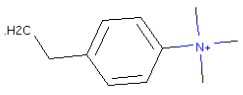	-0.05	-

8	[O]CCc1ccc([N+](C)(C)C)cc1	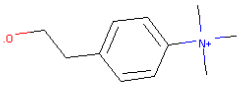	1.03	-
9	COCCc1ccc(C=O)cc1	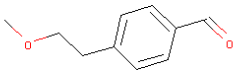	2.12	-2.13
9	[CH]=O		0.99	-1.64
9	[c]1ccc(CCOC)cc1	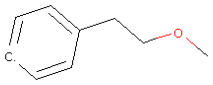	1.35	-1.26
9	[CH2]COC	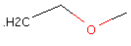	-0.94	-0.51

9	[c]1ccc(C=O)cc1	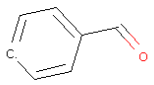	1.71	-0.95
9	[CH2]OC	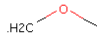	-0.04	-2.2
9	[CH2]c1ccc(C=O)cc1	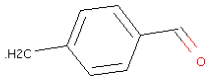	0.91	-0.98
9	[CH2]Cc1ccc(C=O)cc1	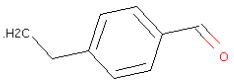	0.43	-1.93
9	[O]C		-	-0.34

9	[CH3]		2.18	-1.8
9	[O]CCc1ccc(C=O)cc1	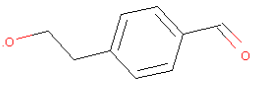	0.21	-0.24
10	COCCc1ccc(C#N)cc1	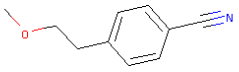	2.08	-2.54
10	[C]#N		7.48	2.09
10	[c]1ccc(CCOC)cc1	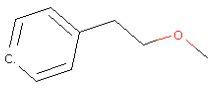	1.35	-1.26

10	[CH2]COC	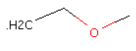	-0.94	-0.51
10	[c]1ccc(C#N)cc1	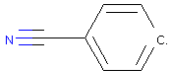	1.86	-0.9
10	[CH2]OC	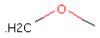	-0.04	-2.2
10	[CH2]c1ccc(C#N)cc1	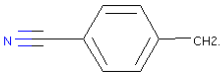	0.94	-1.12
10	[CH2]Cc1ccc(C#N)cc1	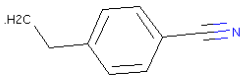	0.47	-1.97

10	[O]C		-	-0.34
10	[CH3]		2.18	-1.8
10	[O]CCc1ccc(C#N)cc1	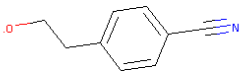	0.25	-0.24
11	COCCc1ccc([N+](=O)[O-])cc1	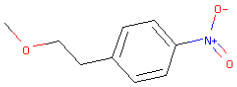	2.2	-1.18
11	[N+](=O)[O-]		2.54	0.39

11	[c]1ccc(CCOC)cc1	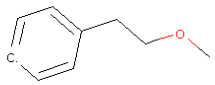	1.35	-1.26
11	[CH2]COC	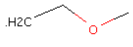	-0.94	-0.51
11	[c]1ccc([N+](=O)[O-])cc1	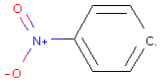	1.98	-0.78
11	[CH2]OC		-0.04	-2.2
11	[CH2]c1ccc([N+](=O)[O-])cc1	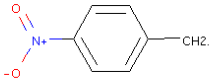	1.12	-0.57

11	[CH2]Cc1ccc([N+](=O)[O-])cc1	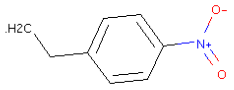	-0.0	-0.89
11	[O]C		-	-0.34
11	[CH3]		2.18	-1.8
11	[O]CCc1ccc([N+](=O)[O-])cc1	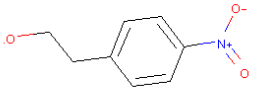	0.56	-0.16

Table S3. Computed gas-phase Gibbs free energy (in eV) of mesolytic cleavage reactions for HBEs **1–11**.

HBE #	Cationic radical parent	Radical Fragment	Cationic Fragment	ΔG
1	CN(C1=CC=C(C=C1)CCOC)C	*COC	*Cc1ccc(cc1)N(C)C	1.86
1	CN(C1=CC=C(C=C1)CCOC)C	*C	*OCCc1ccc(cc1)N(C)C	2.08
1	CN(C1=CC=C(C=C1)CCOC)C	*OC	*CCc1ccc(cc1)N(C)C	2.10
1	CN(C1=CC=C(C=C1)CCOC)C	*C	*N(C)c1ccc(cc1)CCOC	3.12
1	CN(C1=CC=C(C=C1)CCOC)C	*Cc1ccc(cc1)N(C)C	*COC	3.16
1	CN(C1=CC=C(C=C1)CCOC)C	*c1ccc(cc1)N(C)C	*CCOC	3.43
1	CN(C1=CC=C(C=C1)CCOC)C	*CCOC	*c1ccc(cc1)N(C)C	5.14
1	CN(C1=CC=C(C=C1)CCOC)C	*N(C)C	*c1ccc(cc1)CCOC	5.24
1	CN(C1=CC=C(C=C1)CCOC)C	*N(C)c1ccc(cc1)CCOC	*C	5.93
1	CN(C1=CC=C(C=C1)CCOC)C	*c1ccc(cc1)CCOC	*N(C)C	6.01
1	CN(C1=CC=C(C=C1)CCOC)C	*OCCc1ccc(cc1)N(C)C	*C	6.58
2	COC1=CC=C(C=C1)CCOC	*COC	*Cc1ccc(cc1)OC	1.79
2	COC1=CC=C(C=C1)CCOC	*OC	*CCc1ccc(cc1)OC	1.92
2	COC1=CC=C(C=C1)CCOC	*Cc1ccc(cc1)OC	*COC	2.43
2	COC1=CC=C(C=C1)CCOC	*c1ccc(cc1)OC	*CCOC	2.65
2	COC1=CC=C(C=C1)CCOC	*C	*Oc1ccc(cc1)CCOC	3.03
2	COC1=CC=C(C=C1)CCOC	*OC	*c1ccc(cc1)CCOC	4.84
2	COC1=CC=C(C=C1)CCOC	*Oc1ccc(cc1)CCOC	*C	4.92
2	COC1=CC=C(C=C1)CCOC	*CCOC	*c1ccc(cc1)OC	4.95
2	COC1=CC=C(C=C1)CCOC	*OCCc1ccc(cc1)OC	*C	5.78
3	COC1=CC=C(C=C1)C(C)(COC)C	*COC	*C(C)(C)c1ccc(cc1)OC	0.99
3	COC1=CC=C(C=C1)C(C)(COC)C	*C	*OCC(C)(C)c1ccc(cc1)OC	1.23
3	COC1=CC=C(C=C1)C(C)(CO	*C	*C(C)(COC)c1ccc(cc	1.36

	C)C		1)OC	
3	COC1=CC=C(C=C1)C(C)(COC)C	*OC	*CC(C)(C)c1ccc(cc1)OC	1.54
3	COC1=CC=C(C=C1)C(C)(COC)C	*C(C)(C)c1ccc(cc1)OC	*COC	2.16
3	COC1=CC=C(C=C1)C(C)(COC)C	*c1ccc(cc1)OC	*C(C)(C)COC	2.92
3	COC1=CC=C(C=C1)C(C)(COC)C	*C	*Oc1ccc(cc1)C(C)(C)COC	3.02
3	COC1=CC=C(C=C1)C(C)(COC)C	*OC	*c1ccc(cc1)C(C)(C)COC	4.45
3	COC1=CC=C(C=C1)C(C)(COC)C	*C(C)(C)COC	*c1ccc(cc1)OC	4.47
3	COC1=CC=C(C=C1)C(C)(COC)C	*Oc1ccc(cc1)C(C)(C)COC	*C	4.92
3	COC1=CC=C(C=C1)C(C)(COC)C	*C(C)(COC)c1ccc(cc1)OC	*C	5.35
3	COC1=CC=C(C=C1)C(C)(COC)C	*OCC(C)(C)c1ccc(cc1)OC	*C	5.76
4	CC1=CC=C(C=C1)CCOC	*OC	*CCc1ccc(C)cc1	1.22
4	CC1=CC=C(C=C1)CCOC	*COC	*Cc1ccc(C)cc1	1.77
4	CC1=CC=C(C=C1)CCOC	*Cc1ccc(C)cc1	*COC	2.00
4	CC1=CC=C(C=C1)CCOC	*c1ccc(C)cc1	*CCOC	2.19
4	CC1=CC=C(C=C1)CCOC	*CCOC	*c1ccc(C)cc1	4.46
4	CC1=CC=C(C=C1)CCOC	*C	*c1ccc(cc1)CCOC	4.62
4	CC1=CC=C(C=C1)CCOC	*OCCc1ccc(C)cc1	*C	5.41
4	CC1=CC=C(C=C1)CCOC	*c1ccc(cc1)CCOC	*C	6.30
5	COCCC(C=C1)=CC=C1C2=CC=CC=C2	*COC	*Cc1ccc(cc1)-c1ccccc1	1.94
5	COCCC(C=C1)=CC=C1C2=CC=CC=C3	*OC	*CCc1ccc(cc1)-c1ccccc1	2.10
5	COCCC(C=C1)=CC=C1C2=CC=CC=C4	*C	*OCCc1ccc(cc1)-c1ccccc1	2.18
5	COCCC(C=C1)=CC=C1C2=CC=CC=C5	*Cc1ccc(cc1)-c1ccccc1	*COC	2.42
5	COCCC(C=C1)=CC=C1C2=CC=CC=C6	*c1ccc(cc1)-c1ccccc1	*CCOC	2.63
5	COCCC(C=C1)=CC=C1C2=CC=CC=C7	*CCOC	*c1ccc(cc1)-c1ccccc1	4.85
5	COCCC(C=C1)=CC=C1C2=C	*c1ccccc1	*c1ccc(cc1)CCOC	5.53

	C=CC=C8			
5	COCCC(C=C1)=CC=C1C2=CC=CC=C9	*c1ccc(cc1)CCOC	*c1ccccc1	5.65
5	COCCC(C=C1)=CC=C1C2=CC=CC=C10	*OCCc1ccc(cc1)-c1ccccc1	*C	5.79
6	COCCC1=CC=CC=C1	*Cc1ccccc1	*COC	1.74
6	COCCC1=CC=CC=C2	*OC	*CCc1ccccc1	1.78
6	COCCC1=CC=CC=C3	*COC	*Cc1ccccc1	1.81
6	COCCC1=CC=CC=C4	*c1ccccc1	*CCOC	1.90
6	COCCC1=CC=CC=C5	*C	*OCCc1ccccc1	2.03
6	COCCC1=CC=CC=C6	*CCOC	*c1ccccc1	4.31
6	COCCC1=CC=CC=C7	*OCCc1ccccc1	*C	5.14
7	BrC1=CC=C(C=C1)CCOC	*Cc1ccc(Br)cc1	*COC	1.86
7	BrC1=CC=C(C=C1)CCOC	*COC	*Cc1ccc(Br)cc1	1.91
7	BrC1=CC=C(C=C1)CCOC	*OC	*CCc1ccc(Br)cc1	1.97
7	BrC1=CC=C(C=C1)CCOC	*C	*OCCc1ccc(Br)cc1	2.01
7	BrC1=CC=C(C=C1)CCOC	*c1ccc(Br)cc1	*CCOC	2.14
7	BrC1=CC=C(C=C1)CCOC	*Br	*c1ccc(cc1)CCOC	3.98
7	BrC1=CC=C(C=C1)CCOC	*CCOC	*c1ccc(Br)cc1	4.81
7	BrC1=CC=C(C=C1)CCOC	*OCCc1ccc(Br)cc1	*C	5.30
7	BrC1=CC=C(C=C1)CCOC	*c1ccc(cc1)CCOC	*Br	9.63
8	C[N+](C)(C)C1=CC=C(C=C1)CCOC	*Cc1ccc(cc1)[N+](C)(C)C	*COC	-1.26
8	C[N+](C)(C)C1=CC=C(C=C1)CCOC	*c1ccc(cc1)[N+](C)(C)C	*CCOC	-0.94
8	C[N+](C)(C)C1=CC=C(C=C1)CCOC	*[N+](C)(C)C	*c1ccc(cc1)CCOC	0.56
8	C[N+](C)(C)C1=CC=C(C=C1)CCOC	*[N+](C)(C)c1ccc(cc1)CCOC	*C	0.70
8	C[N+](C)(C)C1=CC=C(C=C1)CCOC	*C	*OCCc1ccc(cc1)[N+](C)(C)C	1.53
8	C[N+](C)(C)C1=CC=C(C=C1)CCOC	*OC	*CCc1ccc(cc1)[N+](C)(C)C	1.54
8	C[N+](C)(C)C1=CC=C(C=C1)CCOC	*OCCc1ccc(cc1)[N+](C)(C)C	*C	2.07
8	C[N+](C)(C)C1=CC=C(C=C1)CCOC	*COC	*Cc1ccc(cc1)[N+](C)(C)C	2.40
8	C[N+](C)(C)C1=CC=C(C=C1)CCOC	*CCOC	*c1ccc(cc1)[N+](C)(C)C	5.26
8	C[N+](C)(C)C1=CC=C(C=C1	*c1ccc(cc1)CCOC	*[N+](C)(C)C	8.02

	)CCOC			
9	O=CC1=CC=C(C=C1)CCOC	*Cc1ccc(C=O)cc1	*COC	1.35
9	O=CC1=CC=C(C=C1)CCOC	*c1ccc(C=O)cc1	*CCOC	1.60
9	O=CC1=CC=C(C=C1)CCOC	*OC	*CCc1ccc(C=O)cc1	1.85
9	O=CC1=CC=C(C=C1)CCOC	*C	*OCCc1ccc(C=O)cc1	1.88
9	O=CC1=CC=C(C=C1)CCOC	*COC	*Cc1ccc(C=O)cc1	1.90
9	O=CC1=CC=C(C=C1)CCOC	*C=O	*c1ccc(cc1)CCOC	3.92
9	O=CC1=CC=C(C=C1)CCOC	*c1ccc(cc1)CCOC	*C=O	4.22
9	O=CC1=CC=C(C=C1)CCOC	*CCOC	*c1ccc(C=O)cc1	4.42
9	O=CC1=CC=C(C=C1)CCOC	*OCCc1ccc(C=O)cc1	*C	4.77
10	N#CC1=CC=C(C=C1)CCOC	*Cc1ccc(C#N)cc1	*COC	1.31
10	N#CC1=CC=C(C=C1)CCOC	*c1ccc(C#N)cc1	*CCOC	1.55
10	N#CC1=CC=C(C=C1)CCOC	*OC	*CCc1ccc(C#N)cc1	1.93
10	N#CC1=CC=C(C=C1)CCOC	*COC	*Cc1ccc(C#N)cc1	1.97
10	N#CC1=CC=C(C=C1)CCOC	*CCOC	*c1ccc(C#N)cc1	4.63
10	N#CC1=CC=C(C=C1)CCOC	*OCCc1ccc(C#N)cc1	*C	4.70
10	N#CC1=CC=C(C=C1)CCOC	*C#N	*c1ccc(cc1)CCOC	5.43
10	N#CC1=CC=C(C=C1)CCOC	*c1ccc(cc1)CCOC	*C#N	12.39
11	O=[N+](C1=CC=C(C=C1)CCOC)[O-]	*Cc1ccc(cc1)[N+](=O)[O-]	*COC	1.05
11	O=[N+](C1=CC=C(C=C1)CCOC)[O-]	*c1ccc(cc1)[N+](=O)[O-]	*CCOC	1.32
11	O=[N+](C1=CC=C(C=C1)CCOC)[O-]	*C	*OCCc1ccc(cc1)[N+](=O)[O-]	1.77
11	O=[N+](C1=CC=C(C=C1)CCOC)[O-]	*OC	*CCc1ccc(cc1)[N+](=O)[O-]	1.87
11	O=[N+](C1=CC=C(C=C1)CCOC)[O-]	*COC	*Cc1ccc(cc1)[N+](=O)[O-]	1.97
11	O=[N+](C1=CC=C(C=C1)CCOC)[O-]	*[N+](=O)[O-]	*c1ccc(cc1)CCOC	2.42
11	O=[N+](C1=CC=C(C=C1)CCOC)[O-]	*OCCc1ccc(cc1)[N+](=O)[O-]	*C	4.46
11	O=[N+](C1=CC=C(C=C1)CCOC)[O-]	*CCOC	*c1ccc(cc1)[N+](=O)[O-]	4.54
11	O=[N+](C1=CC=C(C=C1)CCOC)[O-]	*[N+](=O)c1ccc(cc1)CCOC	*[O-]	5.63

Table S4. Spin density surface of oxidized HBEs. Positive and negative regions are shown in turquoise and dark red, respectively.

HBE #	2D Structure	Optimized Geometry
1	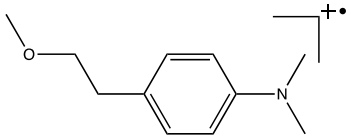	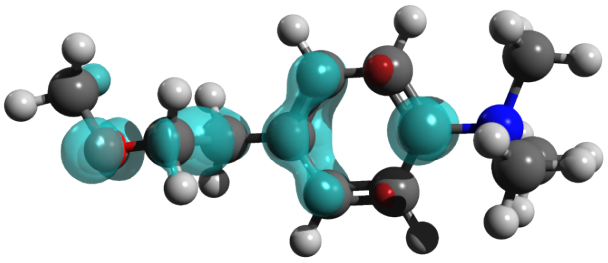
2	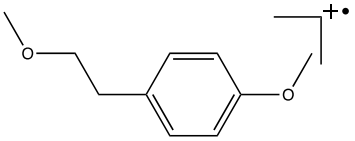	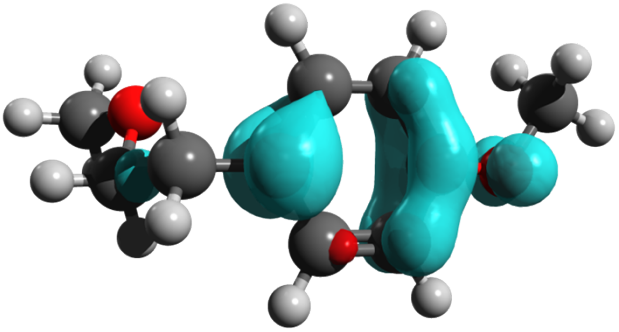
3	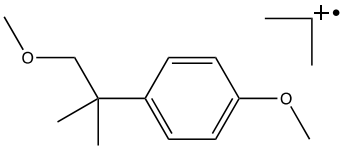	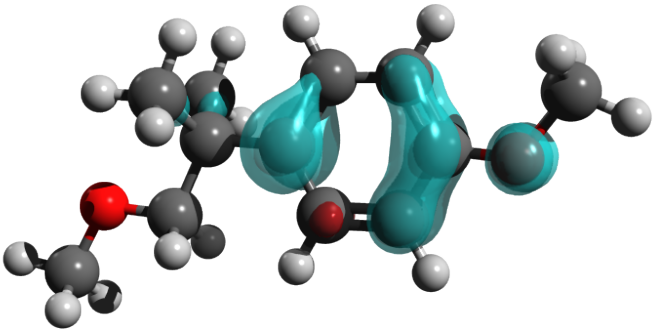
4	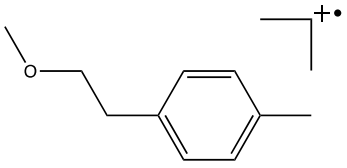	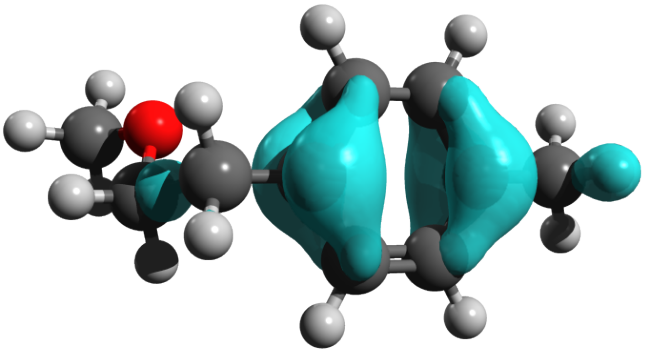

5	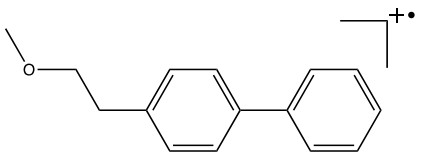	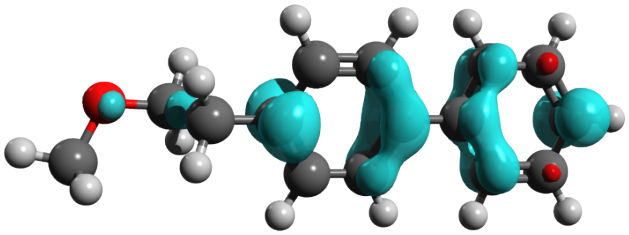
6	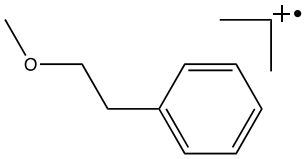	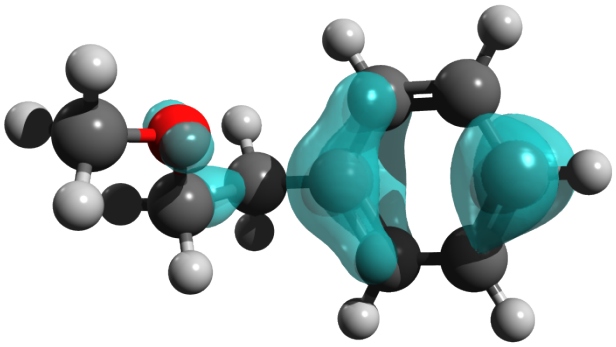
7	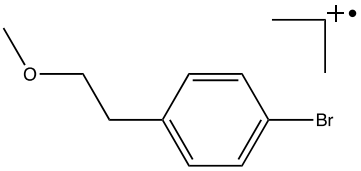	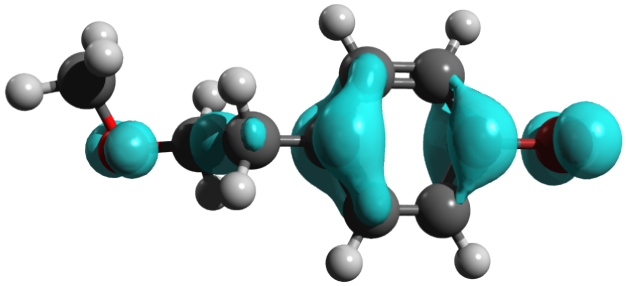
8	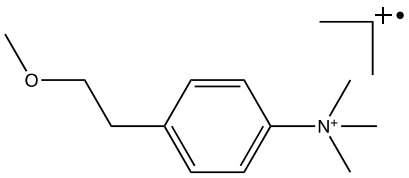	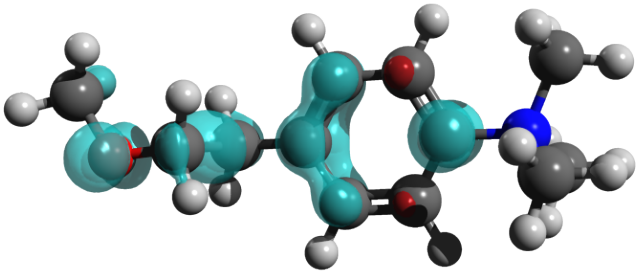
9	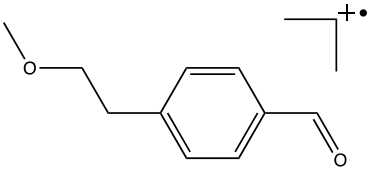	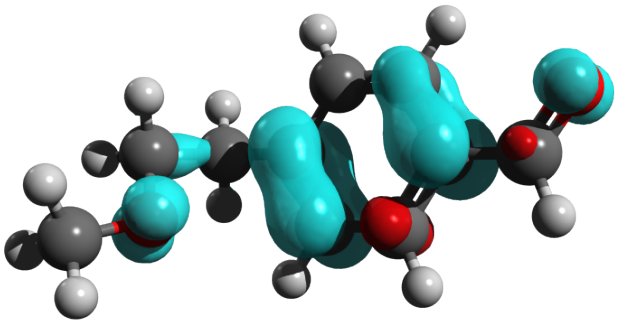

10	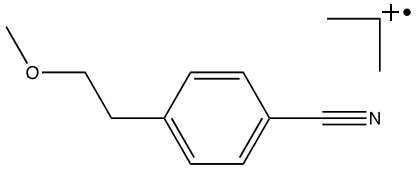	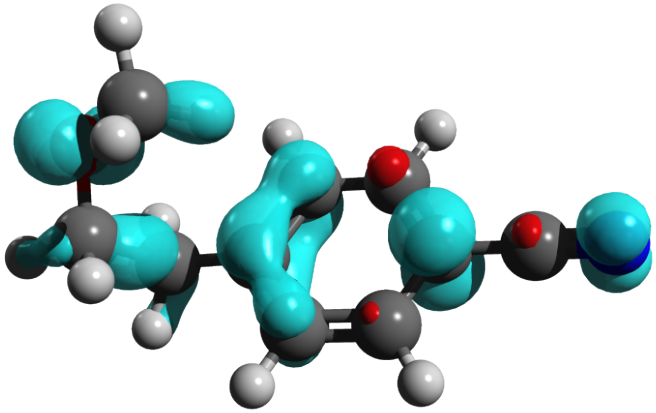
11	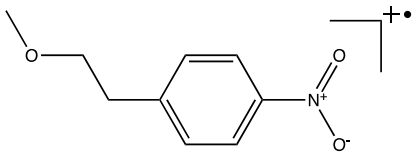	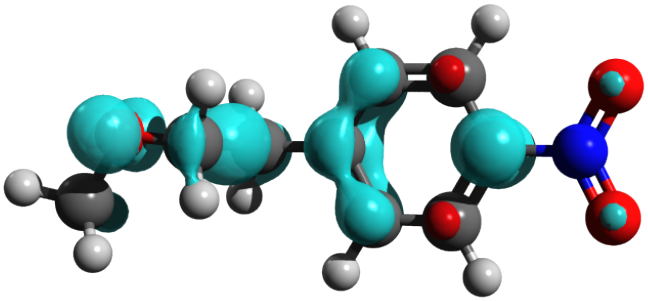

7 NMR Spectra

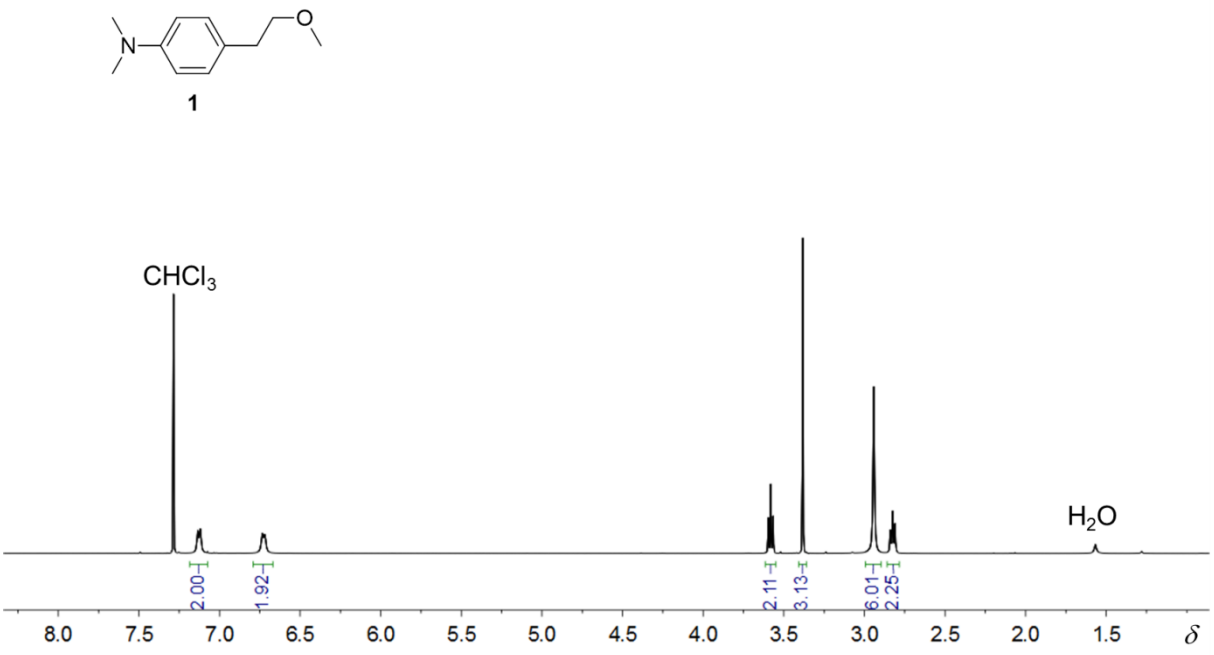

Figure S27. ^{1}H NMR spectrum of **1** (500 MHz, $CDCl_3$).

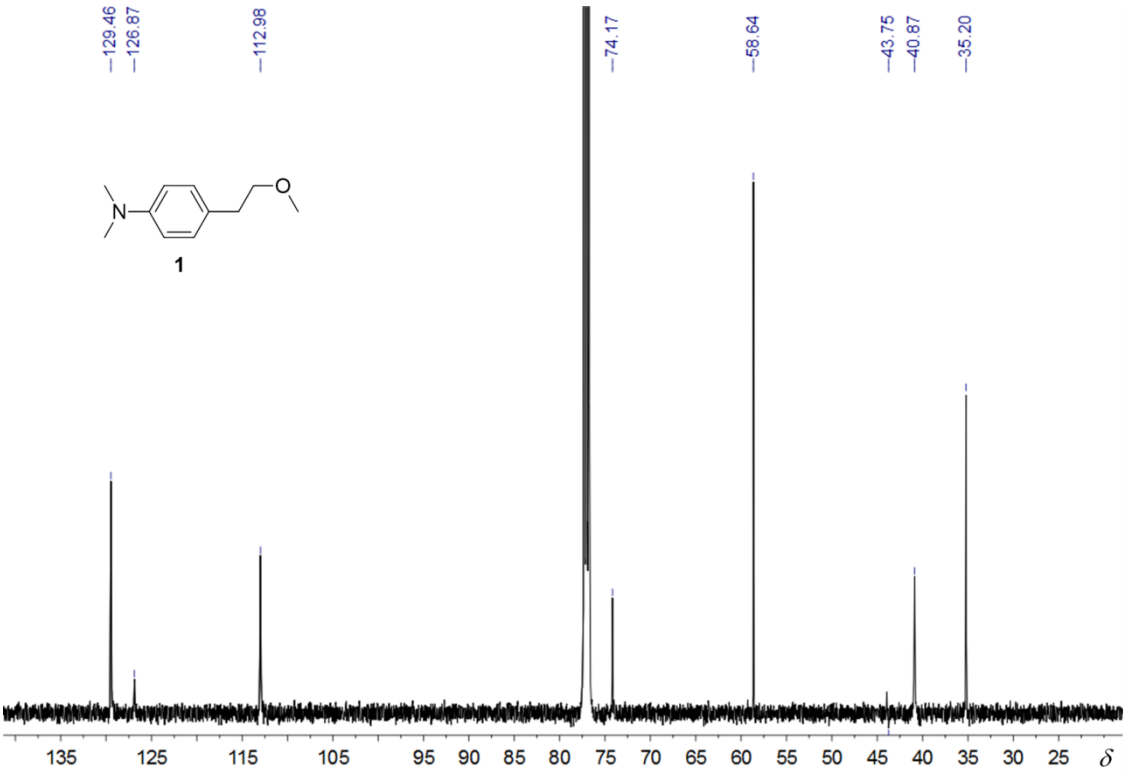

Figure S28. ^{13}C NMR spectrum of **1** (126 MHz, $CDCl_3$).

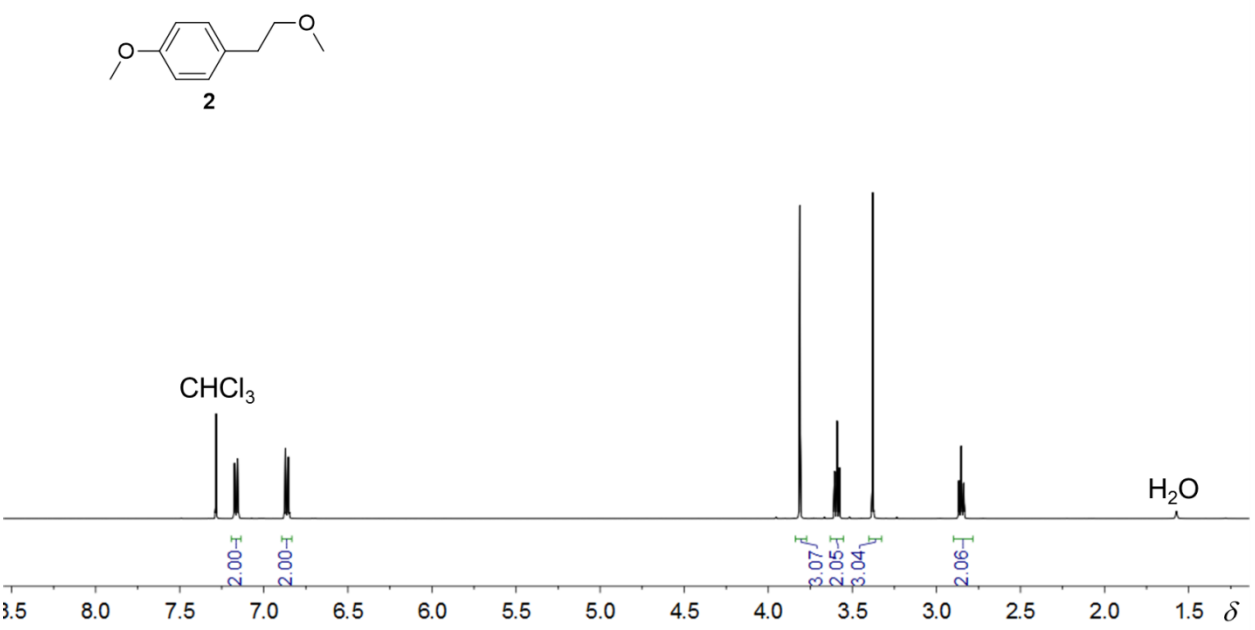

Figure S29. ^{1}H NMR spectrum of **2** (500 MHz, $CDCl_3$).

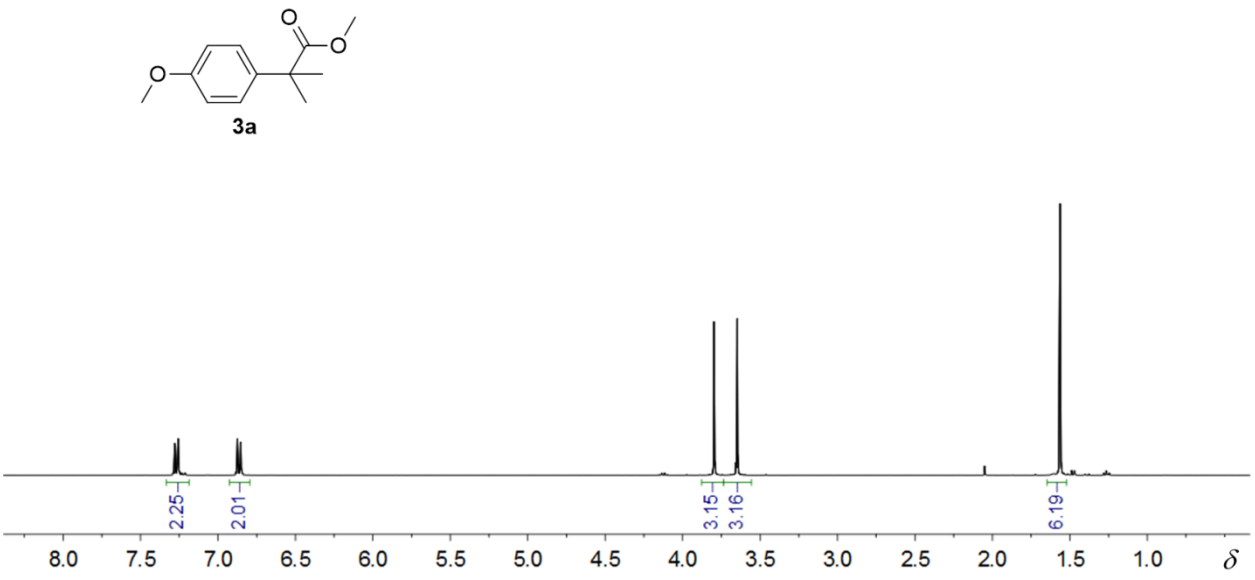

Figure S30. ^{1}H NMR spectrum of **3a** (500 MHz, $CDCl_3$).

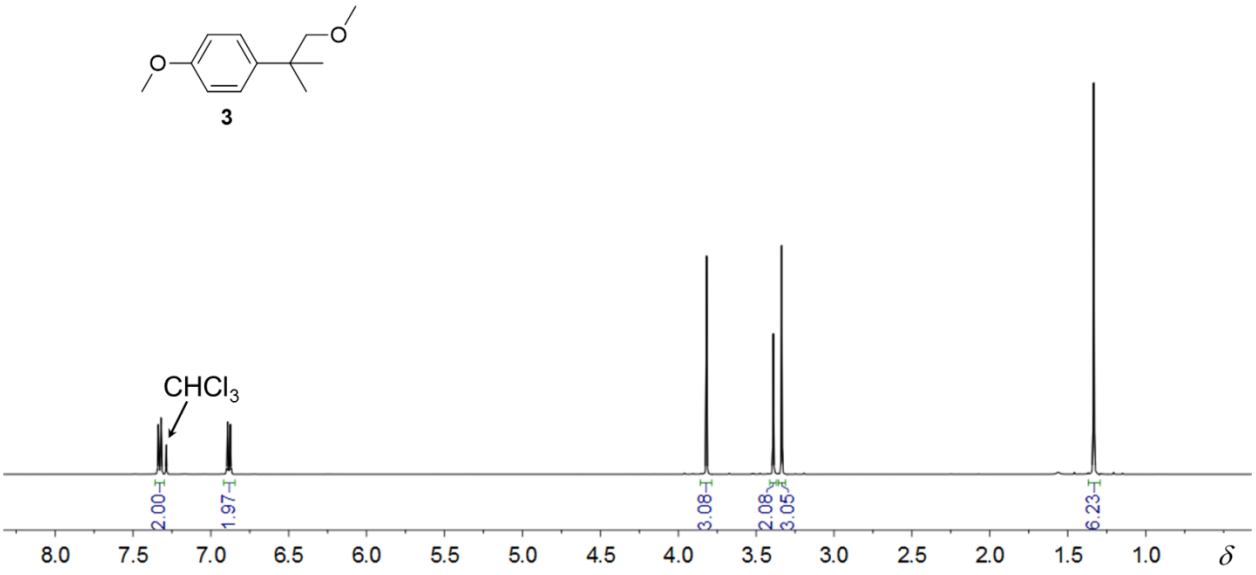

Figure S31. ^{1}H NMR spectrum of **3** (500 MHz, $CDCl_3$).

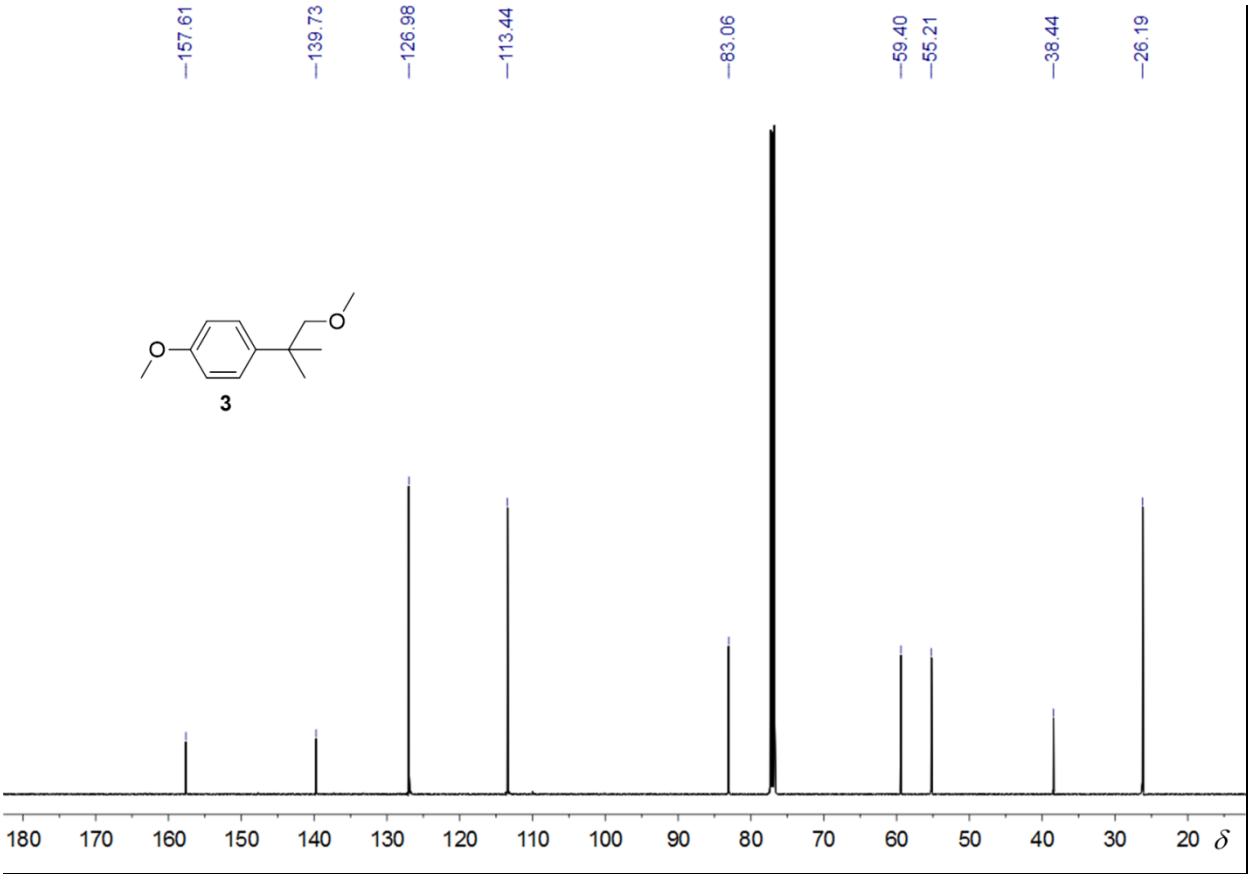

Figure S32. ^{13}C NMR spectrum of **3** (126 MHz, $CDCl_3$).

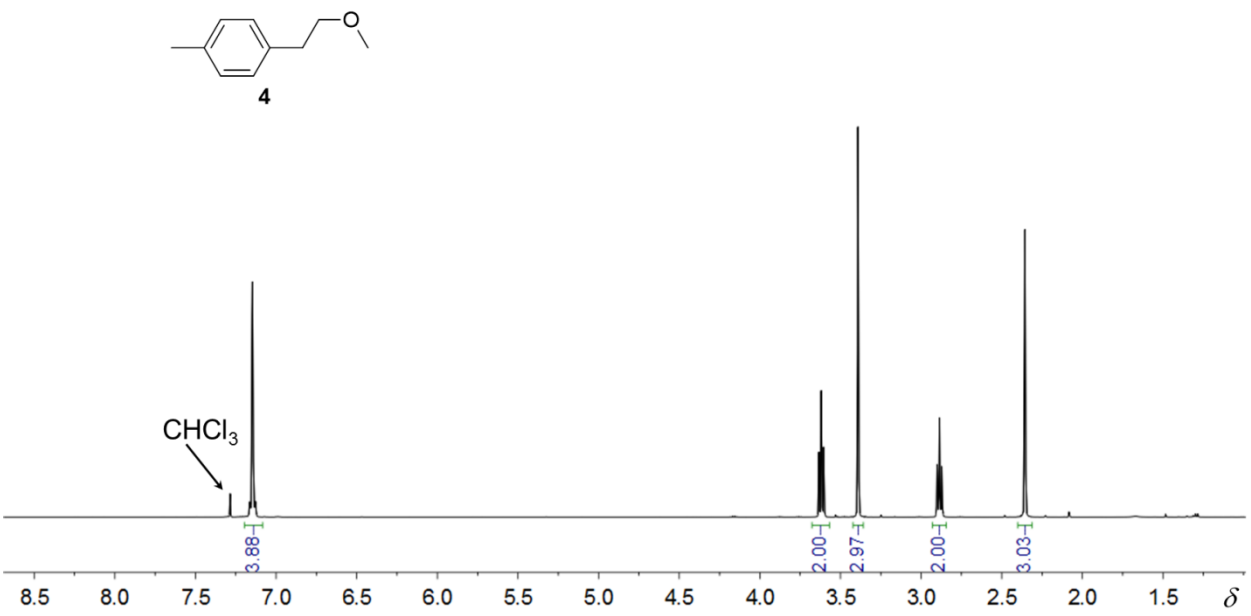

Figure S33. ^{1}H NMR spectrum of **4** (500 MHz, $CDCl_3$).

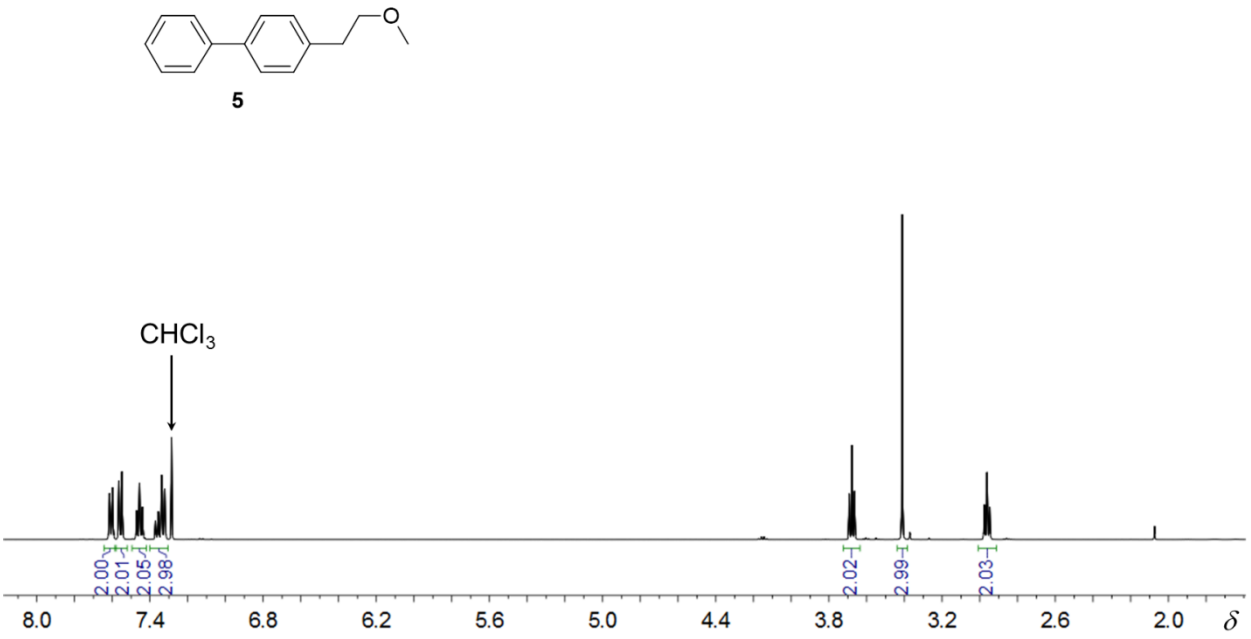

Figure S34. ^{1}H NMR spectrum of **5** (500 MHz, $CDCl_3$).

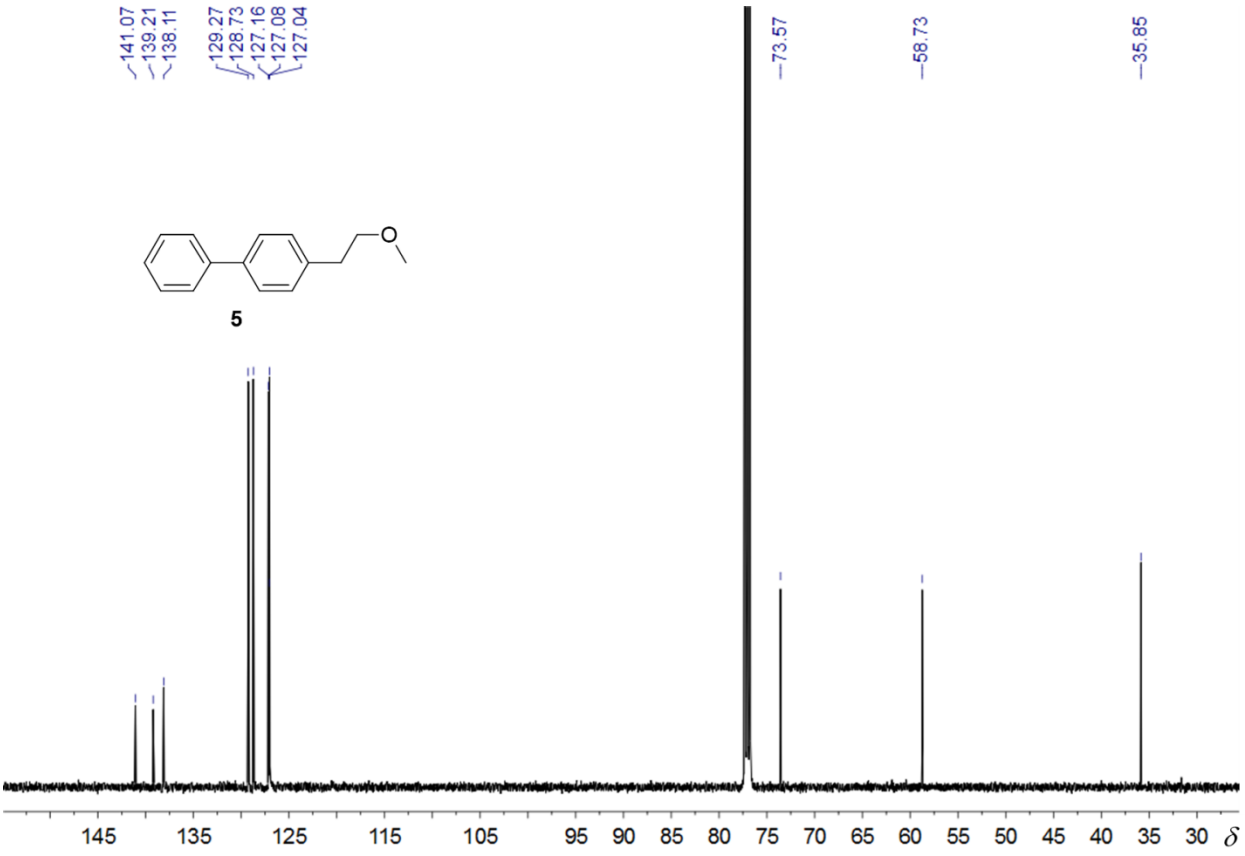

Figure S35. ^{13}C NMR spectrum of **5** (126 MHz, $CDCl_3$).

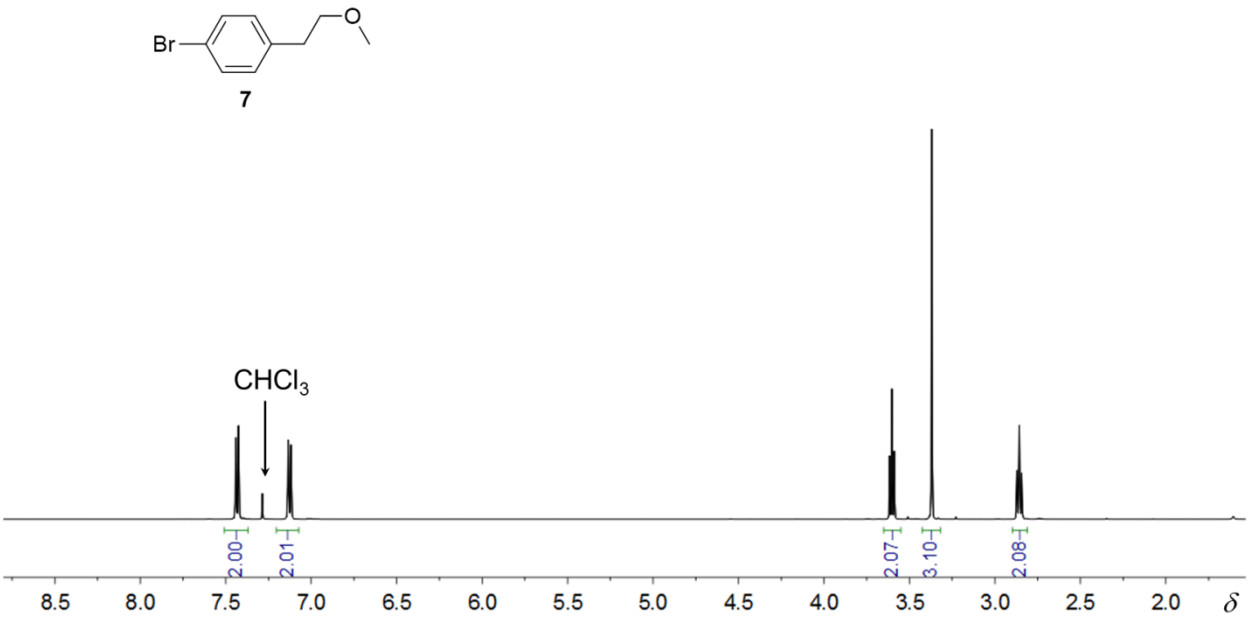

Figure S36. ^{1}H NMR spectrum of **7** (500 MHz, $CDCl_3$).

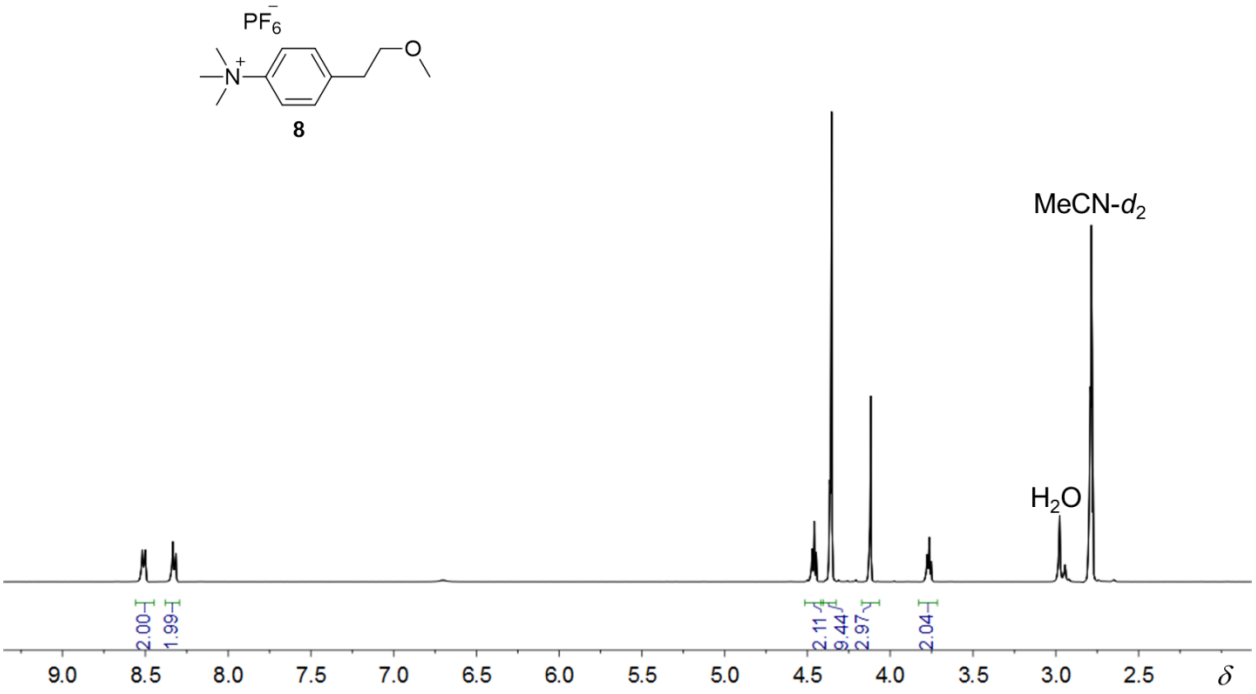

Figure S37. ^{1}H NMR spectrum of **8** (500 MHz, MeCN-d_3).

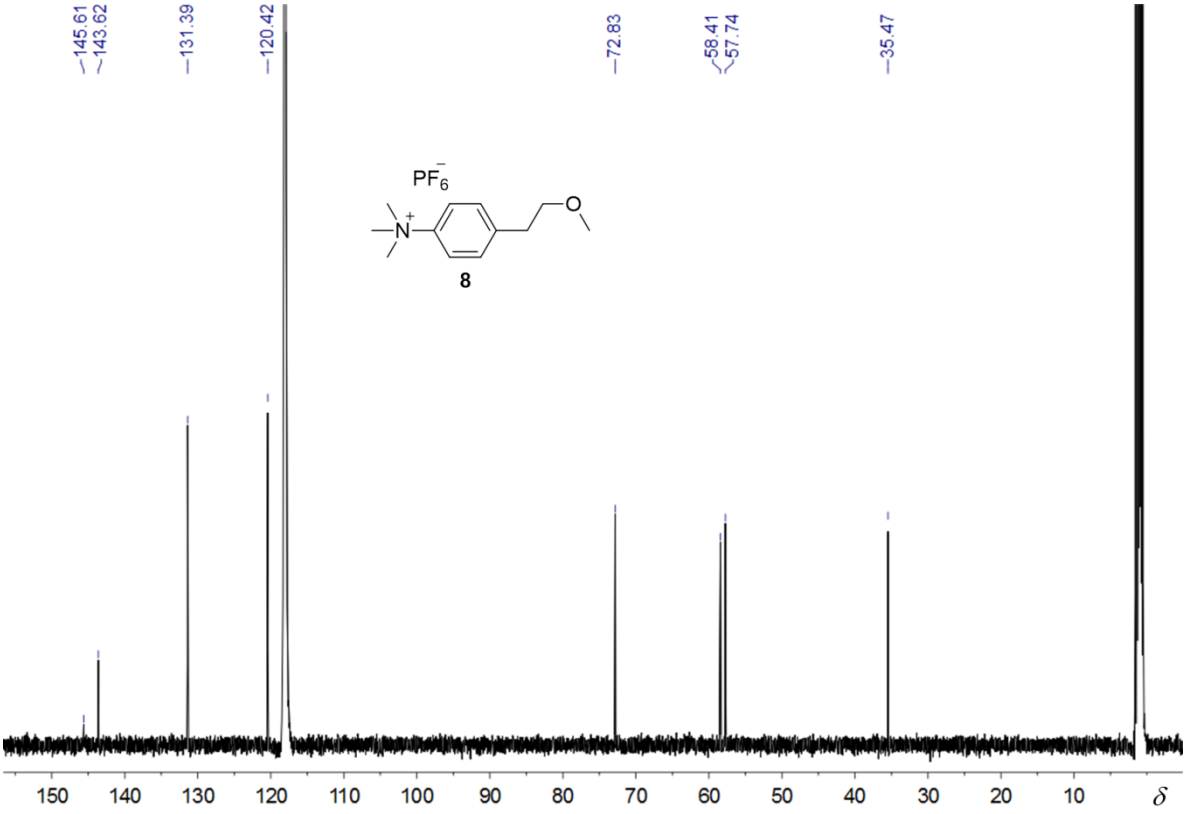

Figure S38. ^{13}C NMR spectrum of **8** (126 MHz, MeCN-d_3).

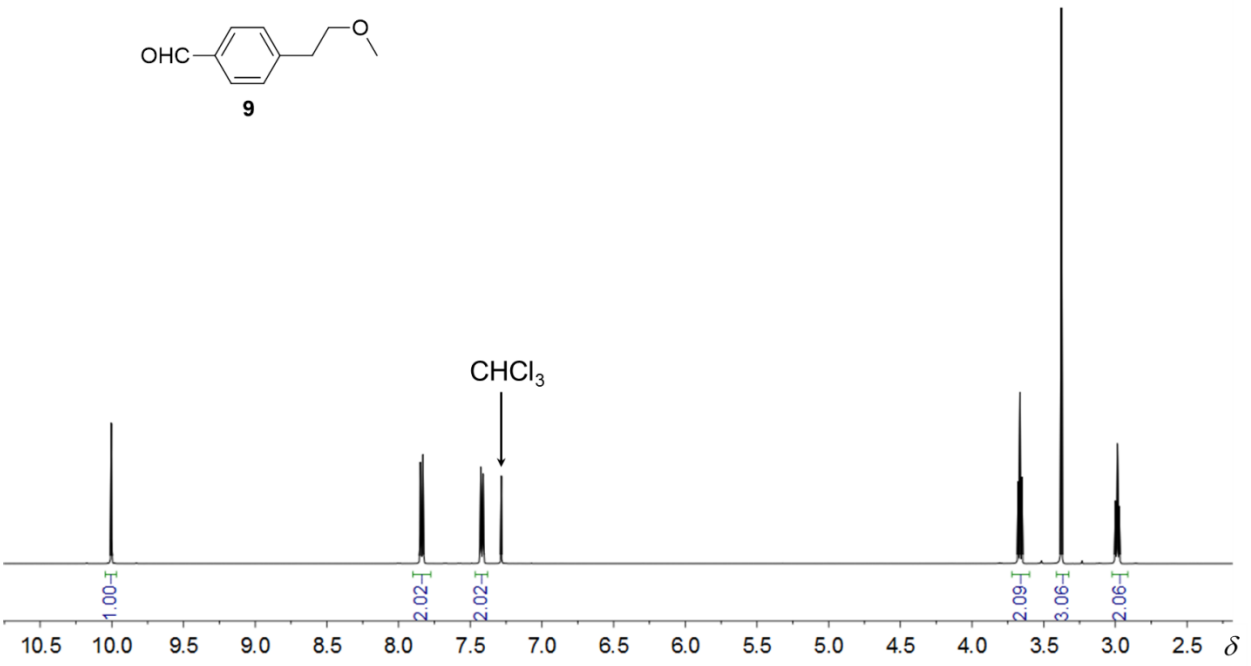

Figure S39. ^{1}H NMR spectrum of **9** (500 MHz, $CDCl_3$).

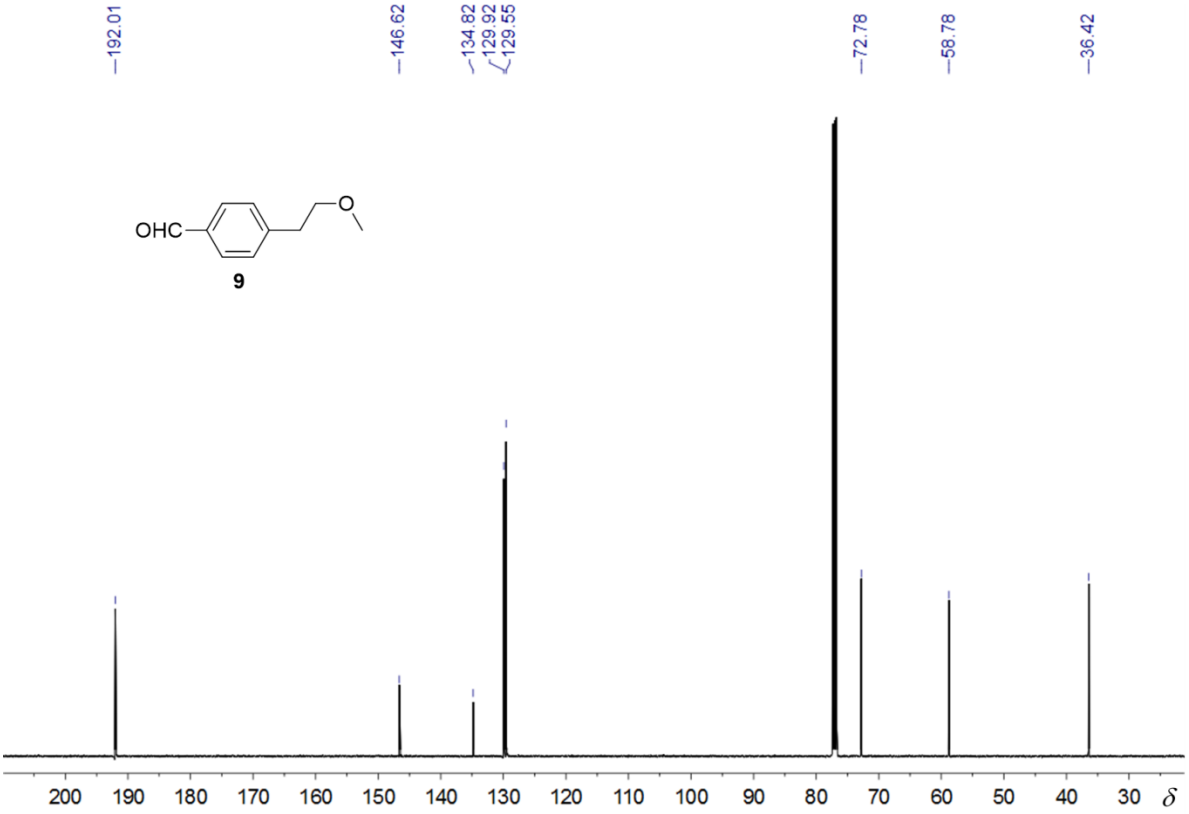

Figure S40. ^{13}C NMR spectrum of **9** (126 MHz, $CDCl_3$).

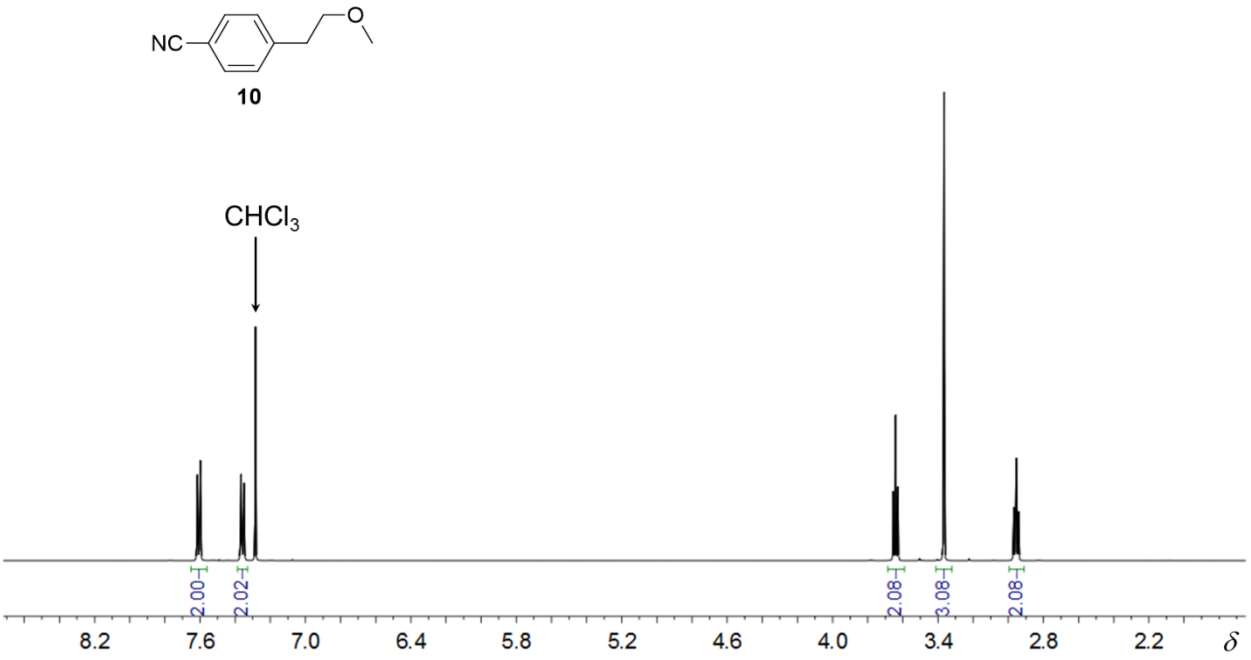

Figure S41. ^{1}H NMR spectrum of **10** (500 MHz, $CDCl_3$).

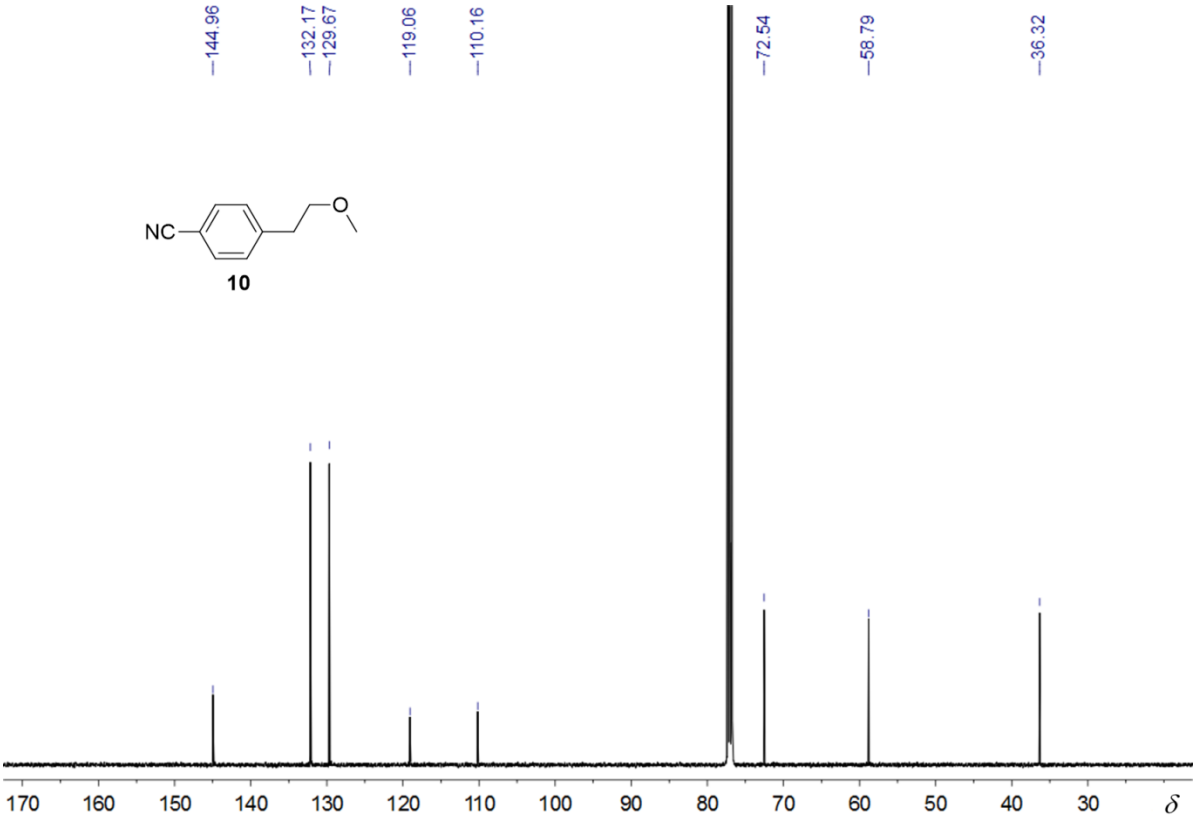

Figure S42. ^{13}C NMR spectrum of **10** (126 MHz, $CDCl_3$).

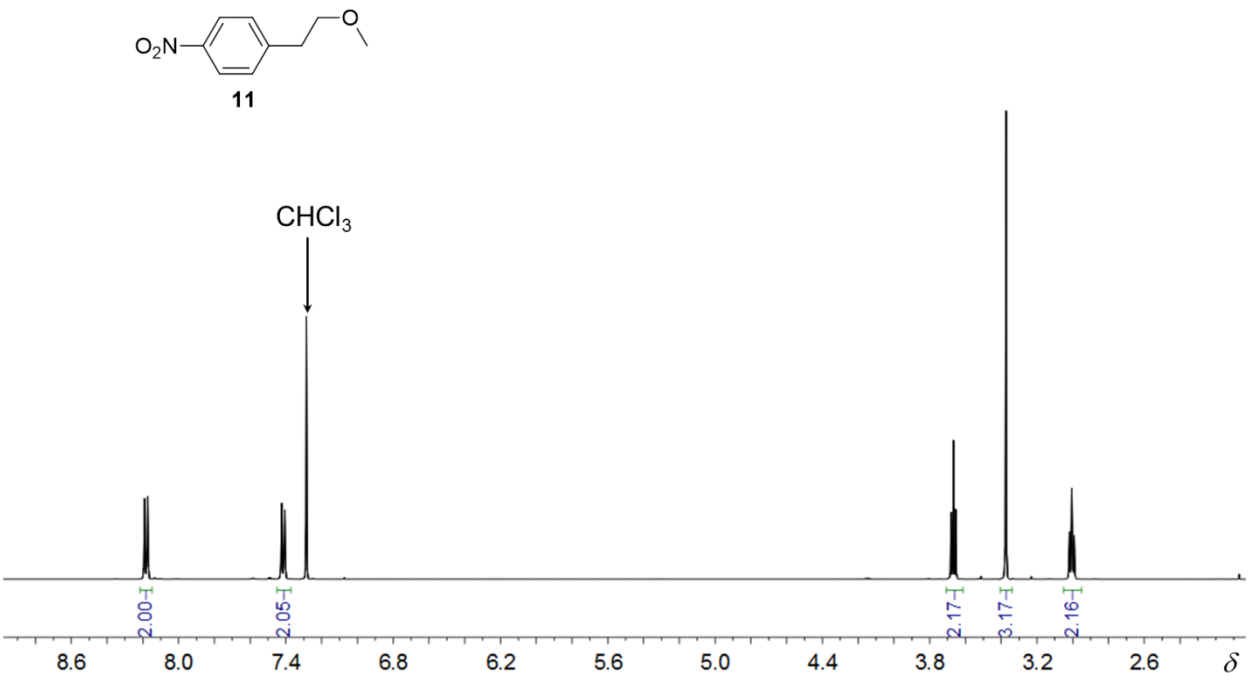

Figure S43. ^{1}H NMR spectrum of **11** (500 MHz, $CDCl_3$).

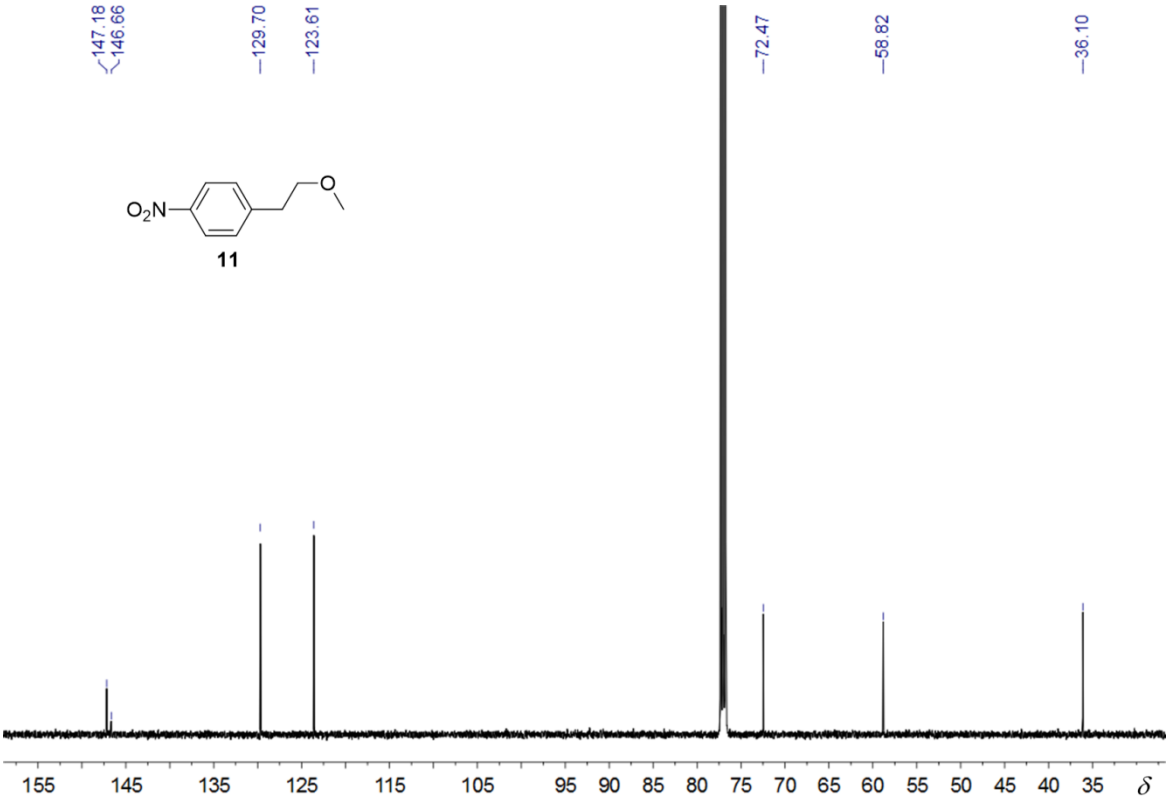

Figure S44. ^{13}C NMR spectrum of **11** (126 MHz, $CDCl_3$).

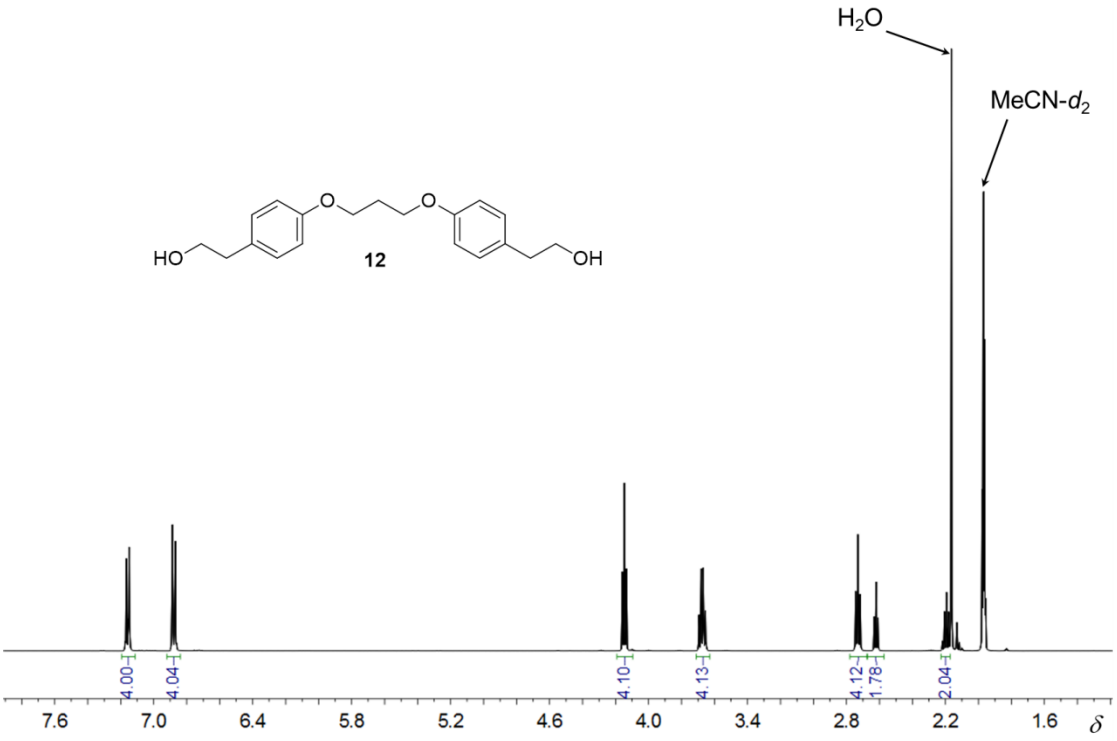

Figure S45. ^{1}H NMR spectrum of **12** (500 MHz, MeCN-d_3).

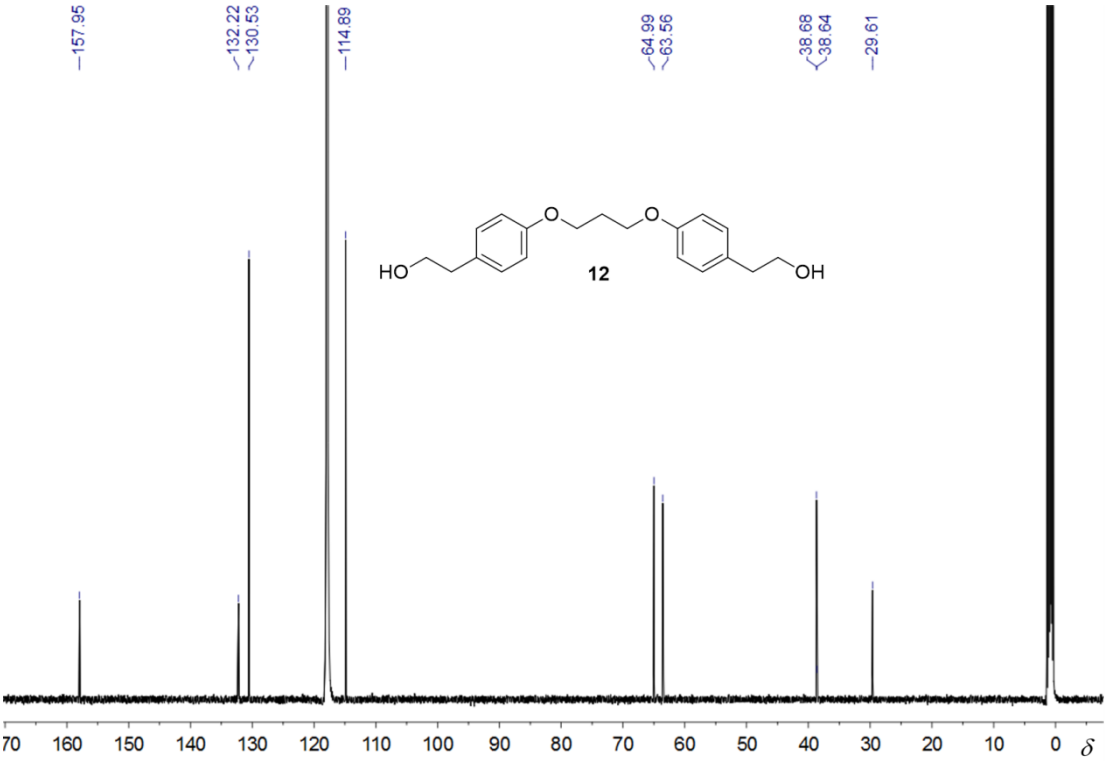

Figure S46. ^{13}C NMR spectrum of **12** (126 MHz, MeCN-d_3).

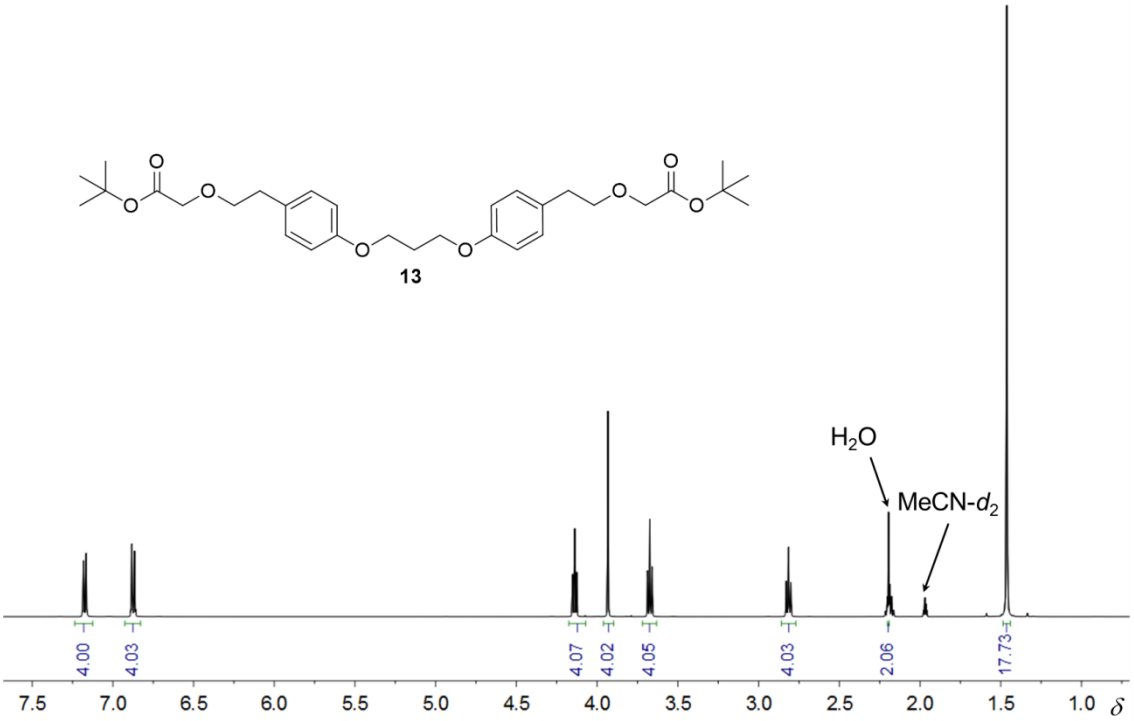

Figure S47. ^{1}H NMR spectrum of **13** (500 MHz, MeCN-d_3).

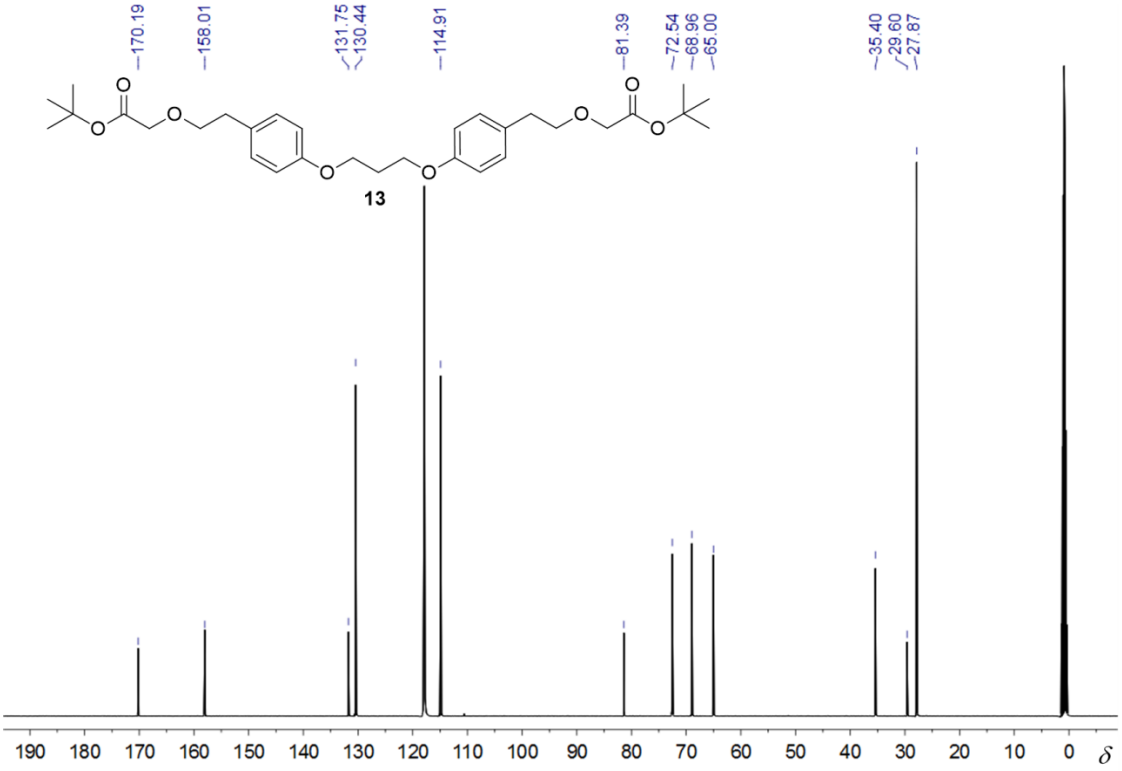

Figure S48. ^{13}C NMR spectrum of **13** (126 MHz, MeCN-d_3).

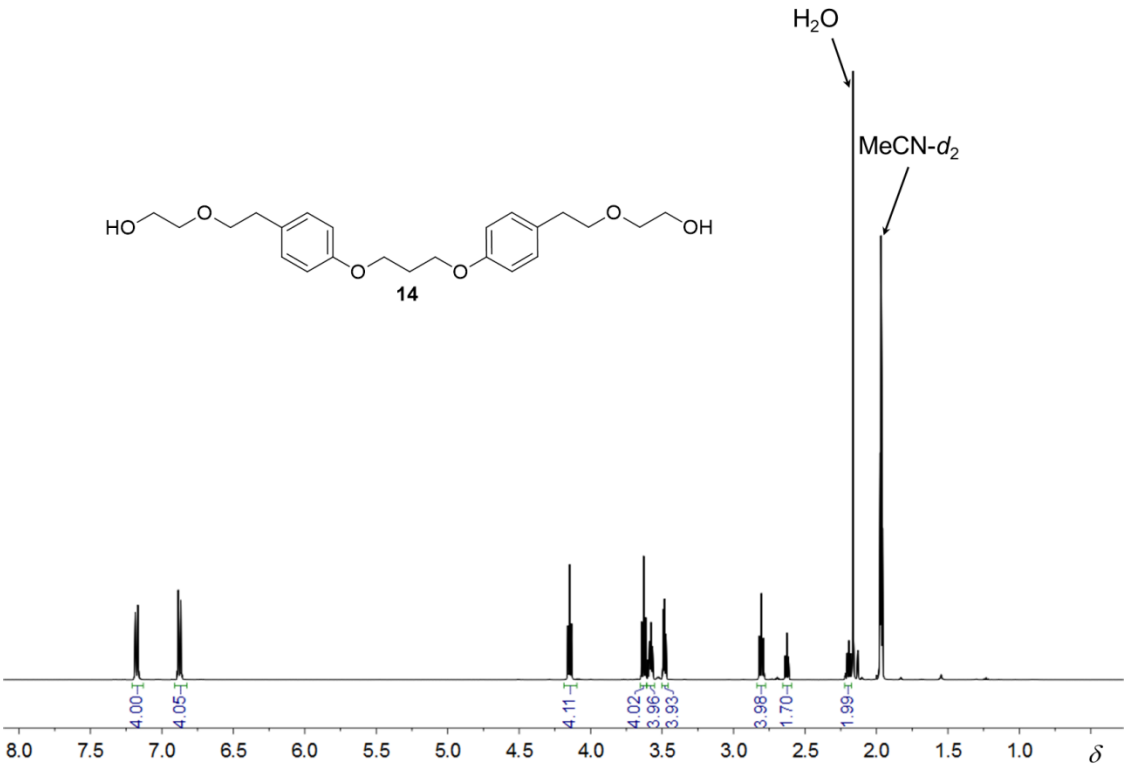

Figure S49. ^{1}H NMR spectrum of **14** (500 MHz, MeCN-d_3).

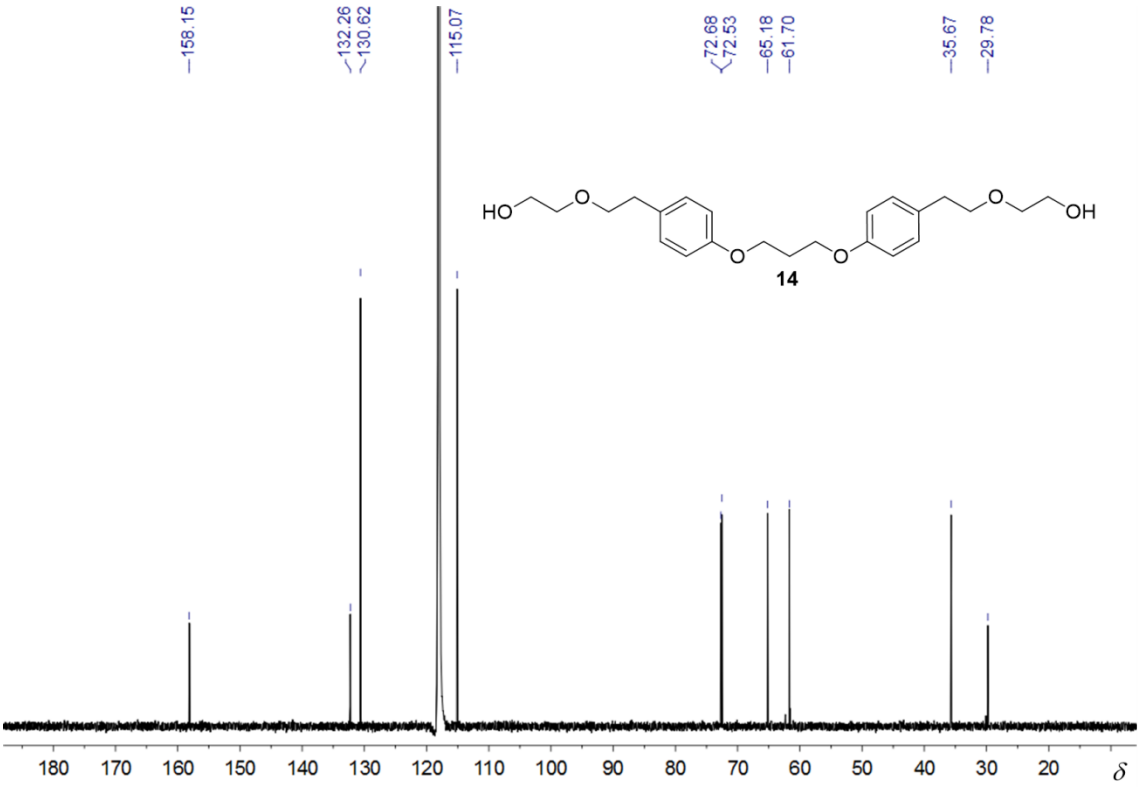

Figure S50. ^{13}C NMR spectrum of **14** (126 MHz, MeCN-d_3).

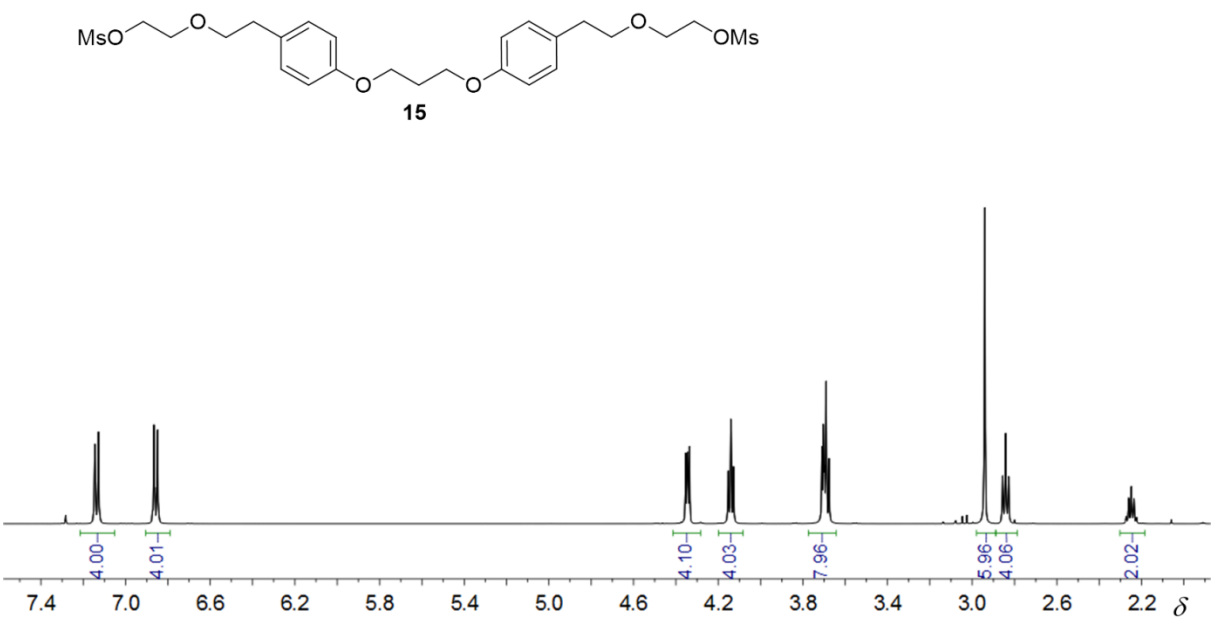

Figure S51. ^{1}H NMR spectrum of **15** (500 MHz, $CDCl_3$).

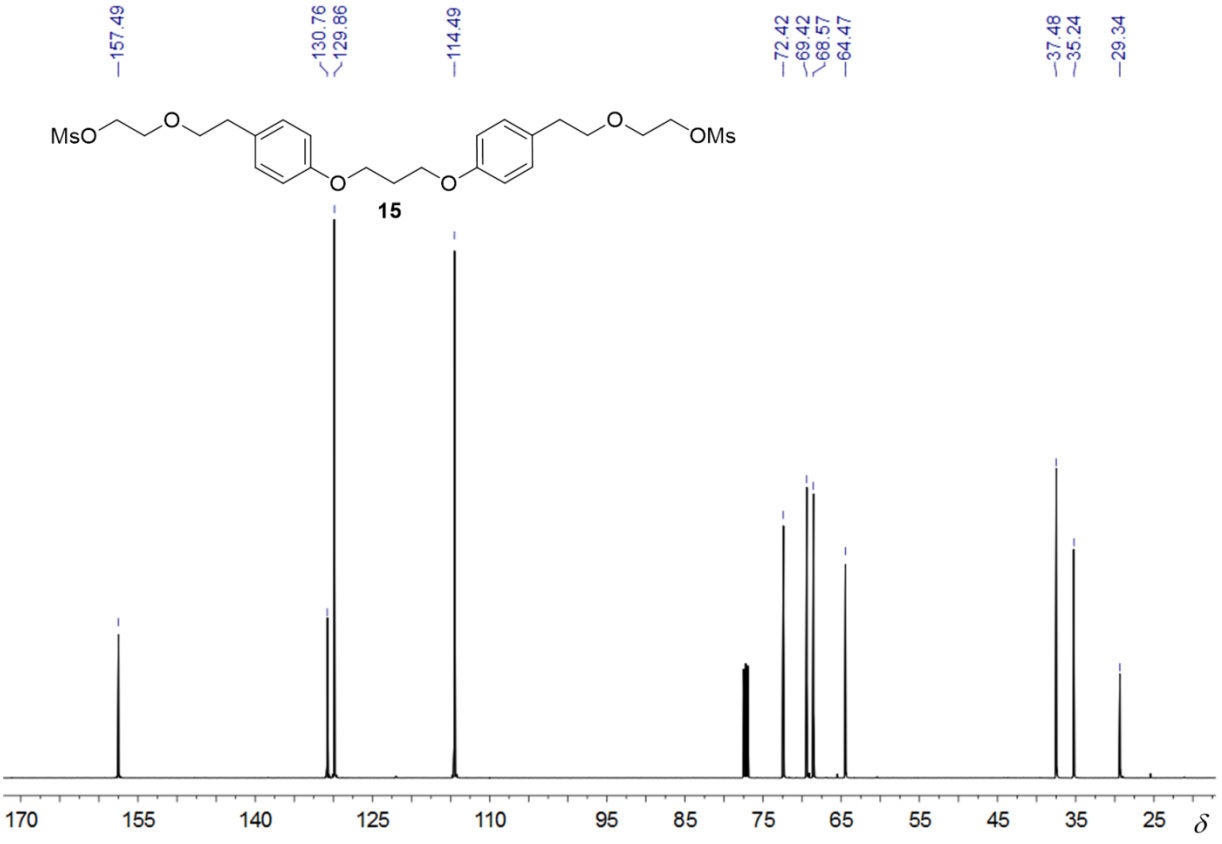

Figure S52. ^{13}C NMR spectrum of **15** (126 MHz, $CDCl_3$).

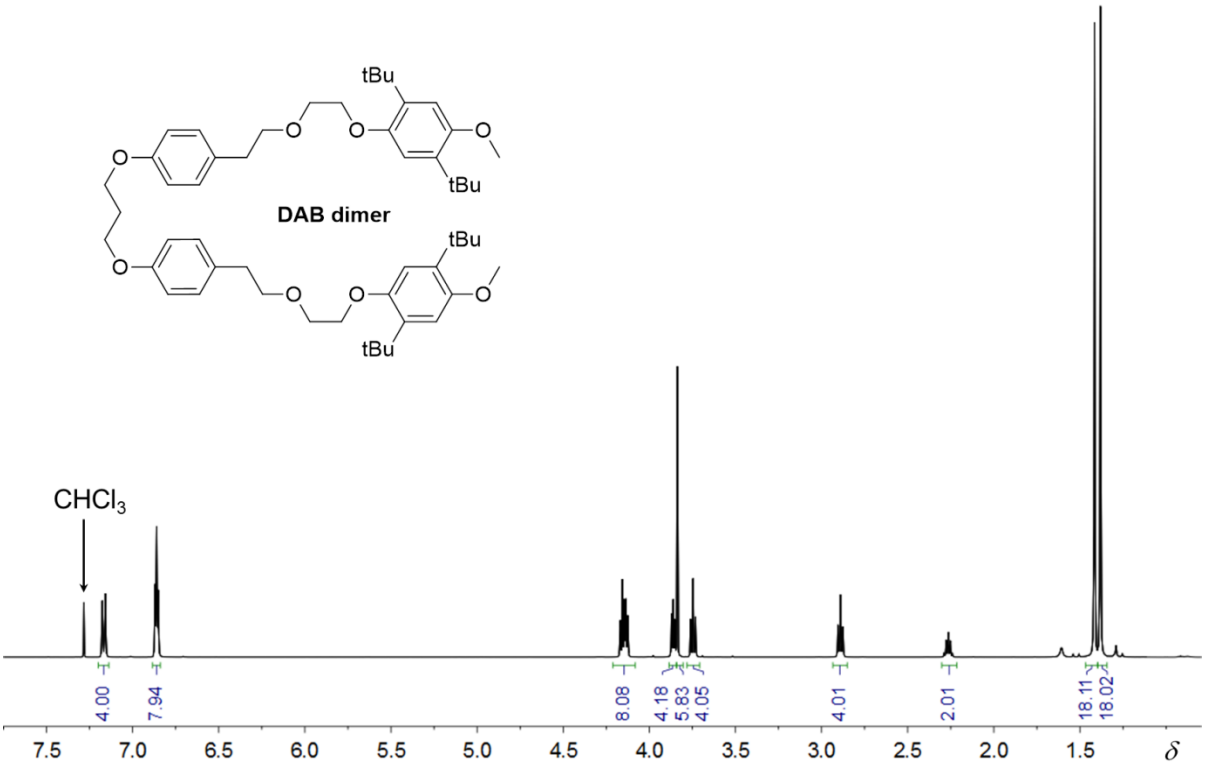

Figure S53. ^{1}H NMR spectrum of **DAB dimer** (500 MHz, $CDCl_3$).

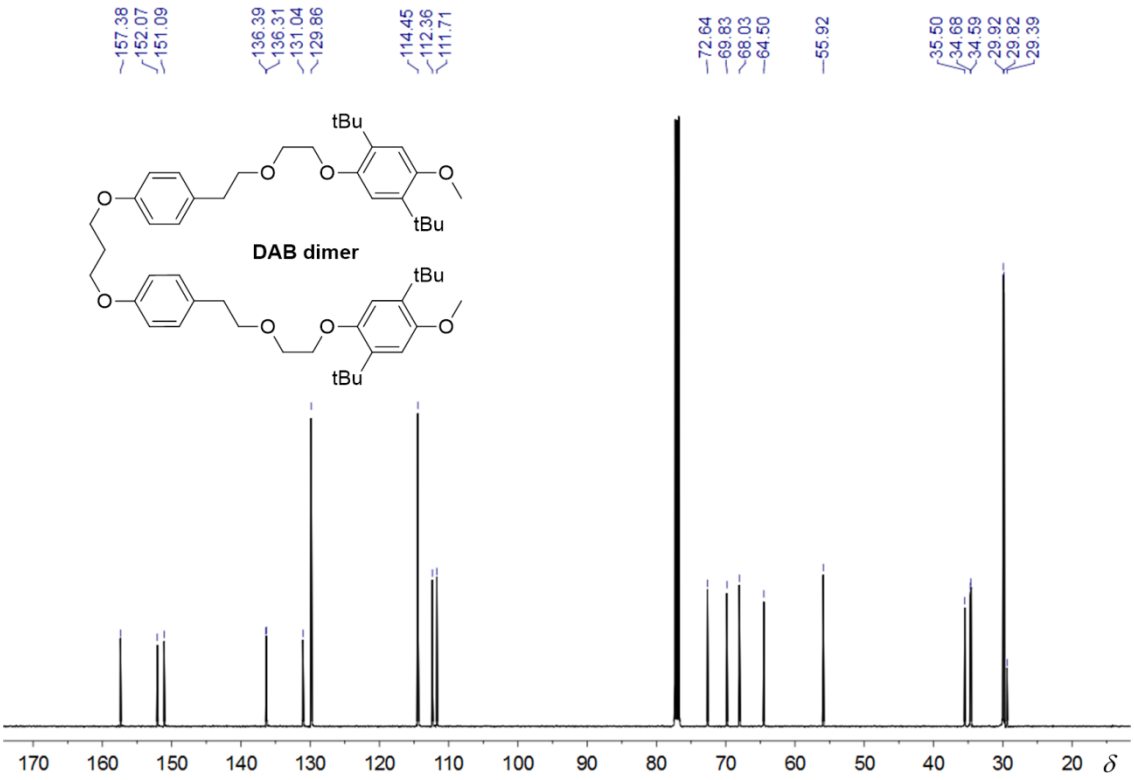

Figure S54. ^{13}C NMR spectrum of **DAB dimer** (126 MHz, $CDCl_3$).

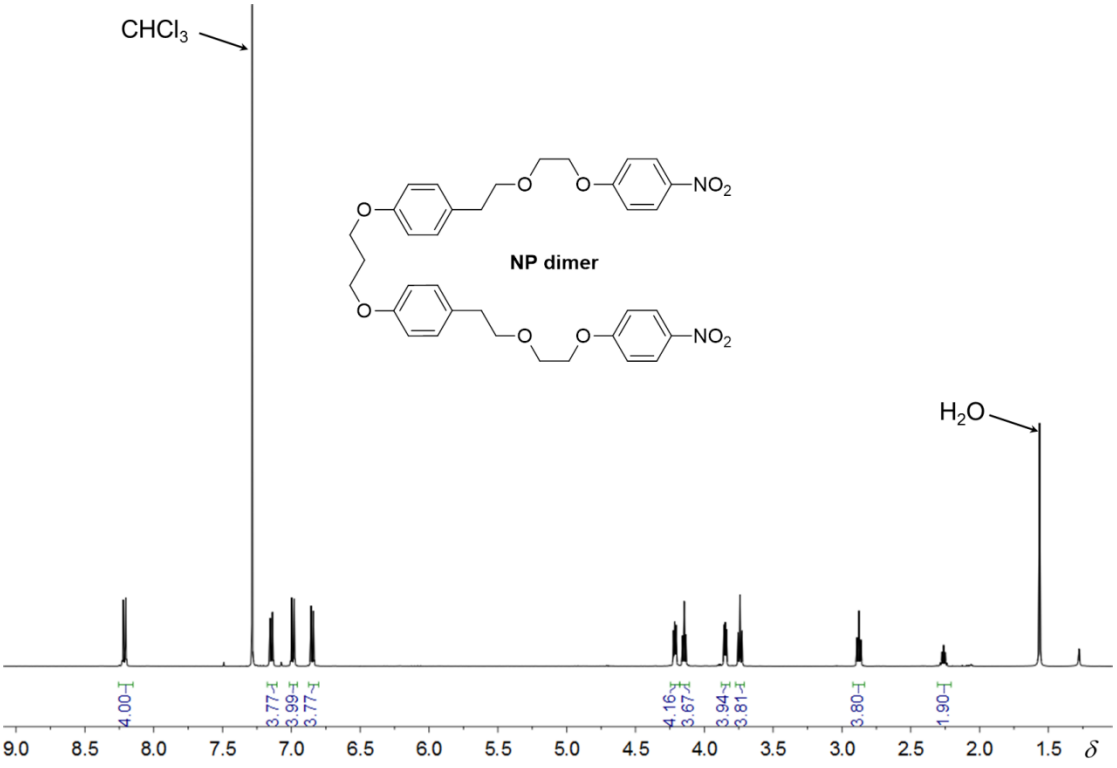

Figure S55. ^{1}H NMR spectrum of **NP dimer** (500 MHz, $CDCl_3$).

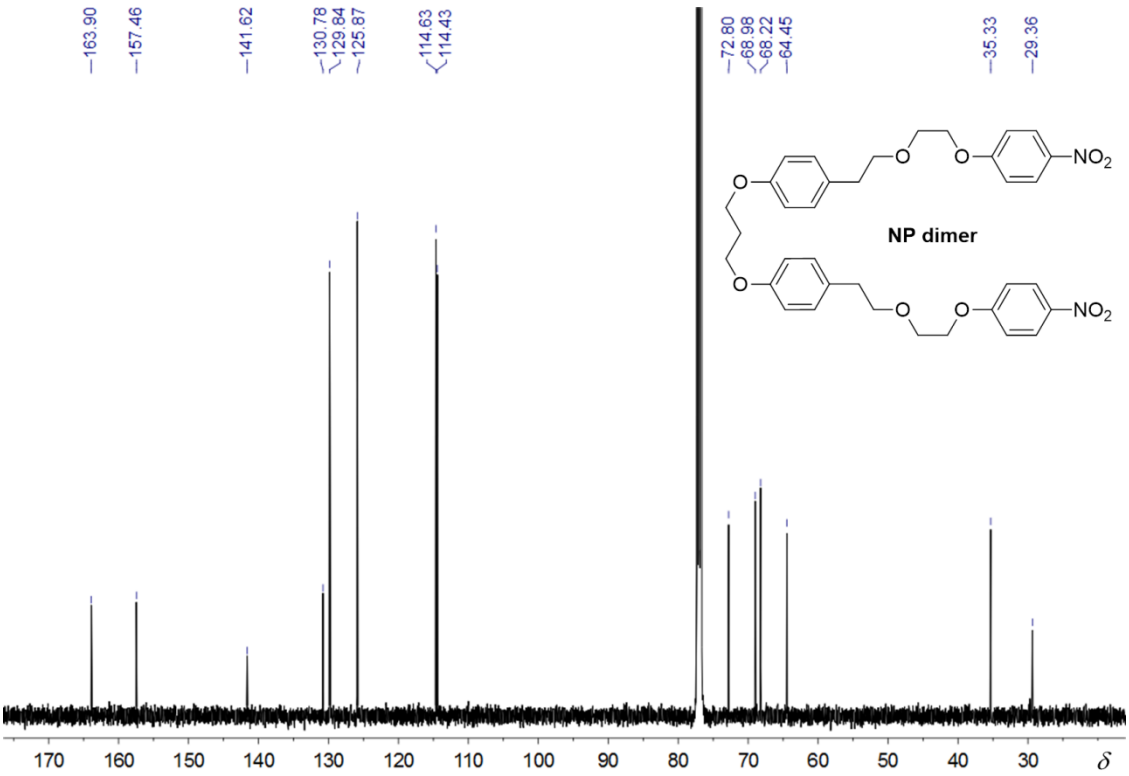

Figure S56. ^{13}C NMR spectrum of **NP dimer** (126 MHz, $CDCl_3$).

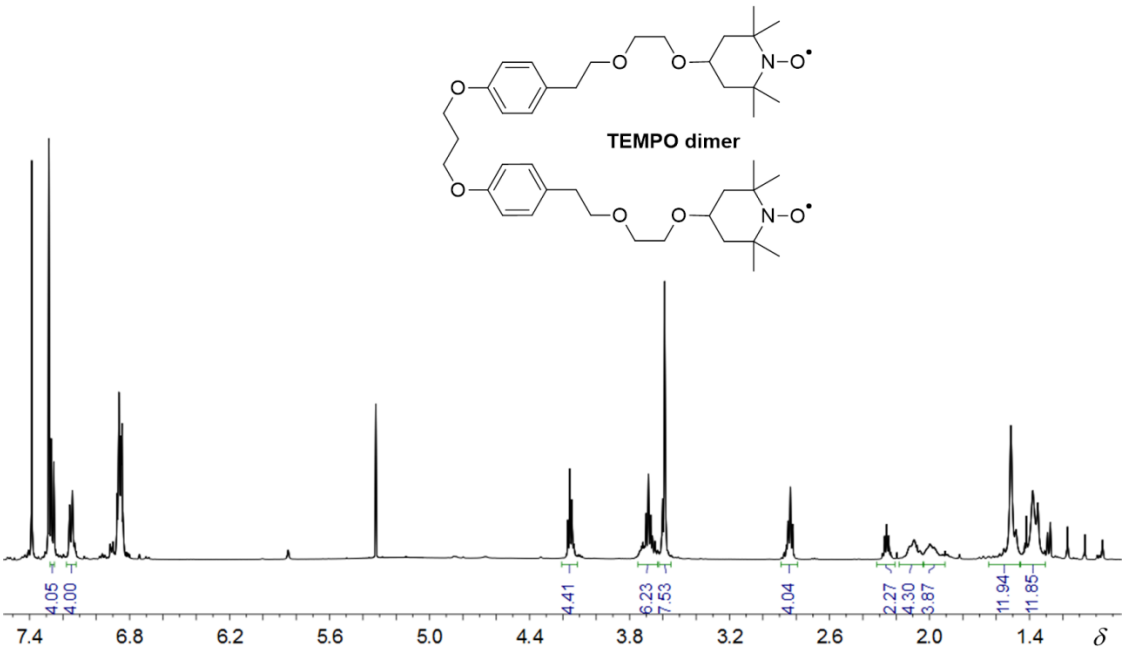

Figure S57. ^{1}H NMR spectrum of **TEMPO dimer** upon reduction by phenylhydrazine (500 MHz, $CDCl_3$).

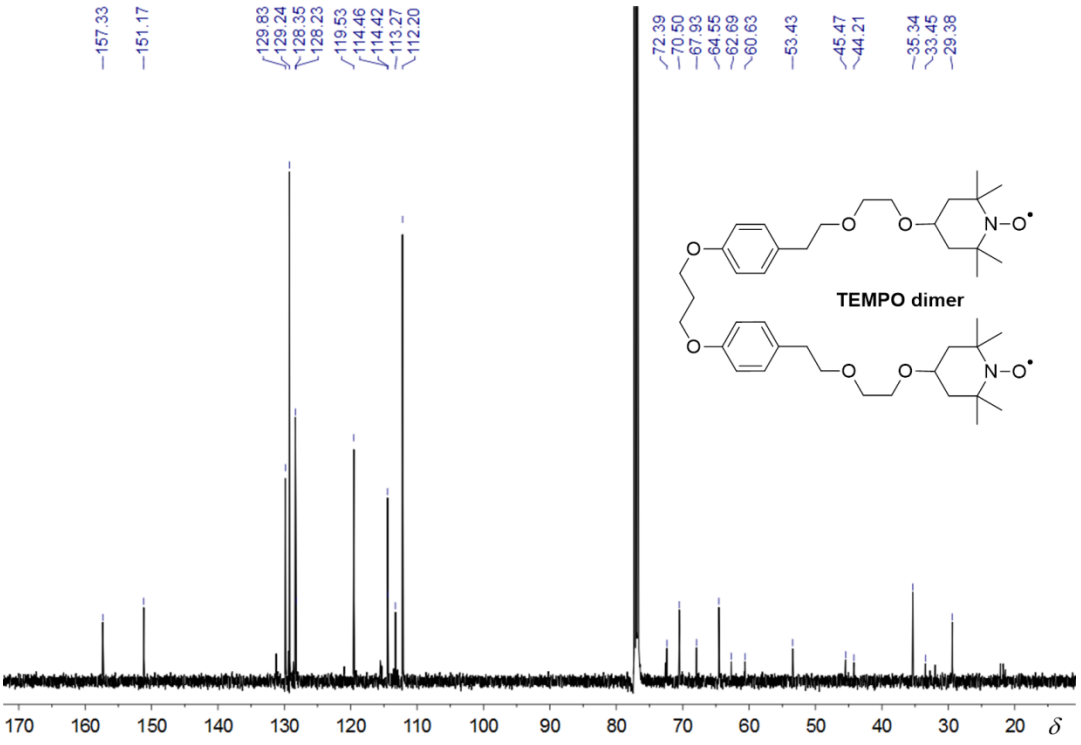

Figure S58. ^{13}C NMR spectrum of **TEMPO dimer** upon reduction by phenylhydrazine (126 MHz, $CDCl_3$).

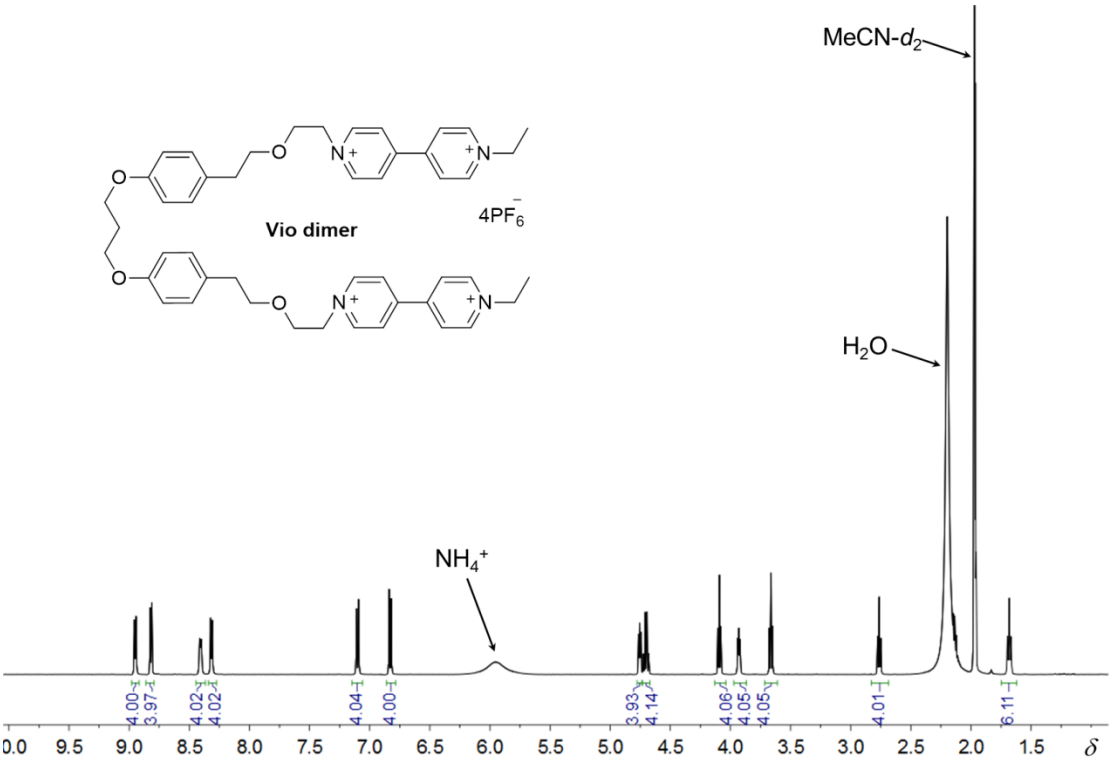

Figure S59. ^{1}H NMR spectrum of **Vio dimer** (500 MHz, MeCN-d_3).

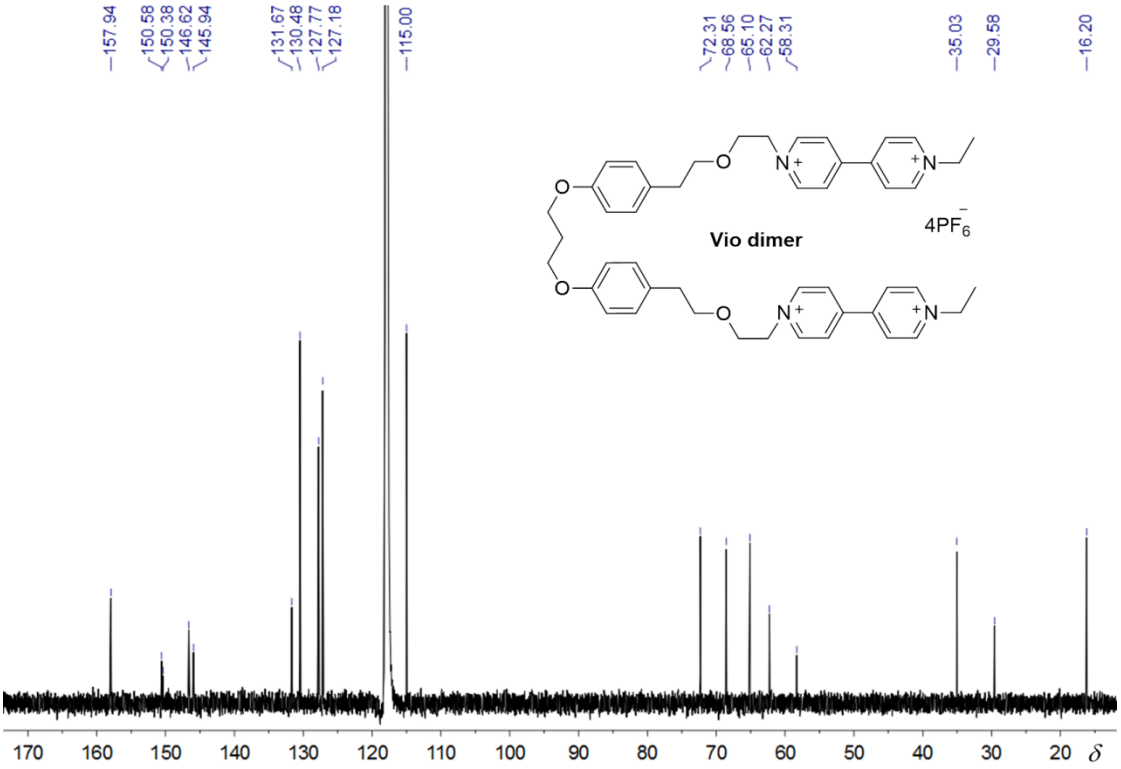

Figure S60. ^{13}C NMR spectrum of **Vio dimer** (126 MHz, MeCN-d_3).

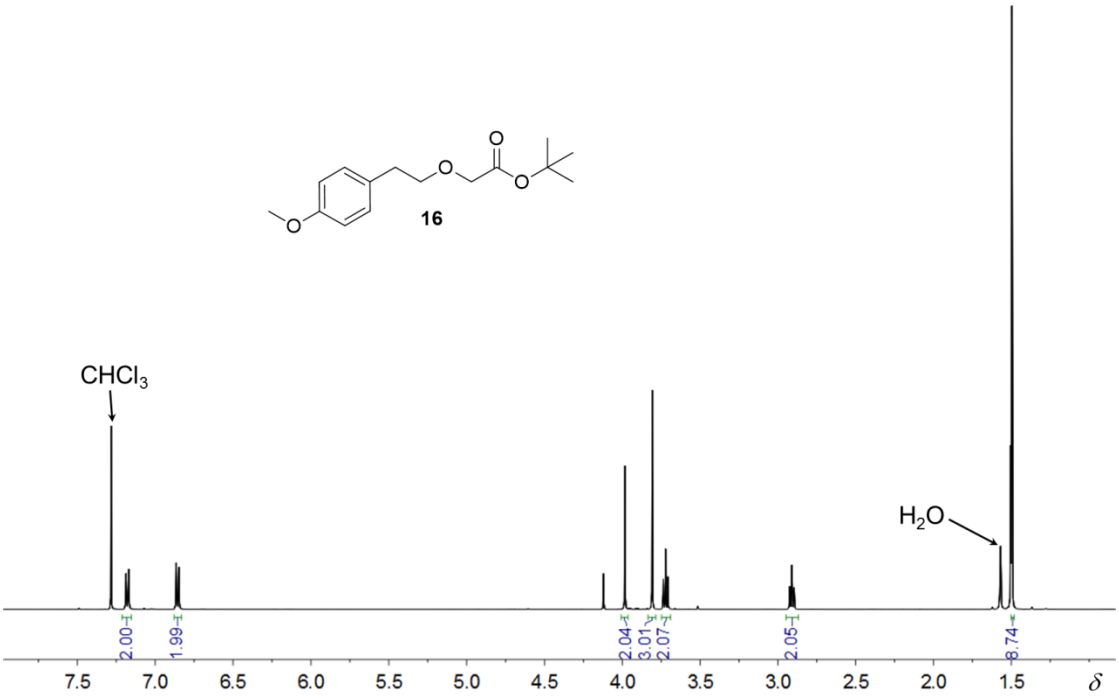

Figure S61. ^{1}H NMR spectrum of **16** (500 MHz, $CDCl_3$).

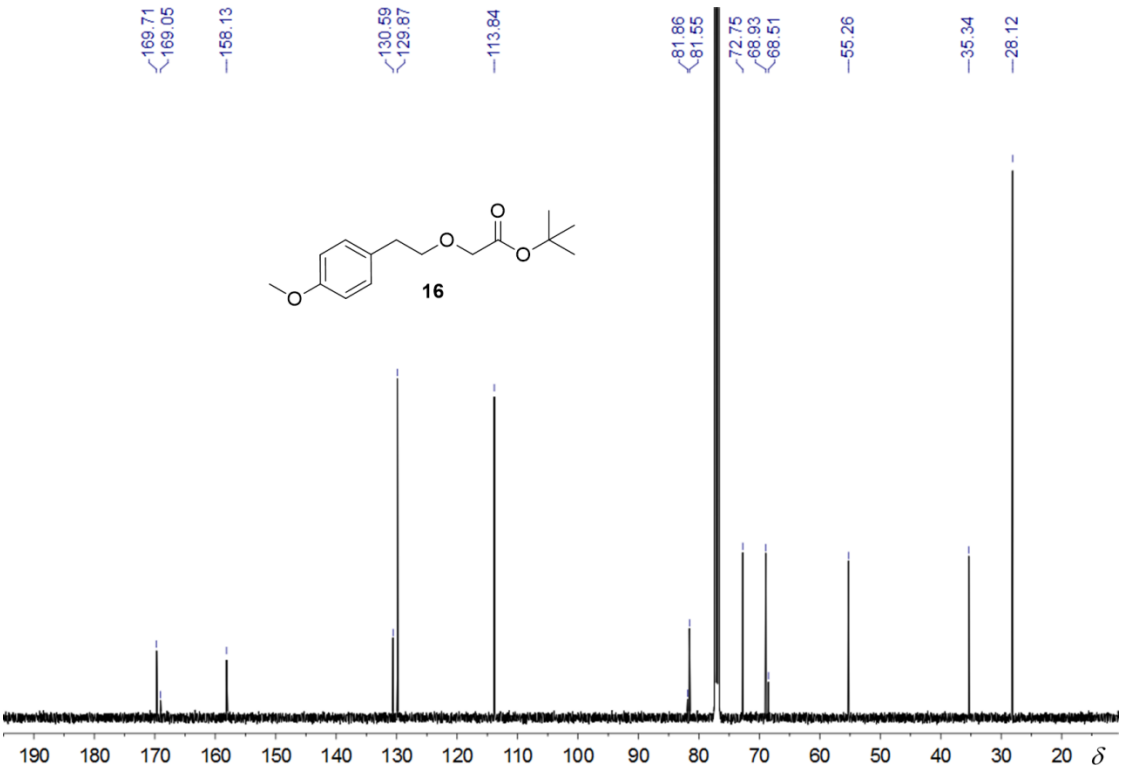

Figure S62. ^{13}C NMR spectrum of **16** (126 MHz, $CDCl_3$).

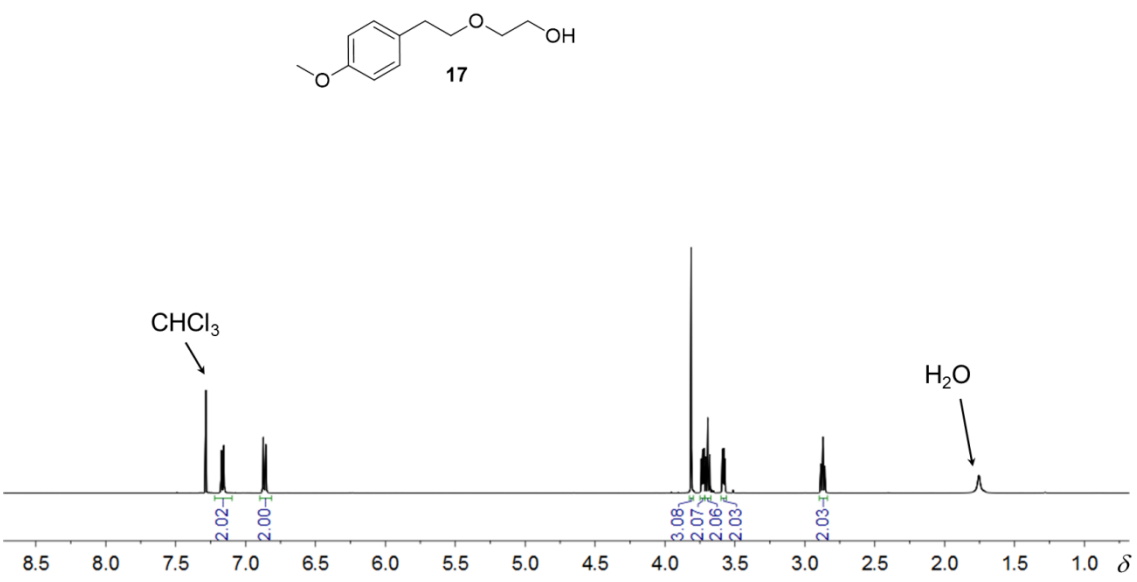

Figure S63. ^{1}H NMR spectrum of **17** (500 MHz, $CDCl_3$).

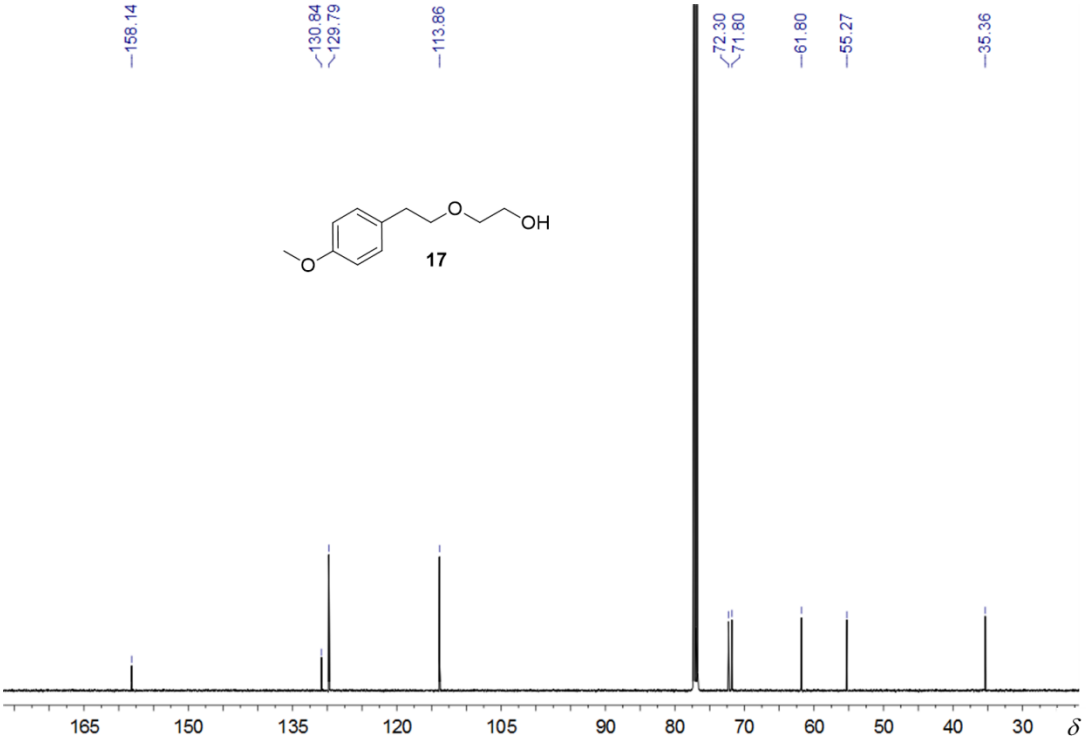

Figure S64. ^{13}C NMR spectrum of **17** (126 MHz, $CDCl_3$).

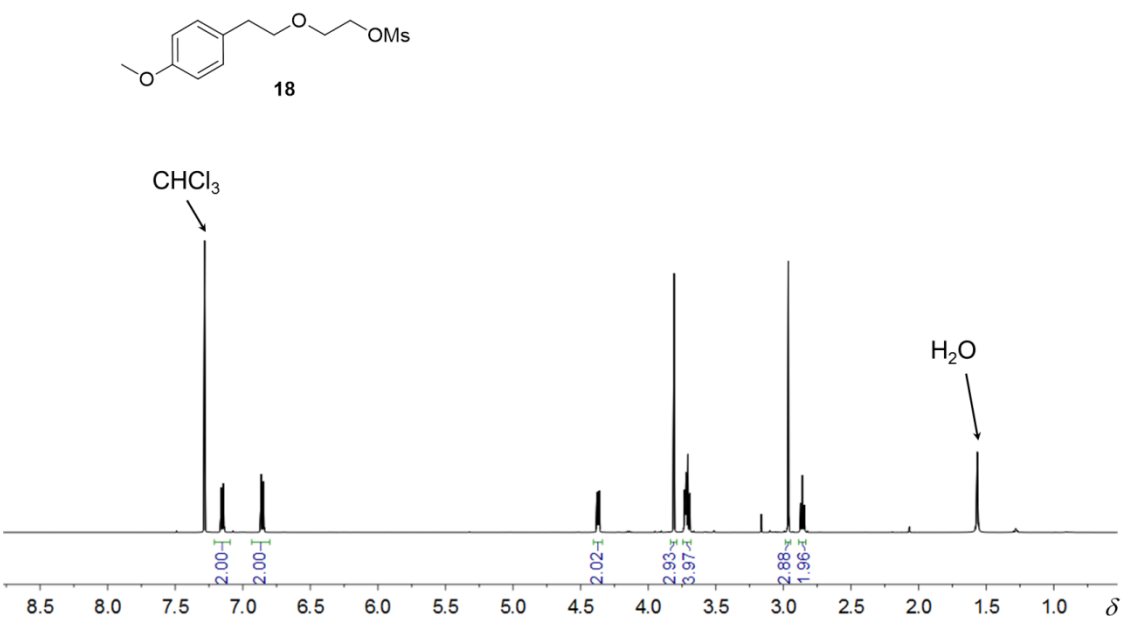

Figure S65. ^{1}H NMR spectrum of **18** (500 MHz, $CDCl_3$).

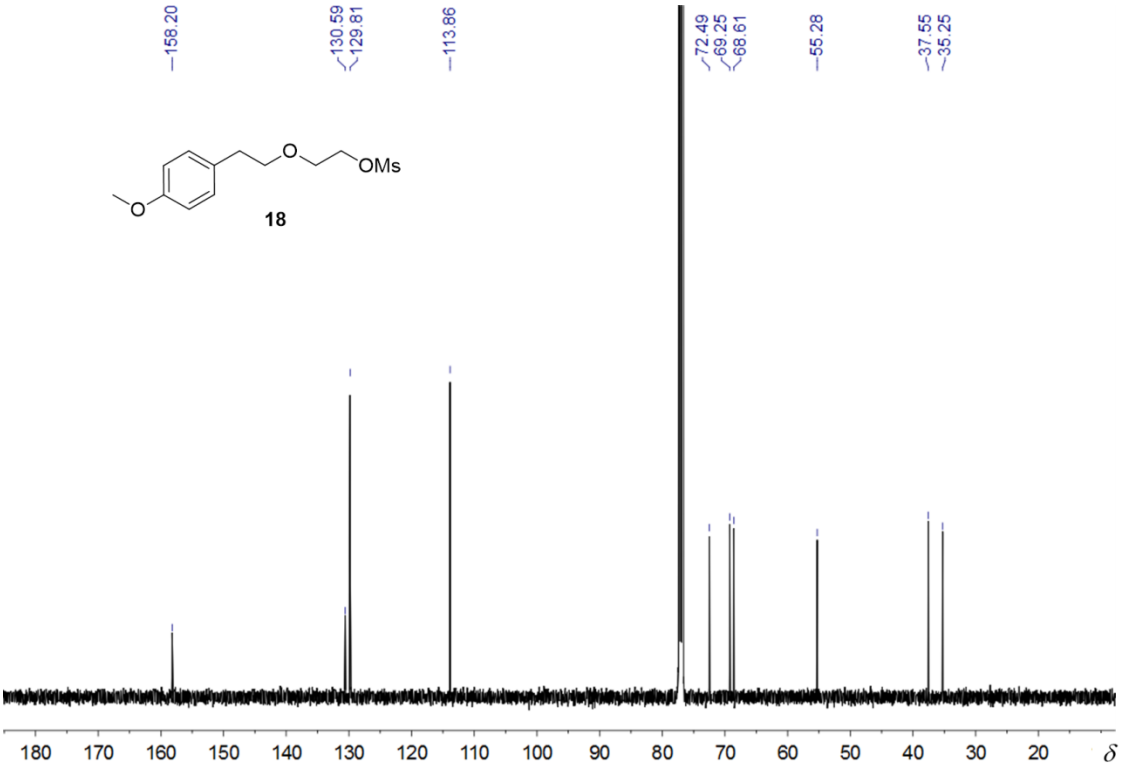

Figure S66. ^{13}C NMR spectrum of **18** (126 MHz, $CDCl_3$).

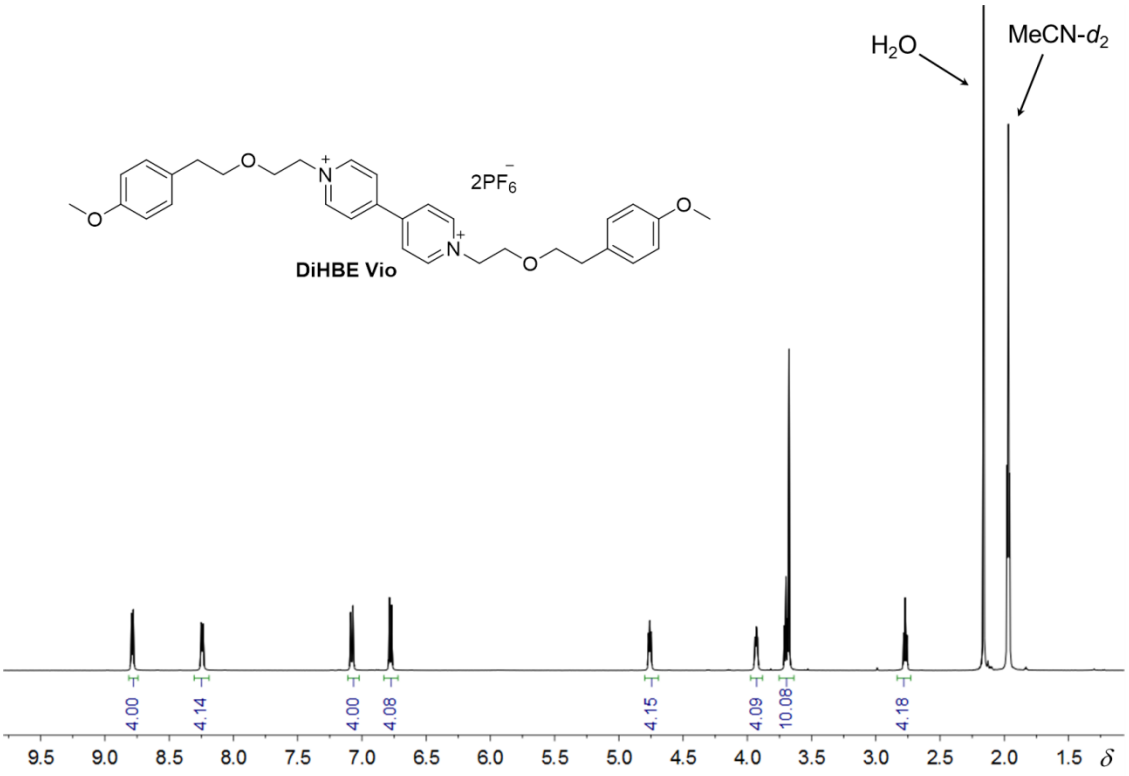

Figure S67. ^{1}H NMR spectrum of **DiHBE Vio** (500 MHz, MeCN-d_3).

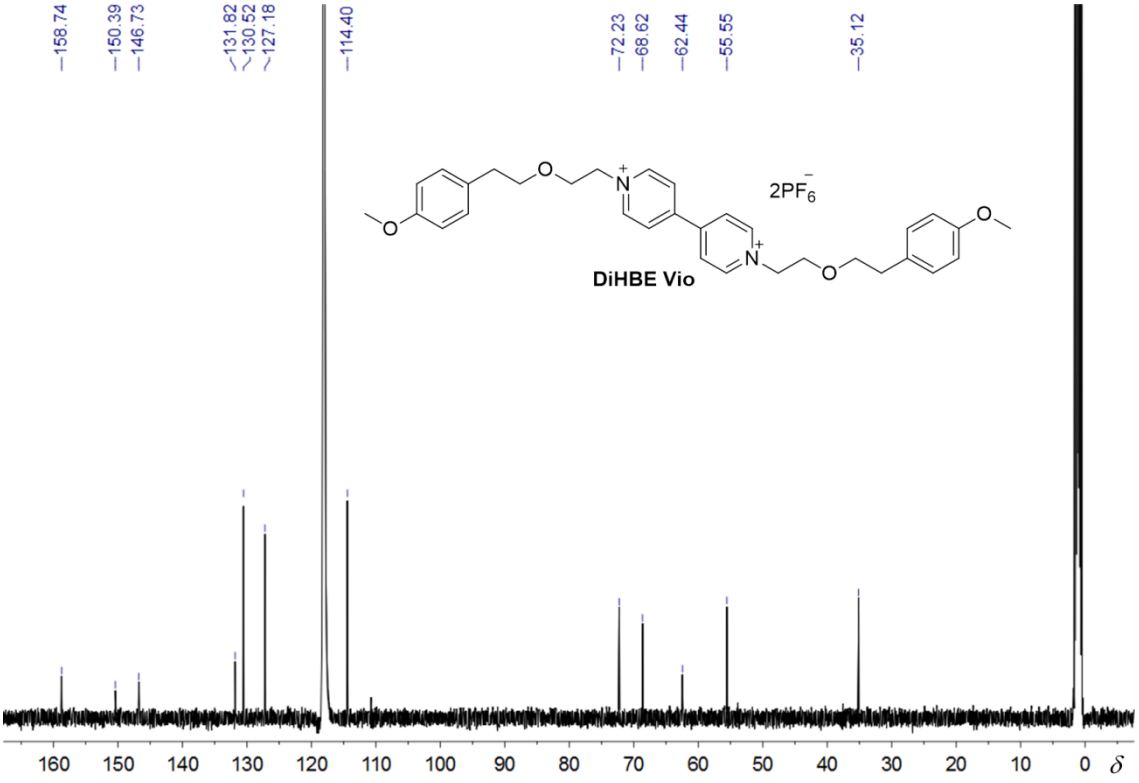

Figure S68. ^{13}C NMR spectrum of **DiHBE Vio** (126 MHz, MeCN-d_3).

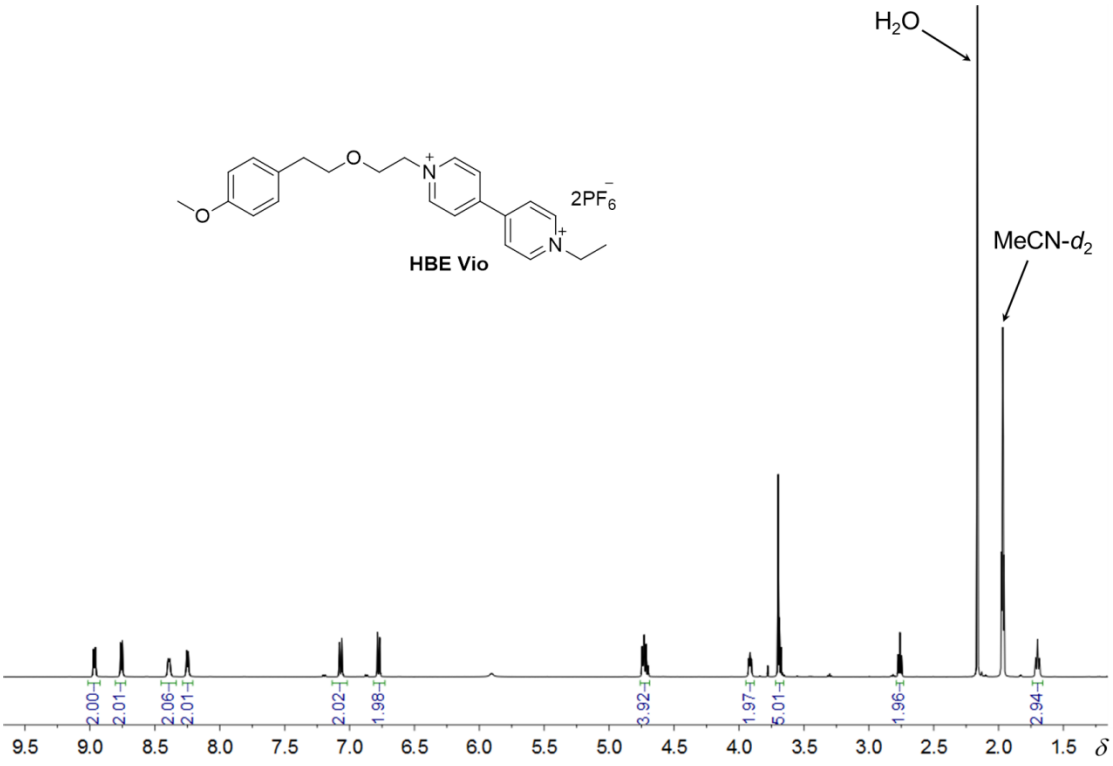

Figure S69. ^{1}H NMR spectrum of **HBE Vio** (500 MHz, MeCN-d_3).

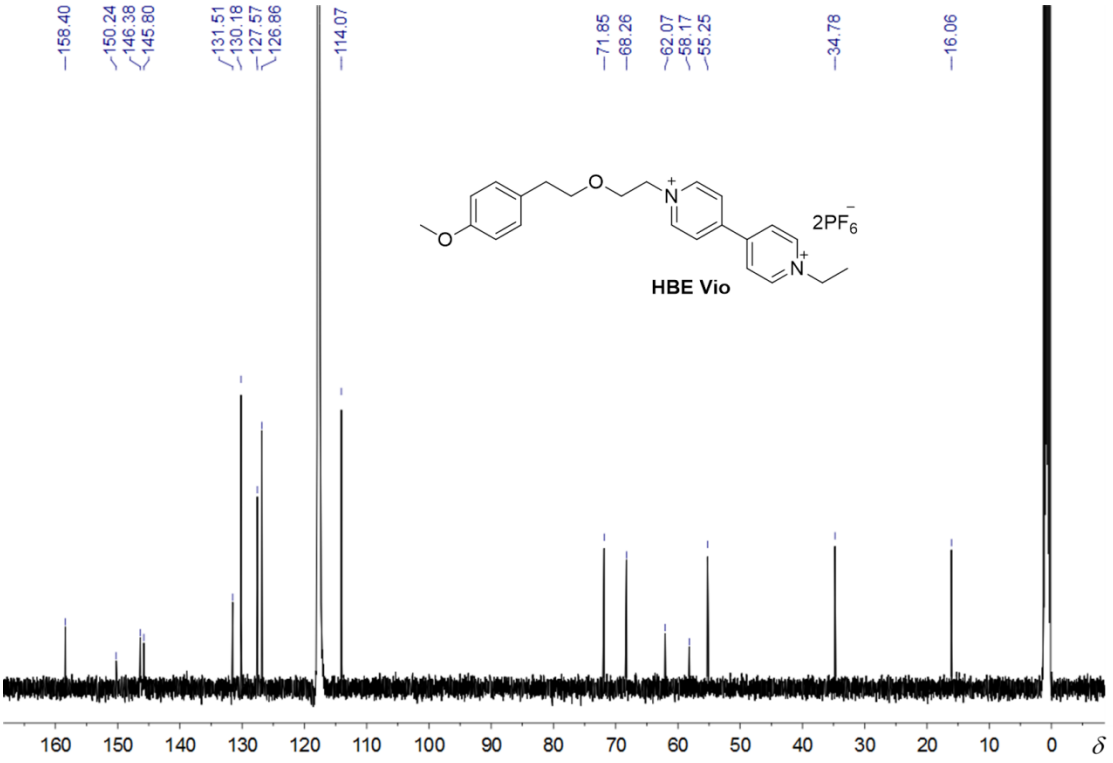

Figure S70. ^{13}C NMR spectrum of **HBE Vio** (126 MHz, MeCN-d_3).

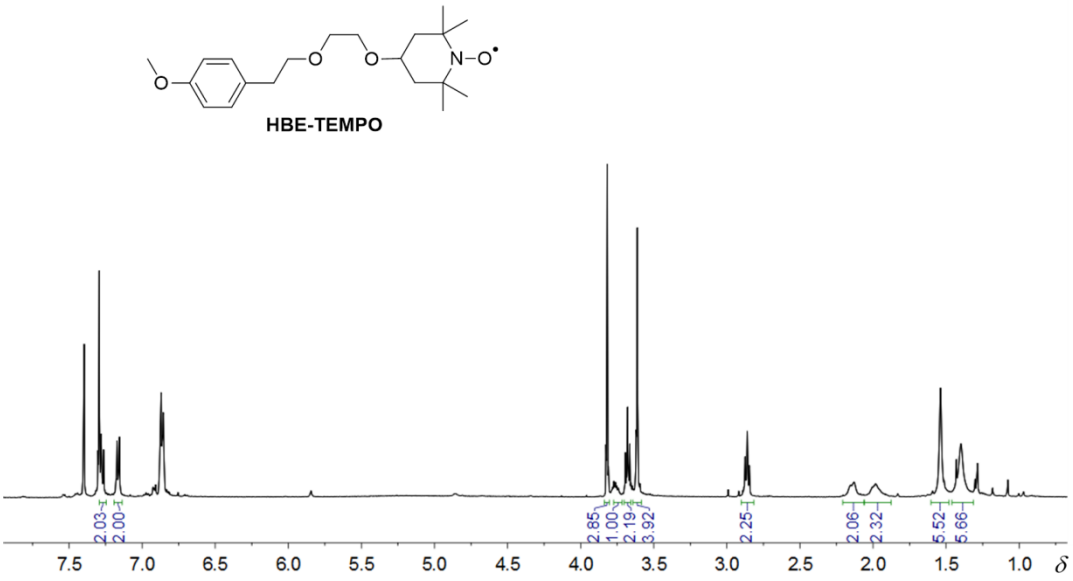

Figure S71. ^{1}H NMR spectrum of **HBE-TEMPO** upon reduction by phenylhydrazine (500 MHz, $CDCl_3$).

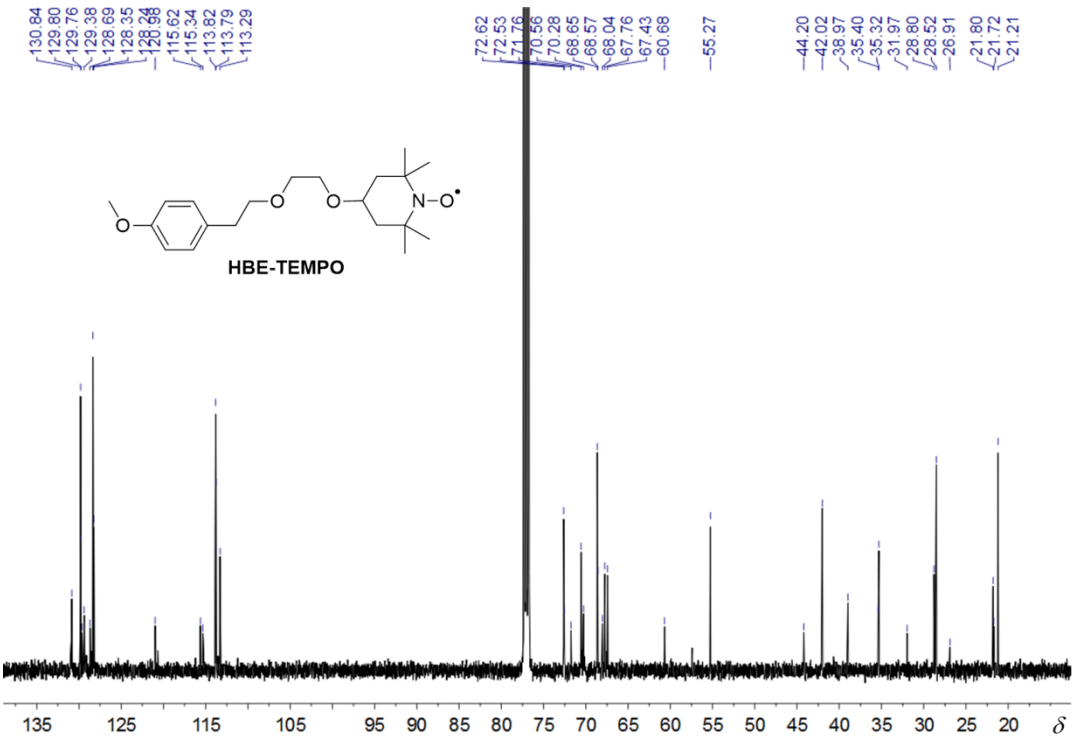

Figure S72. ^{13}C NMR spectrum of **HBE-TEMPO** upon reduction by phenylhydrazine (126 MHz, $CDCl_3$).

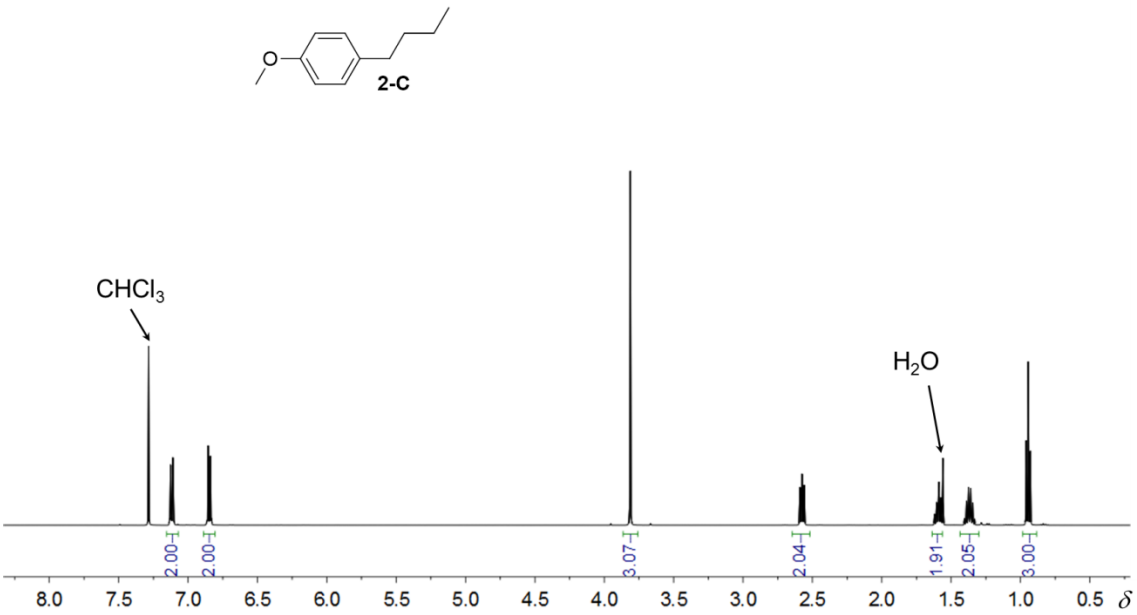

Figure S73. ^{1}H NMR spectrum of **2-C** (500 MHz, $CDCl_3$).

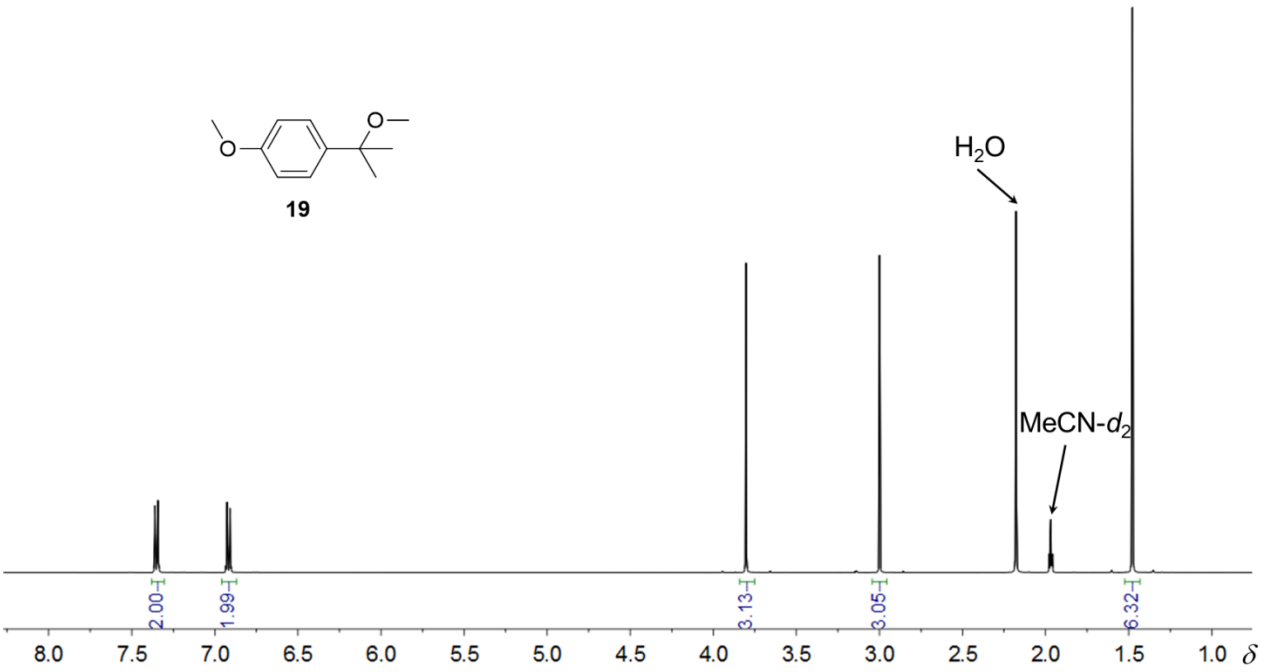

Figure S74. ^{1}H NMR spectrum of **19** (500 MHz, MeCN-d_3).

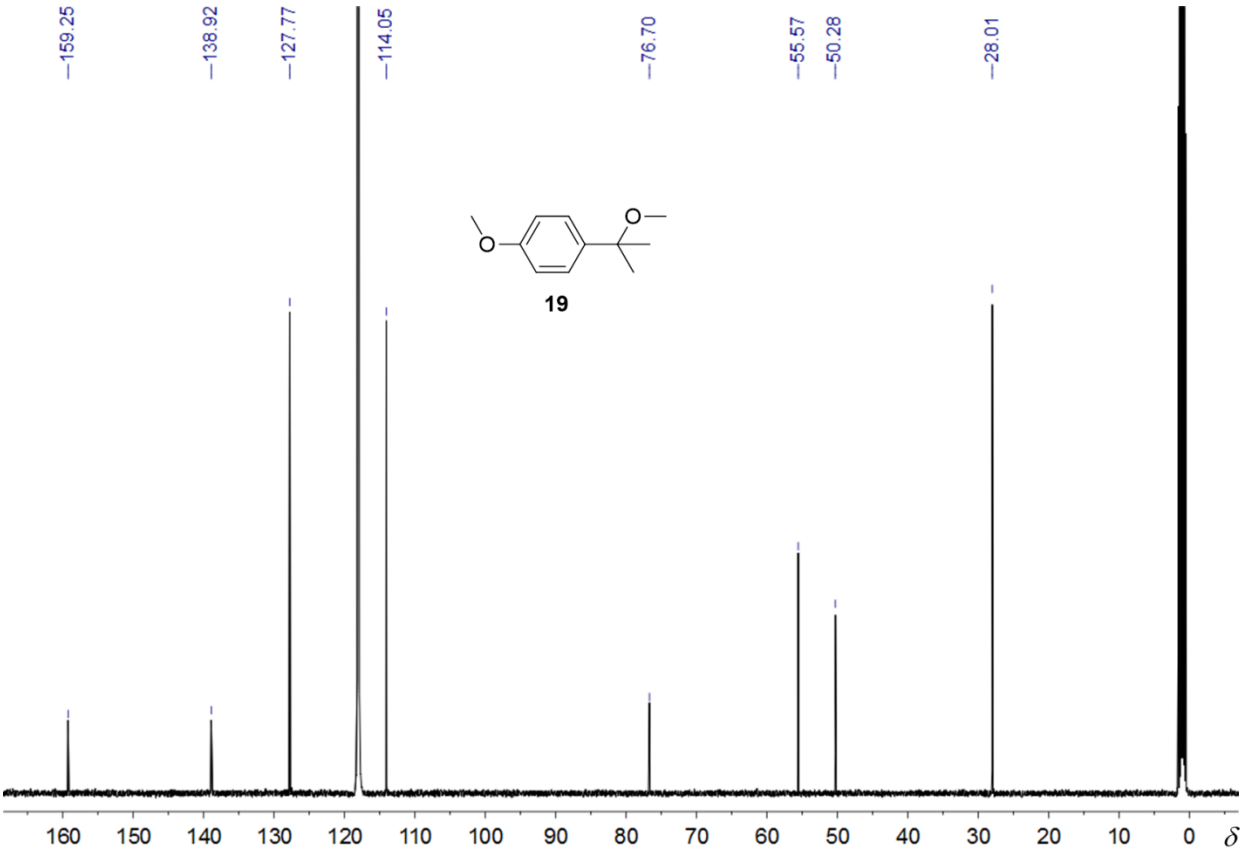

Figure S75. ^{13}C NMR spectrum of **19** (126 MHz, MeCN-d_3).

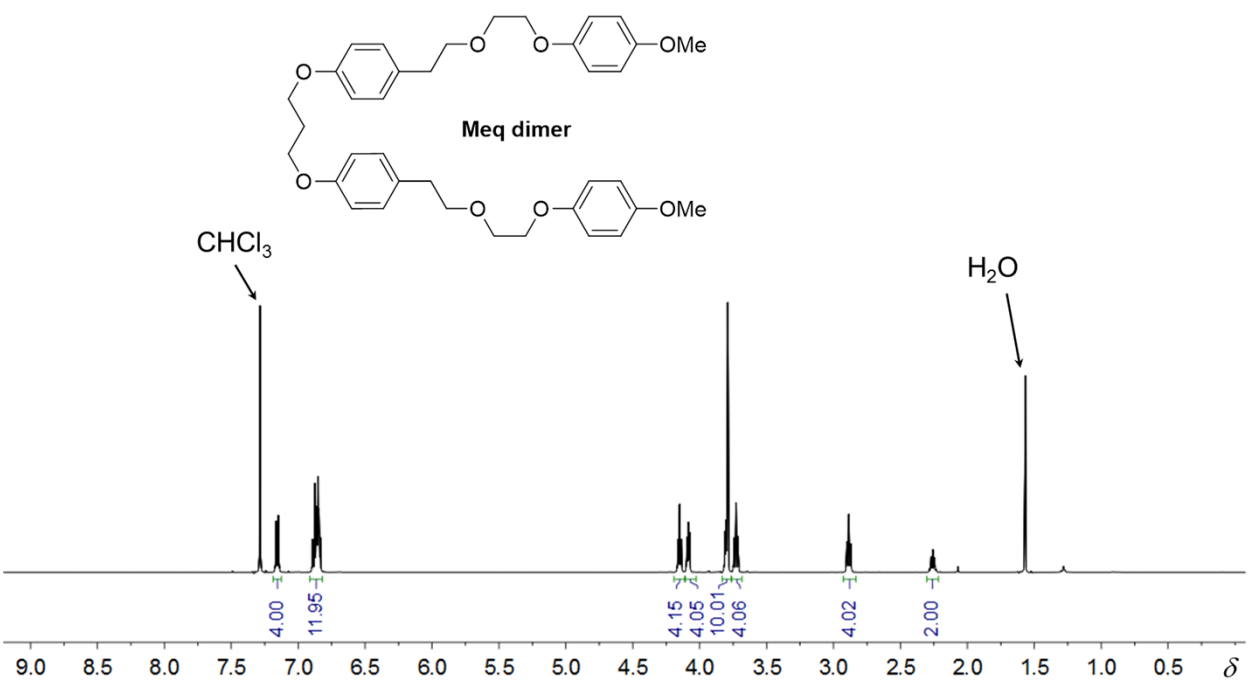

Figure S76. ^{1}H NMR spectrum of **Meq dimer** (500 MHz, $CDCl_3$).

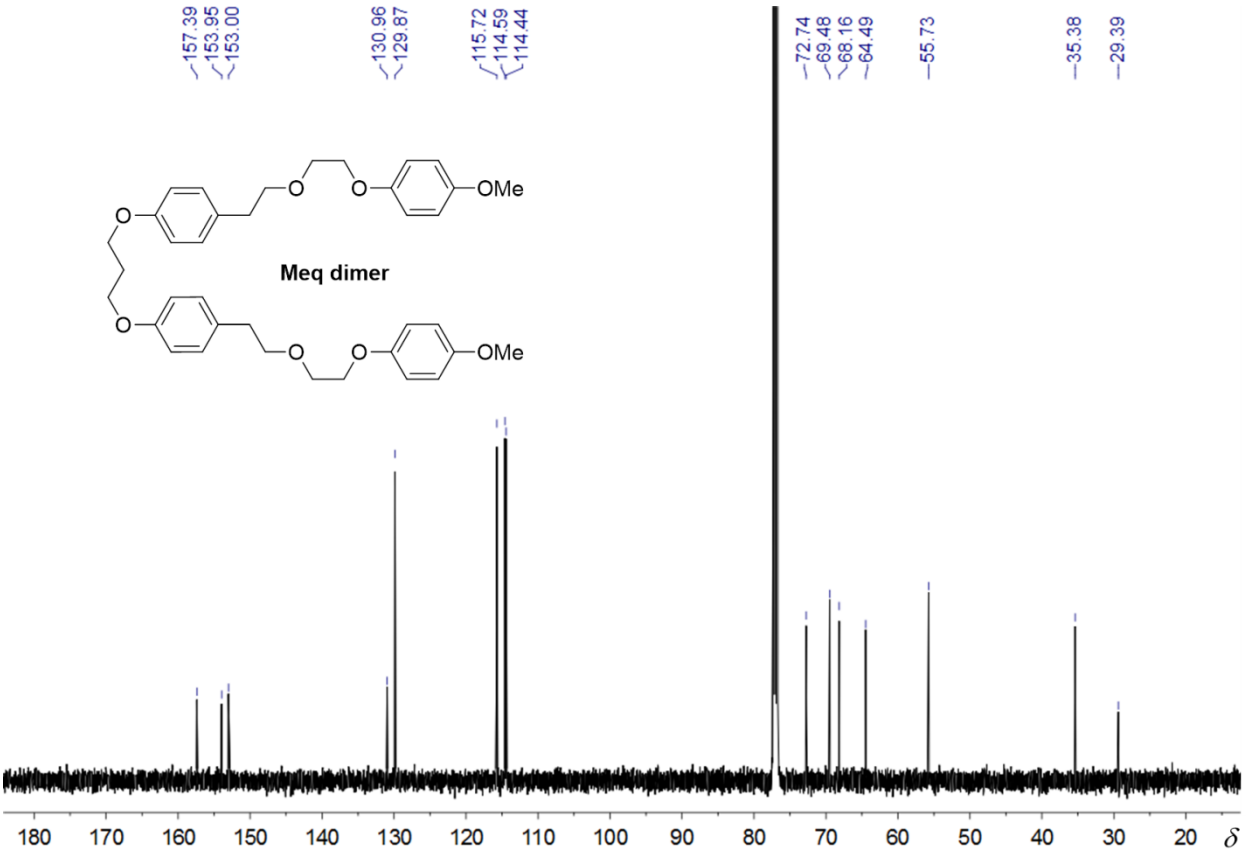

Figure S77. ^{13}C NMR spectrum of **Meq dimer** (126 MHz, $CDCl_3$).

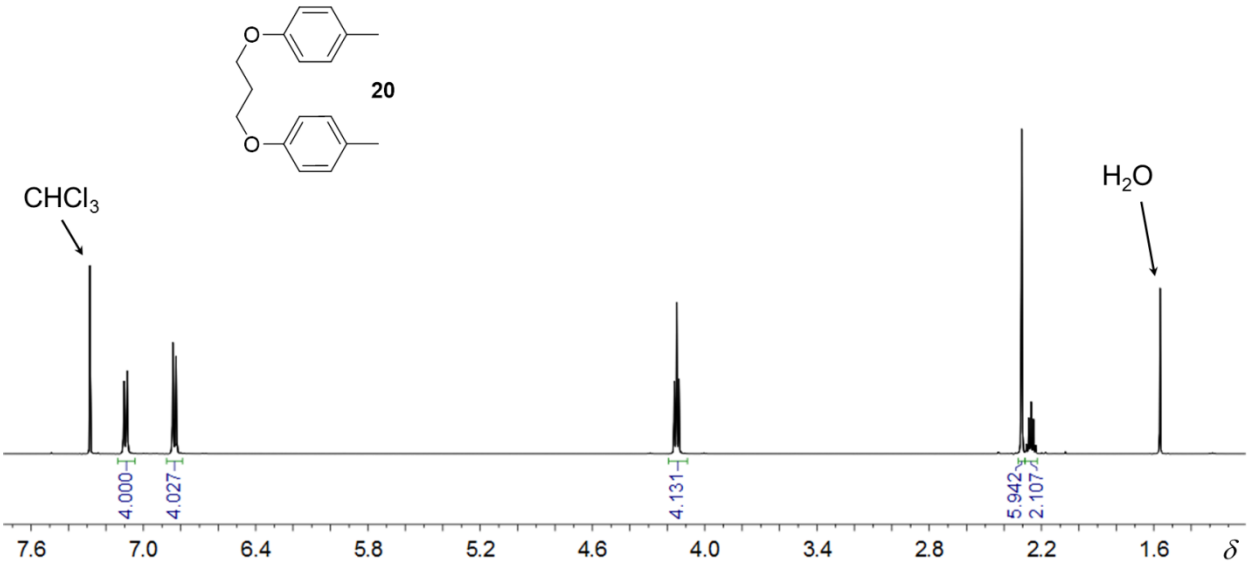

Figure S78. ^{1}H NMR spectrum of **20** (500 MHz, $CDCl_3$).

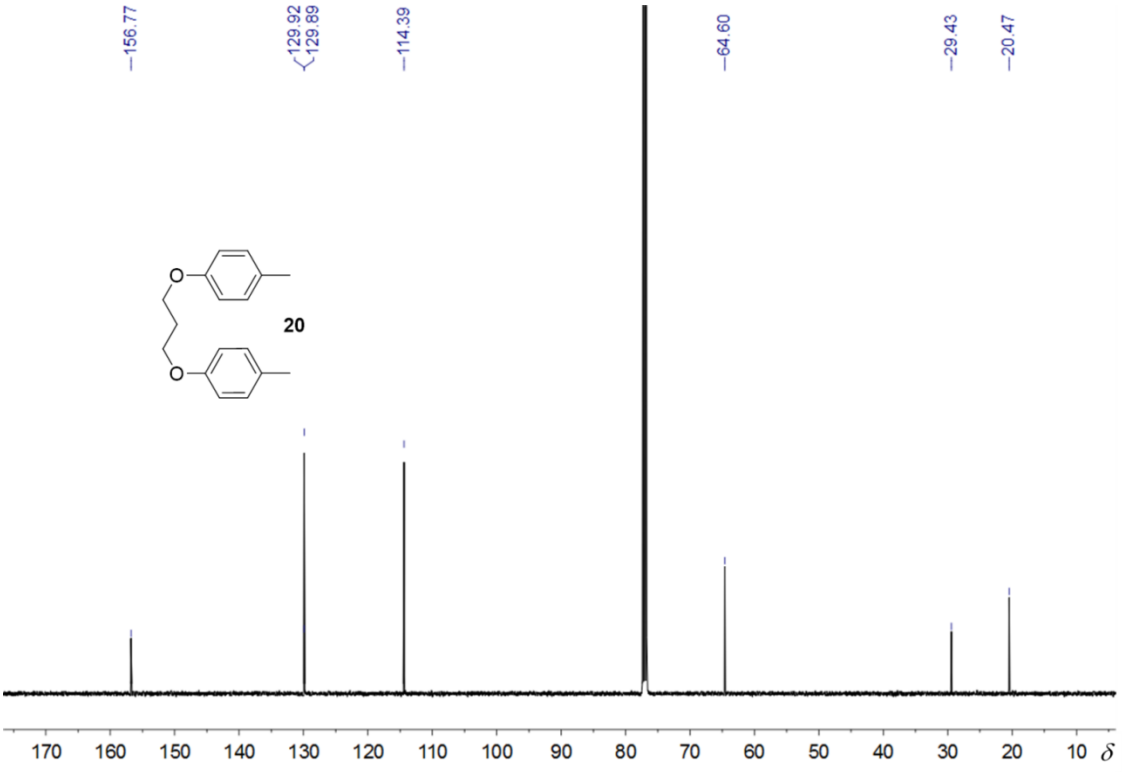

Figure S79. ^{13}C NMR spectrum of **20** (126 MHz, $CDCl_3$).

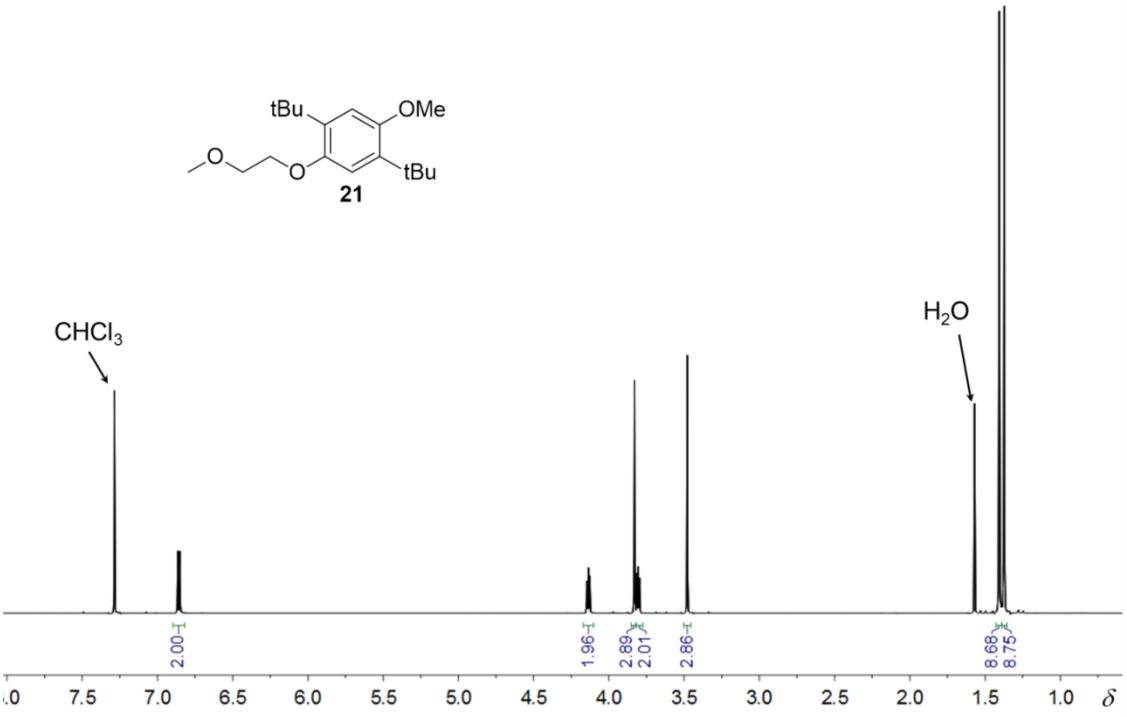

Figure S80. ^{1}H NMR spectrum of **21** (500 MHz, $CDCl_3$).

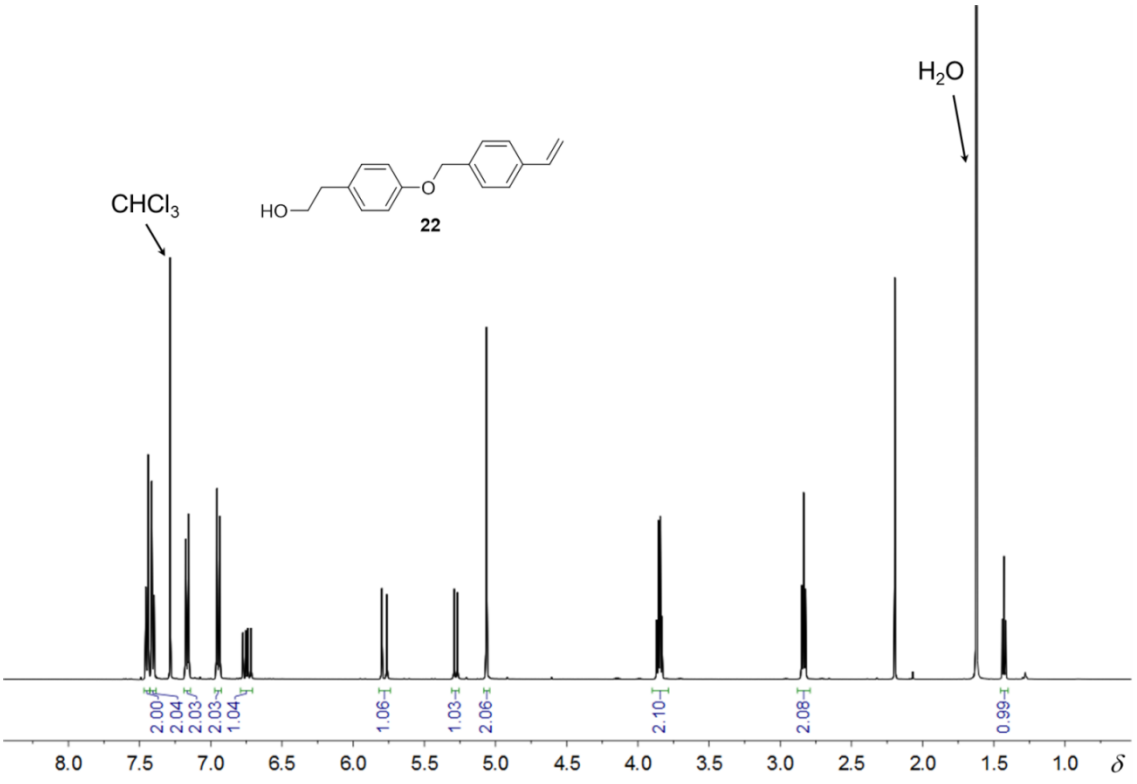

Figure S81. ^{1}H NMR spectrum of **22** (500 MHz, $CDCl_3$).

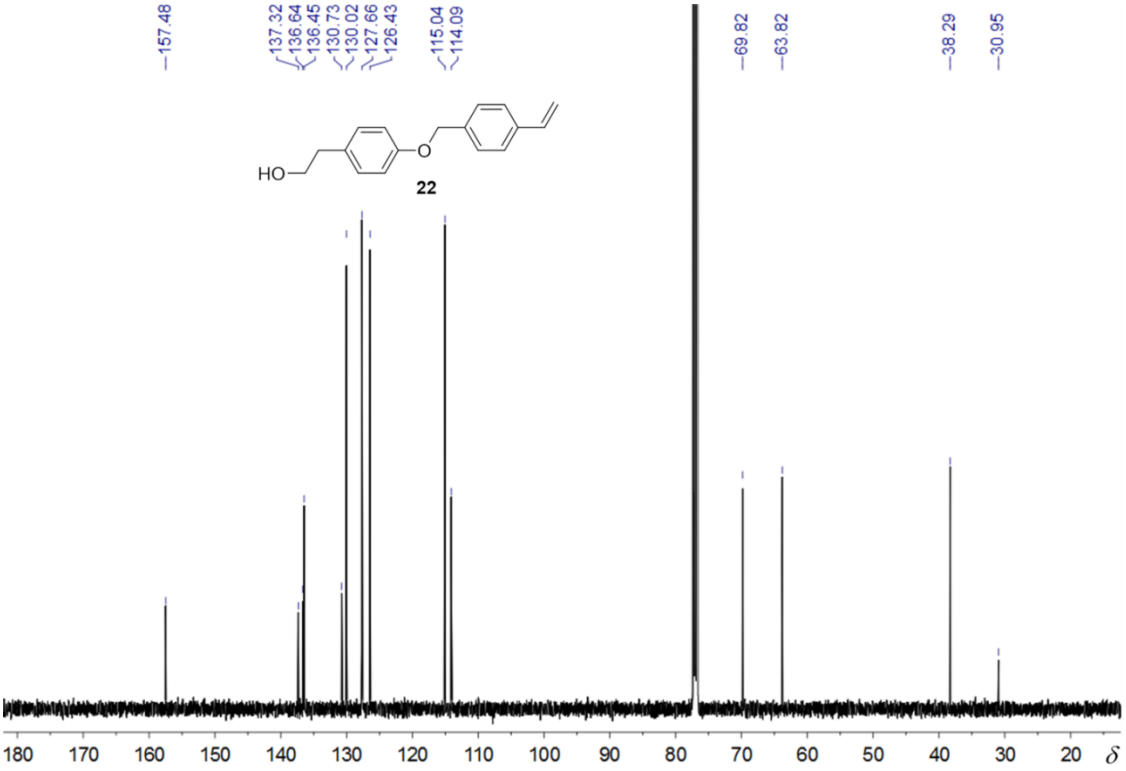

Figure S82. ^{13}C NMR spectrum of **22** (126 MHz, $CDCl_3$).

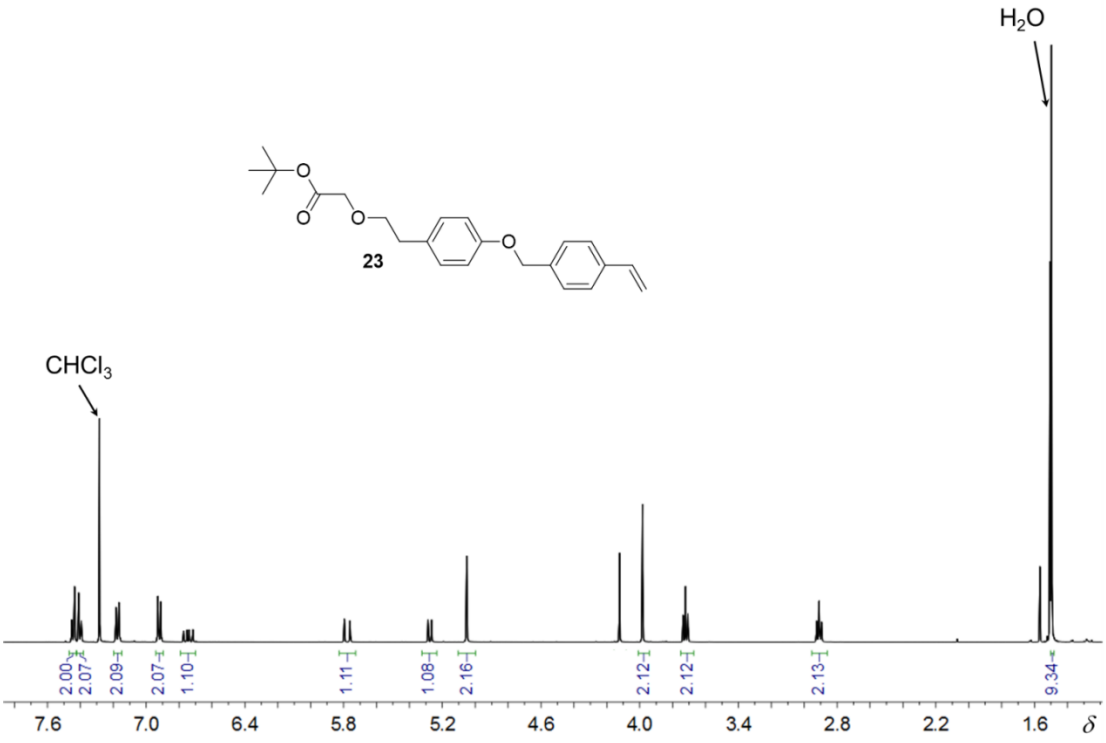

Figure S83. ^{1}H NMR spectrum of **23** (500 MHz, $CDCl_3$).

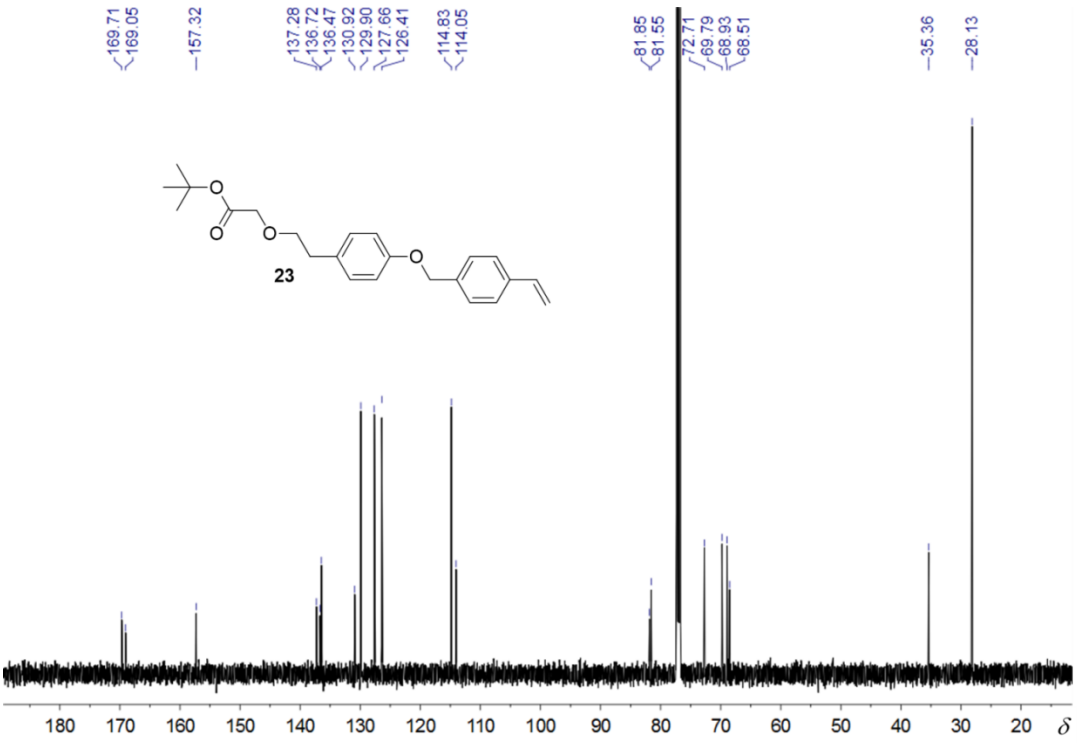

Figure S84. ^{13}C NMR spectrum of **23** (126 MHz, $CDCl_3$).

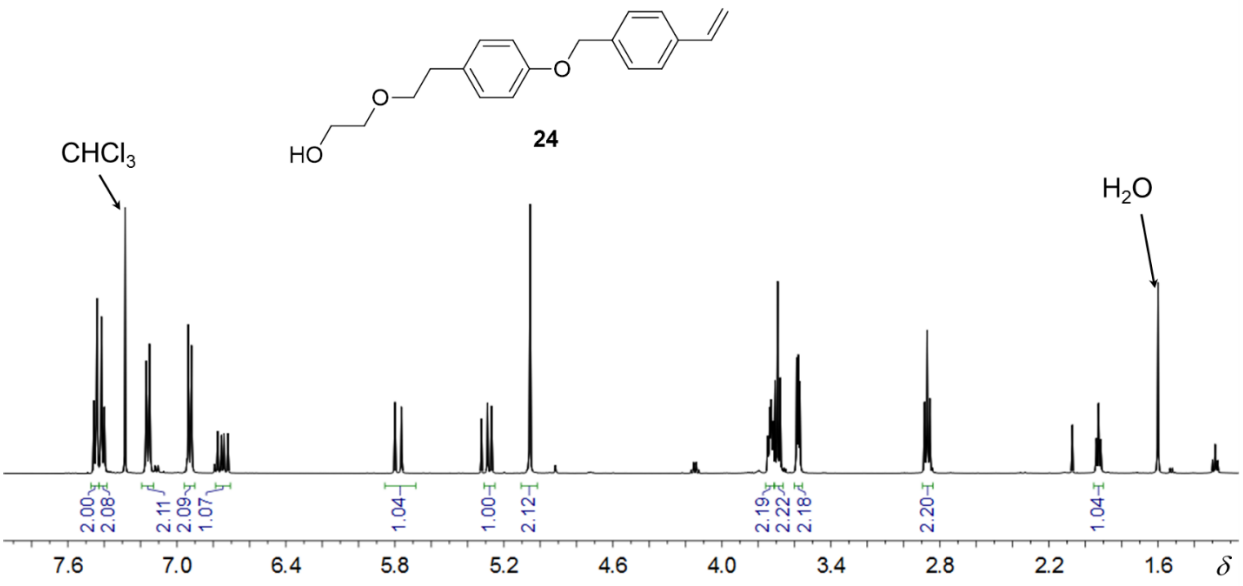

Figure S85. ^{1}H NMR spectrum of **24** (500 MHz, $CDCl_3$).

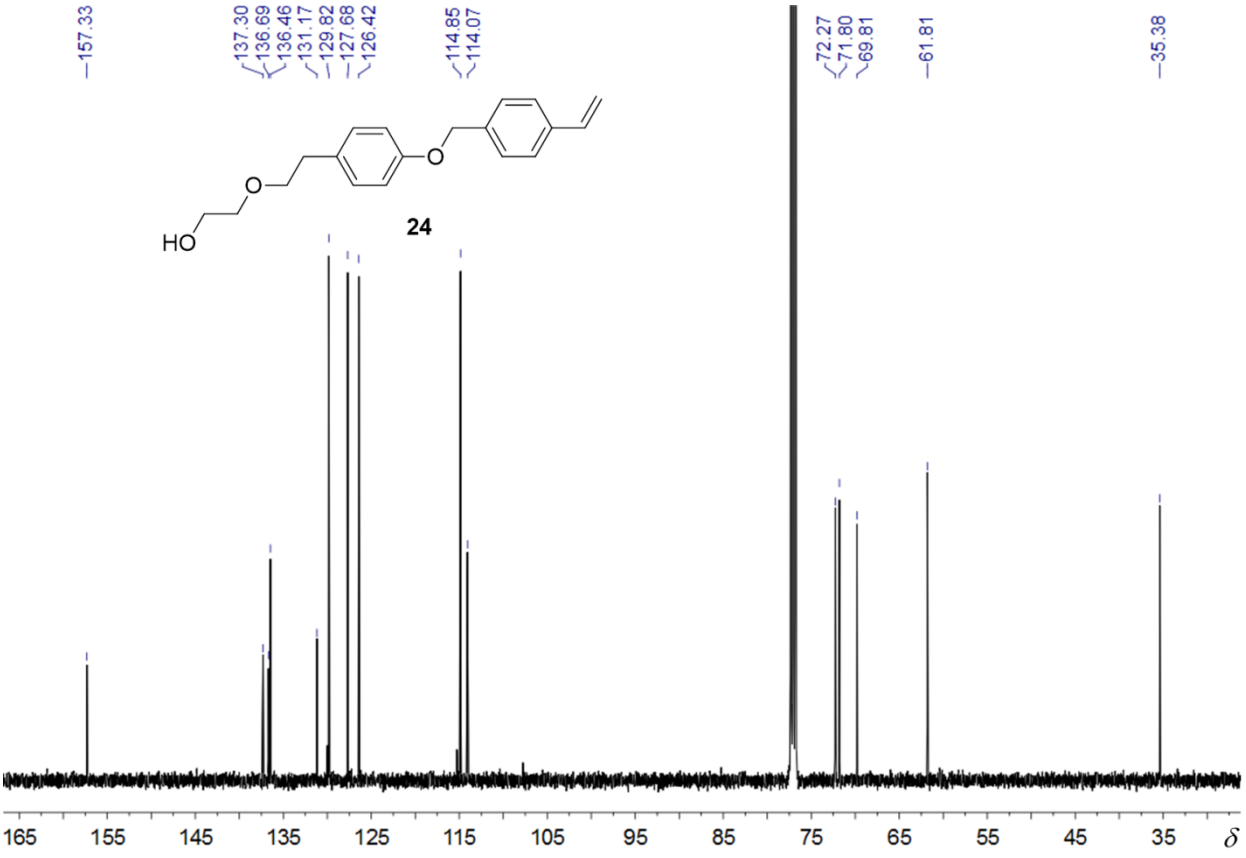

Figure S86. ^{13}C NMR spectrum of **24** (126 MHz, $CDCl_3$).

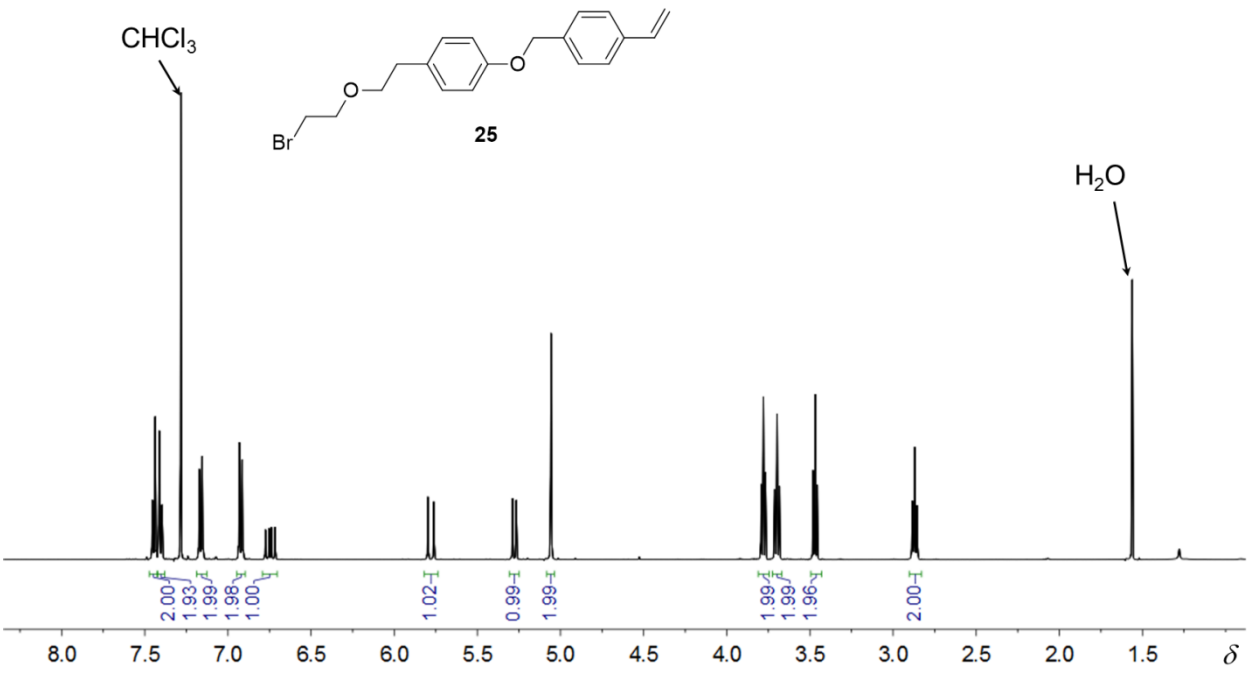

Figure S87. ^{1}H NMR spectrum of **25** (500 MHz, $CDCl_3$).

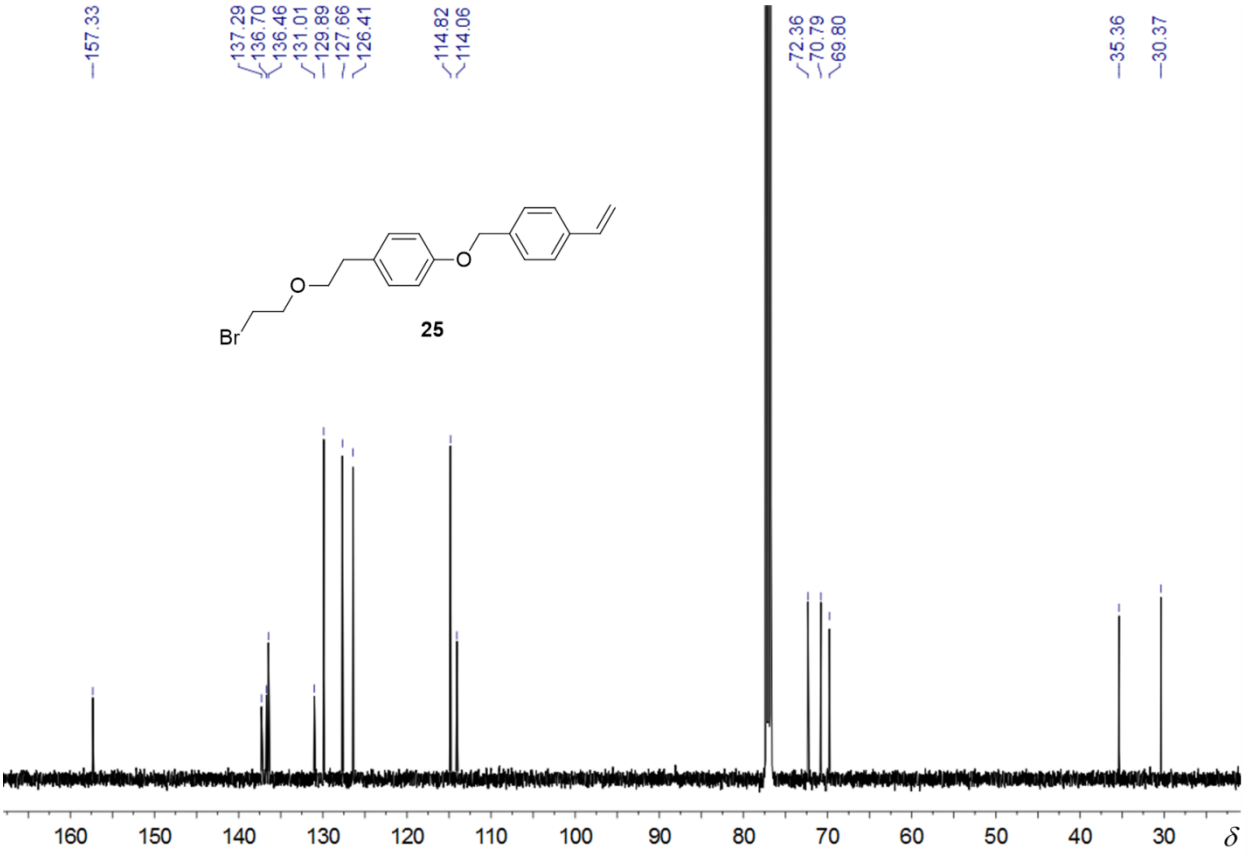

Figure S88. ^{13}C NMR spectrum of **25** (126 MHz, $CDCl_3$).

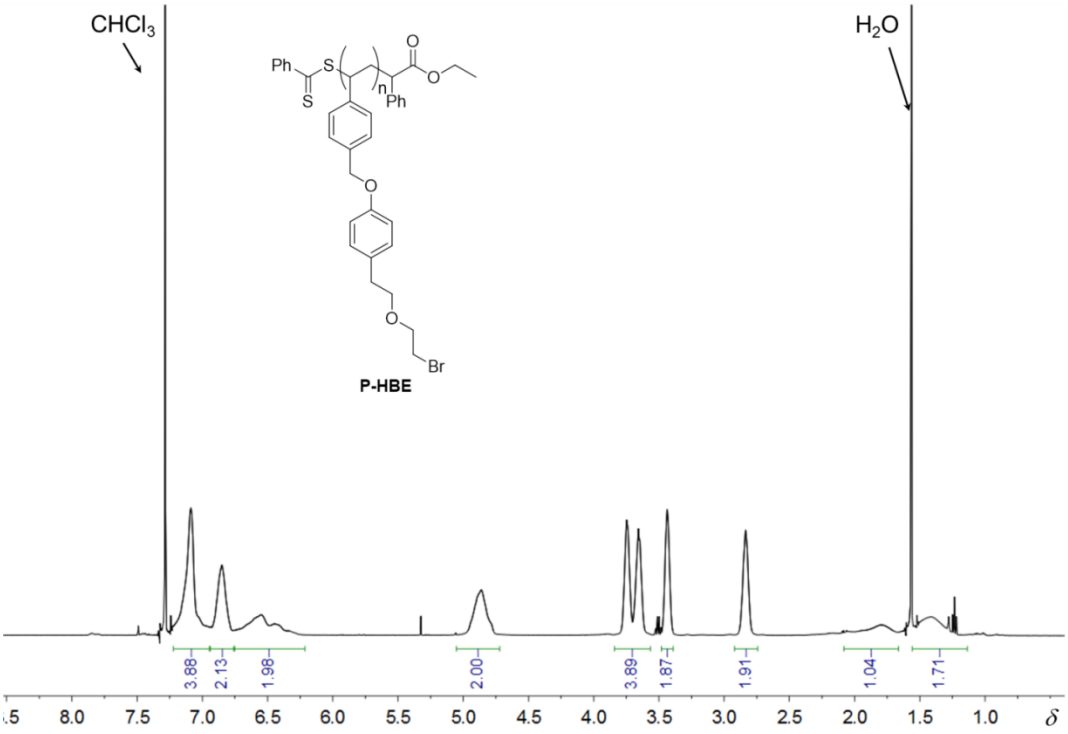

Figure S89. ^{1}H NMR spectrum of **P-HBE** (500 MHz, $CDCl_3$).

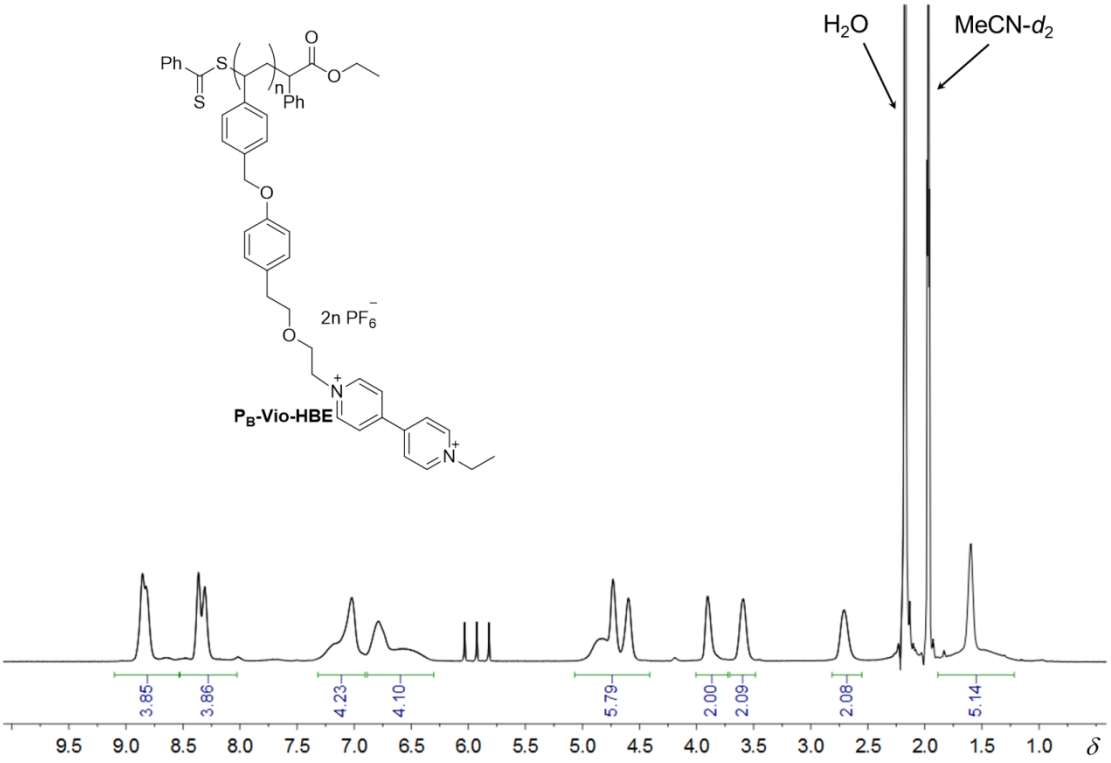

Figure S90. ^{1}H NMR spectrum of **P_B-Vio-HBE** (500 MHz, MeCN-d_3).

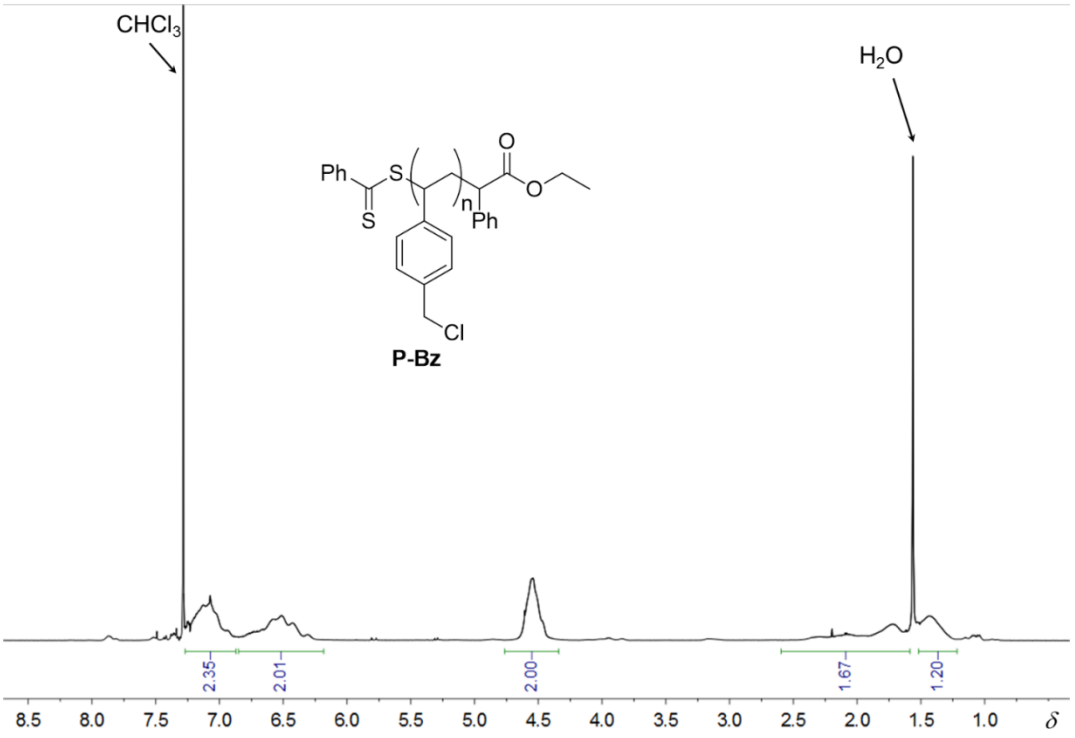

Figure S91. ^{1}H NMR spectrum of **P-Bz** (500 MHz, $CDCl_3$).

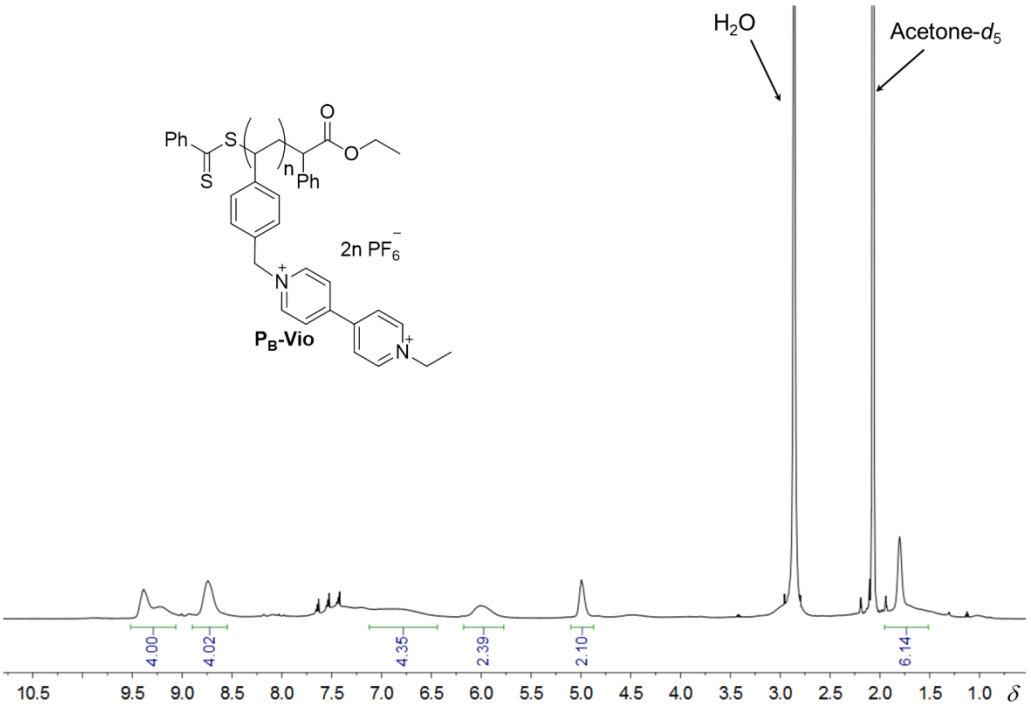

Figure S92. ^{1}H NMR spectrum of **P_B-Vio** (500 MHz, Acetone-d_6).

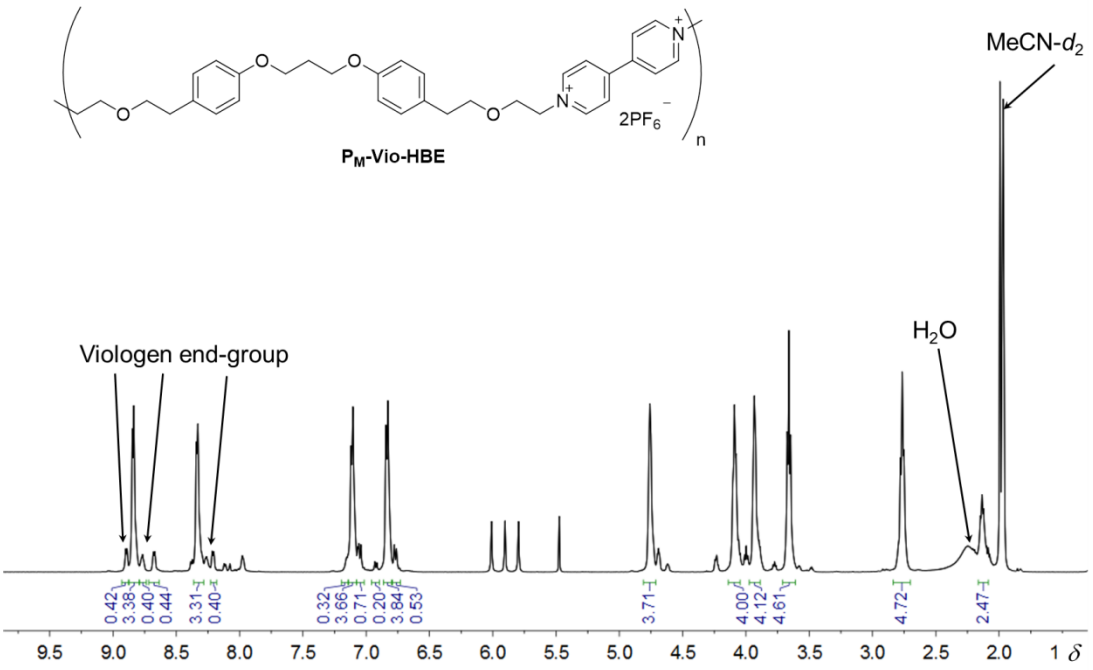

Figure S93. ^{1}H NMR spectrum of $\mathbf{P_M}$**-Vio-HBE** (500 MHz, MeCN-d_3).

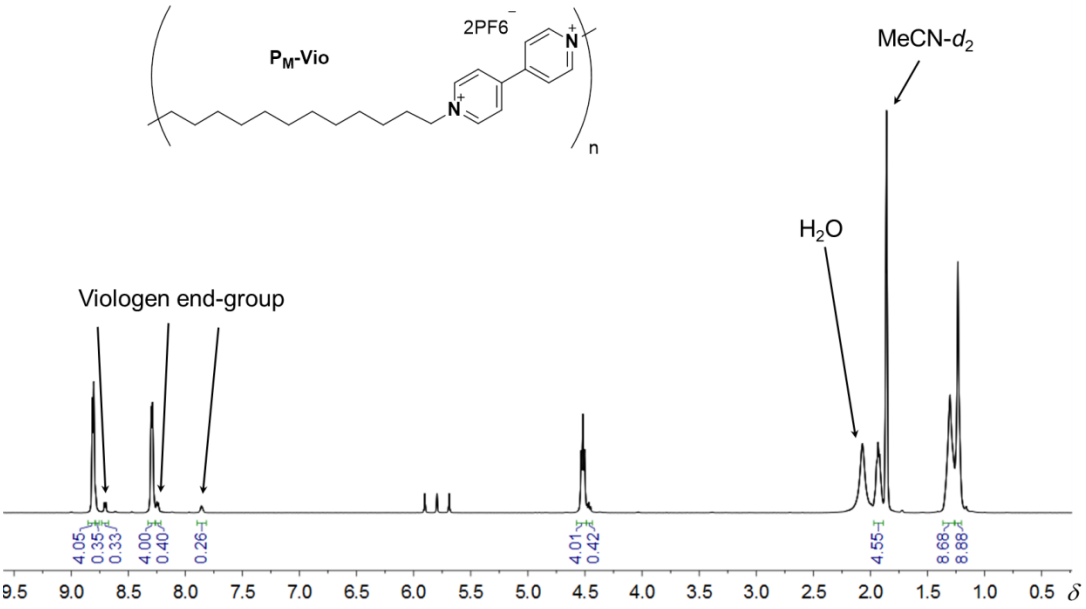

Figure S94. ^{1}H NMR spectrum of $\mathbf{P_M}$**-Vio** (500 MHz, MeCN-d_3).

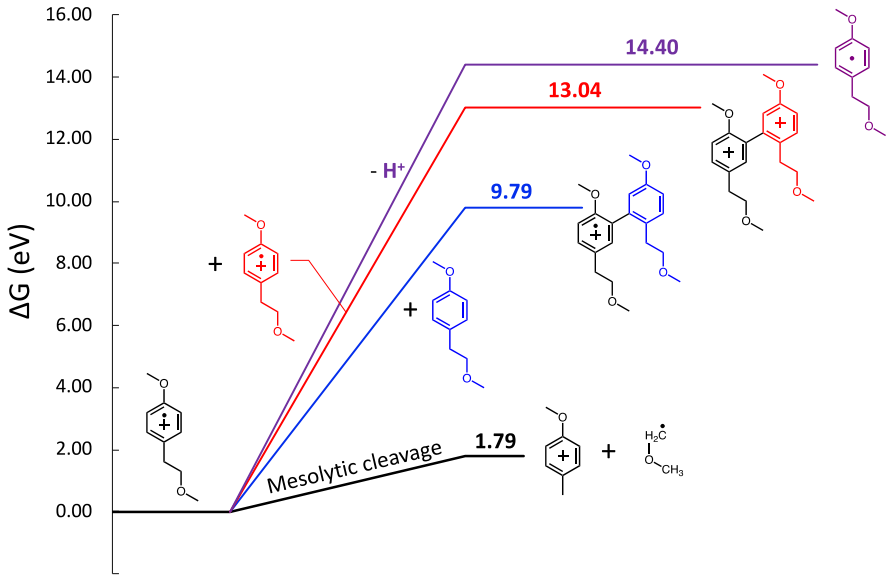

Figure S95. Computed reaction free energies (ΔG) of various reaction pathways starting with the radical cation of **HBE 2**. Mesolytic cleavage, deprotonation, and aryl-aryl coupling with a neutral or radical cation are shown as solid black, purple, blue, and red lines. We note that, mesolytic cleavage is the most likely initial reaction upon 1e oxidation of **HBE 2**.

8 Reference:

S1. H. T. Dao, U. Schneider and S. Kobayashi, *Chem. Commun.*, 2011, **47**, 692-694.

S2. N. A. Paras, B. Simmons and D. W. C. MacMillan, *Tetrahedron*, 2009, **65**, 3232-3238.

S3. M. J. Harper, E. J. Emmett, J. F. Bower and C. A. Russell, *J. Am. Chem. Soc.*, 2017, **139**, 12386-12389.

S4. T. Hama and J. F. Hartwig, *Org. Lett.*, 2008, **10**, 1545-1548.

S5. D. A. Brooks, G. J. Etgen, C. J. Rito, A. J. Shuker, S. J. Dominianni, A. M. Warshawsky, R. Ardecky, J. R. Paterniti, J. Tyhonas, D. S. Karanewsky, R. F. Kauffman, C. L. Broderick, B. A. Oldham, C. Montrose-Rafizadeh, L. L. Winneroski, M. M. Faul and J. R. McCarthy, *J. Med. Chem.*, 2001, **44**, 2061-2064.

S6. C. Berti and L. Greci, *J. Org. Chem.*, 1981, **46**, 3060-3063.

S7. S. Ushijima and H. Togo, *Synlett*, 2010, DOI: 10.1055/s-0029-1219935, 1562-1566.

S8. J. Zhang, Y. Li, F. Y. Zhang, C. C. Hu and Y. Y. Chen, *Angew. Chem. Int. Ed.*, 2016, **55**, 1872-1875.

S9. S. P. Bai, S. H. Li, J. B. Xu, X. Peng, K. Sai, W. H. Chu, Z. D. Tu, C. B. Zeng and R. H. Mach, *J. Med. Chem.*, 2014, **57**, 4239-4251.

S10. M. J. Baran, M. N. Braten, E. C. Montoto, Z. T. Gossage, L. Ma, E. Chenard, J. S. Moore, J. Rodriguez-Lopez and B. A. Helms, *Chem. Mater.*, 2018, **30**, 3861-3866.

S11. G. Dilauro, A. F. Quivelli, P. Vitale, V. Capriati and F. M. Perna, *Angew. Chem. Int. Ed.*, 2019, **58**, 1799-1802.

S12. X. Q. Xing, Q. H. Liu, B. G. Wang, J. P. Lemmon and W. Q. Xu, *J. Power Sources*, 2020, **445**, 227330.

S13. Y. Sagara, M. Karman, E. Verde-Sesto, K. Matsuo, Y. Kim, N. Tamaoki and C. Weder, *J. Am. Chem. Soc.*, 2018, **140**, 1584-1587.

S14. G. Nagarjuna, J. S. Hui, K. J. Cheng, T. Lichtenstein, M. Shen, J. S. Moore and J. Rodriguez-Lopez, *J. Am. Chem. Soc.*, 2014, **136**, 16309-16316.

S15.

S16. W. H. Ding and P. C. Tsai, *Anal. Chem.*, 2003, **75**, 1792-1797.

S17. E. Baciocchi, M. Bietti and O. Lanzalunga, *Acc. Chem. Res.*, 2000, **33**, 243-251.

S18. J. J. Guerard and J. S. Arey, *J. Chem. Theory Comput.*, 2013, **9**, 5046-5058.

S19. A. Lewis, J. A. Bumpus, D. G. Truhlar and C. J. Cramer, *J. Chem. Educ.*, 2007, **81**, 596-603.

S20. M. Haga, E. S. Dodsworth and A. B. P. Lever, *Inorg. Chem.*, 1986, **25**, 447-453.

S21. J. A. Bellefeuille, C. A. Grapperhaus, R. M. Buonomo, J. H. Reibenspies and M. Y. Darensbourg, *Organometallics.*, 1998, **17**, 4813-4821.